University of Alberta

Moving Horizon Estimation for Continuum and Noncontinuum States with Applications in Distillation Processes

by

Moshood Jide Olanrewaju

A thesis submitted to the Faculty of Graduate Studies and Research in partial fulfillment of the requirements for the degree of

Doctor of Philosophy

in

Process Control

Department of Chemical and Materials Engineering

Fall 2011
Edmonton, Alberta

To my wife, Mariam, and sons: Mubaraq, Maliq, and Mishal

Abstract

This thesis focuses on the development of advanced state estimators for continuum and noncontinuum state estimations in a switching dynamic system, and the demonstration of their applications in addressing some important process monitoring problems of distillation processes.

First, the theoretical and experimental investigations of applying a sequential continuum and noncontinuum state estimator to composition estimation in a distillation process with switching dynamics are explored. A moving horizon estimator (MHE), which has the capability to handle process constraints, is developed to estimate product composition in a distillation process under known switching mode criteria using the available temperature measurements. For situations when the system operating mode transition is unknown, an approach to state estimation under unknown switching functions is developed. The proposed method combines a MHE for composition estimation with a mode change detector to detect a change in the system operating mode and an operating mode estimator to identify the functioning mode.

Next, a noncontinuum state estimator, which is based on a moving horizon method for a class of switching system that follows a hidden Markov model, is developed. An approach to arrival cost development and constraint handling in moving horizon estimation of noncontinuum state is discussed. The effectiveness of the proposed method is illustrated by considering mode estimation problems in a simulated leakage detection system as well as a continuous stirred tank reactor.

Last, the development and application of a hybrid moving horizon estimator (HMHE) to achieve simultaneous estimation of both continuum and noncontinuum

states in a constrained dynamic system is explored. One of the major issues in a moving horizon estimation approach is the development of an arrival cost to summarize the effect of past and a prior information. In this work, we have developed a generalized arrival cost, which accounts for both continuum and noncontinuum states. A generalized hybrid state estimator, which can be used as a stand-alone continuum state estimator, or as a simultaneous continuum and noncontinuum state estimator, is developed. The effectiveness of the HMHE is demonstrated through simulation studies, while its practical reliability is tested by conducting experimental studies on distillation processes.

Acknowledgements

All thanks to Allah, The Beneficent, The Merciful. I wish to thank my thesis advisor, Dr. Biao Huang, whose encouragement, guidance, and support enabled me to complete this work. I consider it an honor and a privilege to work with him. His dedication to a quality research work and commitment to providing insightful suggestions are a source of inspiration to me.

I must also thank Artin Afacan. I appreciate his tireless effort, visionary leading role in the lab, and consistent support in making this work a reality. I thank you for being patient enough for me to learn a lot during the experimental studies.

I gratefully acknowledge my committee members, Dr. Sirish Shah, Dr. Amos Ben-zvi, Dr. Stevan Dubljevic, Dr. Qing Zhao, and Dr. Nael H. El-Farra (External examiner), for their co-operation, support and contributions. Their suggestions and advice are highly valued and appreciated.

The technical support provided by Fadi Ibrahim during the early stage of my research work is highly appreciated, while the financial supports from Syncrude Canada Ltd, and Natural Sciences and Engineering Research Council of Canada (NSERC) are acknowledged.

For my wife, Taiwo, and sons, Mubaraq, Maliq, and Mishal, we have been in this journey together. I thank you all for being there with me through thick and thin. I am very grateful to my parents, Mr. and Mrs. Olanrewaju for their patience, love, and support.

I also owe thanks to a number of other persons whose presence made my experience at University of Alberta both amusing and rewarding. These include but not limited to all my fellow graduate students of Dr. Huang, namely, Fei, Xinguang, Seyi, Xing, Yuri, Ruben, and others. I thank my friends: AbdulJelill Bello, Gideon Lambiv, Animu Bello, and their families, for making my living in Michener Park a memorable period.

Contents

List of Tables

List of Figures

List of Symbols

A, B, C	dynamic linear system matrices
B	bottoms flow rate (kmol/h)
D	distillate flow rate (kmol/h)
E_{mv}	tray efficiency
F	feed flow rate (kmol/h)
$F^{(m_k)}$	Jacobian Matrix for a switching linear state transition function
$H^{(m_k)}$	Jacobian Matrix for a switching linear output function
H_i	liquid holdup on stage i (kmol)
$\mathbf{K}$	Kalman filter gain matrix
L	liquid flow rate (kmol/hr)
m	operating modes
N	horizon length
N_s	total number of stages including reboiler and reflux drum
P_i	operating pressure on tray i
Q, $\mathcal{R}$	weighting matrices
r_k	output measurement residual at time instant k
R	reflux flow rate (kmol/h)
RR	reflux ratio
$\mathbf{T}$	temperature
T_i	temperature on tray i

T	Final time instant
u_k	input(s) at sampling time instant k
v	measurement noise
V	vapor boilup (kmol/h)
w	process noise
$\hat{w}$	estimated process noise
w_{lo}	process noise lower bound
w_{up}	process noise upper bound
$x_{i,j}$	liquid mole fraction of component j on tray i
x, X	vector of the state variables
$\hat{x}, \hat{X}$	vector of the state estimates
$y_{i,j}$	vapor composition of component j on a stage i
y_k	output(s) at sampling time instant k
y, Y	vector of the output measurements
z	feed composition
ΔH_{vap}	heat of vaporization
Δu_k	change in input at instant time k
ε	mode change index
α_j	relative volatility of component j with respect to heavy component
θ and β	system parameters
δ_w	standard deviation of the process noise
δ_v	standard deviation of the measurement noise

List of Abbreviations

AMR	Average Missing Rate
CSTR	Continuous Stirred Tank Reactor
DEKF	Discrete Extended Kalman Filter
EKF	Extended Kalman Filter
ELO	Extended Luenberger observer
FIR	Finite Impulse Response
HMHE	Hybrid Moving Horizon Estimator (Estimation)
KF	Kalman Filter
MAP	Maximum a Posterior
MMAP	Marginal Maximum a Posterior
MHE	Moving Horizon Estimator (Estimation)
MHENS	Moving Horizon Estimator for Noncontinuum state
HMM	Hidden Markov Model
MeOH	Methanol
MR	Missing Rate
MCD	Mode Change Detector
RMSE	Root Mean Square Error
MLD	Mixed Logical Dynamical
OME	Operating Mode Estimator
Off-VA	Offline Viterbi Algorithm

On-VA	Online Viterbi Algorithm
PDF	Probability Density Function
PWA	Piecewise Affine
PF	Particle Filter
SHMHE	Sequential Hybrid Moving Horizon Estimator (Estimation)
UKF	Unscented Kalman Filter
VA	Viterbi Algorithm

Chapter 1

Introduction

1.1 Motivation and Objectives

Chemical process plant safety, environmental regulations, plant economics, decision-making under uncertainties, and the demand for effective process monitoring and control are some of the main reasons that are driving an upward research interest in the development of more advanced methods for state estimation. Most process monitoring and control schemes rely on the assumption that the states of the system are explicitly available. But in reality, most process states are either not directly measurable or can only be measured with a considerable level of noise. State estimator, a tool to infer the process states from the available measurement, is important and a necessity to achieve effective process monitoring, diagnosis, and control.

State estimation of a continuum dynamic system has been well studied in the literature. The Kalman filter (KF) [50], extended Kalman filter (EKF) [63], unscented Kalman filter (UKF) [49], moving horizon estimation (MHE) [72], and particle filter [18] are among the well established estimation techniques that can be used for a dynamic estimation of a continuous-valued or continuum state. In reality, the problems to address in a chemical system can take a discrete-event or noncontinuum forms. Typical examples of noncontinuum form representation in process monitoring problems are stiction versus non-stiction problems of control valves [47], normal versus abnormal conditions in fault detection and isolation problems [47, 55], and a hybrid control system design [23]. Even for a continuum dynamic process, the problem of interest to address may still take a noncontinuum representation such as "desired" or "undesired" operating regions in process monitoring [43, 44] and "good", "bad", or "optimum" in control performance assessment problems [41]. Noncontinuum states also play a key role in embedded control systems that interact with the physical world [8, 23, 58].

Studies in the literature have also shown that dynamic behavior of a nonself-oscillatory chemical system can switch periodically between two nearby stable sta-

tionary states [96], while a steady state multiplicity effect [44, 51] and a phase change behavior in chemical systems [45] are other factors that make it difficult to describe a system with a single continuum dynamics. However, existing studies on noncontinuum state estimation have been limited in the literature. For advanced process monitoring, fault detection and control purposes, it is necessary to interpret and model chemical processes as hybrid systems (i.e., containing continuum and noncontinuum states) and seek for a more general, practical and effective hybrid estimation method, which has the capability to estimate both the continuum and noncontinuum states.

Distillation is perhaps one of the most important and widely used unit operations in process industry. Distillation operations consume large amount of energy. Thus, in the face of rising prices of energy and raw materials, it has become imperative to operate distillation columns more efficiently through effective process monitoring and control. With the evidence of the industrially operated distillation columns having multiple steady state solutions as well as unstable operating points [43, 44, 45, 51], the development of advanced state estimators for distillation processes modeled as hybrid systems will help address some of the outstanding process monitoring problems such as simultaneous composition estimation, fault detection, operating mode determination, as well as unmeasurable disturbance input estimation in a unified and systematic way.

At present, the most widely used approximate nonlinear state estimator in process monitoring and control of distillation columns is the extended Kalman filter (EKF) [9, 10, 62]. However, it has the disadvantage that the covariance propagation and update are carried out through linearization around some operating points, and this suggests that the region of stability may be small since nonlinearities in the system dynamics are not fully accounted for. Therefore, it is necessary to investigate new and more advanced nonlinear state estimators and demonstrate their practical reliability by conducting both theoretical and experimental investigation on an industrial-type distillation column.

The objective of this thesis is to develop advanced state estimators, which are based on a moving horizon approach, for the estimation of both continuum and noncontinuum states, and demonstrate their practical applications in addressing some important process monitoring problems of distillation processes with switching dynamics. Our contributions in this work will be on three major areas, which are: improving the theoretical foundation of dynamic estimation methods and developing new state estimators for a class of hybrid system, investigating the practical reliability of a hybrid state estimator through experimental studies on distillation processes, and developing computational algorithms that can be used for industrial applications. Investigation of convergence issues of the estimators is not considered

in this thesis.

1.2 Main Contributions of This Thesis

The specific contributions of this thesis are summarized as follows:

1. **Theoretical contributions:** A generalized hybrid state estimator, which can be used as a stand-alone noncontinuum state estimator, or as a stand-alone continuum estimator, or as a simultaneous continuum and noncontinuum state estimator, is developed. In this work, we considered the following estimation problems:

    - The development of a noncontinuum state estimation technique, which is based on a moving horizon method for a class of switching system. An approach to arrival cost development as well as constraint handling in noncontinuum state estimation is discussed.
    - The development of a sequential continuum and noncontinuum state estimator for a class of a switched hybrid system. This approach combines a moving horizon estimator to estimate the continuum state with a mode change detector to detect a change in the system operating mode, and an operating mode estimator to identify the real-time functioning mode.
    - The development of a hybrid moving horizon estimator to achieve a simultaneous estimation of both continuum and noncontinuum states in a constrained switching dynamic system. A generalized arrival cost, which accounts for both continuum and noncontinuum states, is derived.

2. **Simulation evaluation:** The application of a hybrid state estimator to the process monitoring of some chemical processes such as a storage water tank system, continuous stirred tank reactor (CSTR), and distillation processes is explored.

3. **Experimental investigation:** The practical reliability of the developed estimation techniques is investigated by conducting an experimental studies on distillation processes with switching dynamics. The effects of constraints presence, measurement noise, plant mismatch, and horizon length variation on the estimation of both the continuum and noncontinuum states are analyzed.

1.3 Thesis Organization

Chapter 2 provides a detailed background for this work. An overview on the existing filtering and estimation techniques is provided. A review of a moving horizon state

estimation (MHE) formulation for a continuum state system is provided. A detailed literature review of a hybrid state estimation and the history of state estimation applications to distillation processes are presented in this chapter.

Chapter 3 explores both the theoretical and experimental investigations of applying a sequential continuum and noncontinuum state estimator to composition estimation in a distillation process with switching dynamics. In a hybrid distillation modeling, the column compositions are considered as continuum states while the operating modes are modeled as noncontinuum states. A moving horizon estimator (MHE), which has the capability to handle process constraints, is developed for composition estimation in a distillation process under known switching mode criteria using the available temperature measurements. The performance of a MHE is shown to be superior to that of EKF in handling process and measurement noise under switching dynamics. For situations when the system operating mode transition is unknown, an approach to state estimation under unknown switching functions is investigated. The proposed method combines a MHE for composition estimation with a mode change detector to detect a change in the system operating mode and an operating mode estimator to identify the functioning mode. In the presence of both the measurement noise and plant-model mismatch, the developed estimator is shown to be effective in estimating both the column composition and the system operating mode.

In Chapter 4, a noncontinuum state estimator, which is based on a moving horizon method for a class of switching system that follows a hidden Markov model, is developed. An approach to arrival cost development and constraint handling in moving horizon estimation of noncontinuum state is discussed. The effectiveness of the proposed method is illustrated by considering mode estimation problems in a simulated leakage detection system as well as a continuous stirred tank reactor.

The development and application of a hybrid moving horizon estimator (HMHE) to achieve simultaneous estimation of both continuum and noncontinuum states in a constrained switching dynamic system is the focus of Chapter 5. One of the major issues in a moving horizon estimation approach is the development of an arrival cost to summarize the effect of past and *a prior* information. In this work, we developed a generalized arrival cost, which accounts for both continuum and noncontinuum states. A generalized hybrid state estimator, which can be used as a stand-alone continuum state estimator, or as a simultaneous continuum and noncontinuum state estimator, is developed. The effects of constraints, process and measurement noise levels, as well as a moving horizon length on the simultaneous estimation of both the continuum and noncontinuum states are analyzed. The effectiveness of the HMHE is demonstrated through simulation studies, while its practical application is examined on a constrained continued stirred tank reactor system.

Chapter 6 details extensive experimental investigation studies carried out on a distillation process. This experimental work aims at examining the practical reliability of the developed hybrid moving horizon estimator to infer the composition of methanol in the distillate product as well as the operating modes using the available temperature measurements. The effects of constraints presence, process and measurement noise levels, and the horizon length variation on the estimation of the continuum and noncontinuum states are also analyzed in this chapter.

Chapter 2

Thesis Background

2.1 State Estimation

In most of the chemical, biochemical, and petrochemical processes, effective process monitoring and advanced control system designs are often difficult because of the absence of frequent and delay-free measurements of important process variables and the presence of unknown disturbances in the process. A state estimator has been recognized as a tool that can be designed to estimate the values of these process variables from the available measurements. As shown in Figure 2.1 for instance, a state estimator is required to provide the system states in order to implement a state feedback controller. Besides, state estimators can also play a key role in process control and monitoring wherein an early detection of hazardous conditions is needed for a safe operation [80, 89].

2.2 Continuum State Estimation

Continuum state estimation generally involves the estimation of a continuous-valued state, x, given the measurable input, u, and observable measurement, y. There are several continuum state estimation techniques available in the literature. These include the static partial least-square regression estimator [57, 13], Kalman filter [9, 10, 50, 62, 85], H_∞ filter [84], a high gain observer [101], Bayesian state estimation [18, 19], Luenberger observer [69, 101], moving horizon estimator (MHE) [77], and particle filter [18, 19, 92]. Most of these methods are well developed for continuum state estimation problems with various limitations in the handling of process nonlinearity, constraints, measurement noise, and plant-model mismatch.

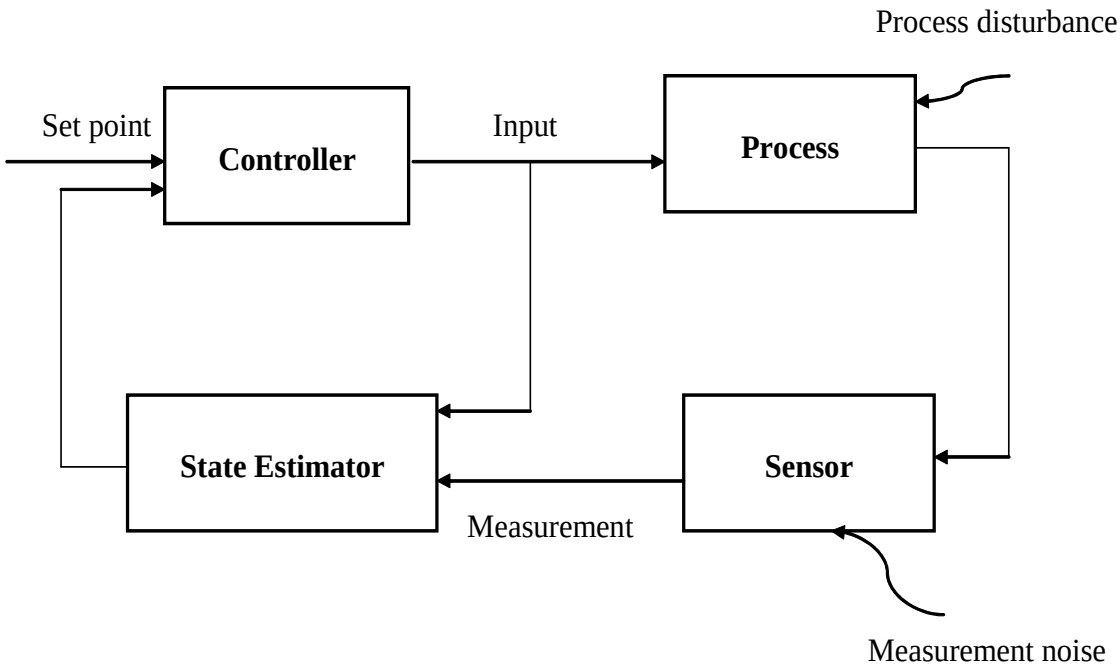

Figure 2.1: Application of a state estimator in a feedback control system.

2.2.1 Dynamic process model

To elaborate on the estimation problem for continuum state, let us consider the following discrete state space models:

$$\begin{aligned} x_k &= f(x_{k-1}, u_{k-1}; \theta) + w_{k-1}, \\ y_k &= g(x_k; \beta) + v_k, \end{aligned} \tag{2.1}$$

where $x_k \in \mathbb{R}^n$ denotes the model state, $u_k \in \mathbb{R}^p$ is the input and $y_k \in \mathbb{R}^q$ denotes the observed output from the system at time k. $f : \mathbb{R}^n \times \mathbb{R}^p \longrightarrow \mathbb{R}^n$ is the deterministic transition function determining the mean of x_k given x_{k-1} and u_{k-1}. $w_{k-1} \in \mathbb{R}^n$ is the zero-mean Gaussian noise vector at time $k-1$. $g : \mathbb{R}^n \times \mathbb{R}^q \longrightarrow \mathbb{R}^q$ is the deterministic output function determining the mean of the y_k given x_k. An additive measurement noise vector to the output measurement is given as $v_k \in \mathbb{R}^q$. θ and β denote the system parameters. The process follows a hidden Markov process as shown in Figure 2.2, and the observation data are generated from the sequence of hidden states in the presence of measurement noise.

The main interest in the state estimation problem is to find the best state estimates (i.e., $\hat{x}_{0:T}$) of the hidden process states (i.e., $x_{0:T}$) from the available measurements (i.e., $y_{0:T}$). Probabilistically, it means either the state estimates are the conditional expectation of the states $x_{0:T}$ given the measurement $y_{0:T}$,

$$\hat{x}_{0:T} = \mathbb{E}(x_{0:T}|y_{0:T}) \tag{2.2}$$

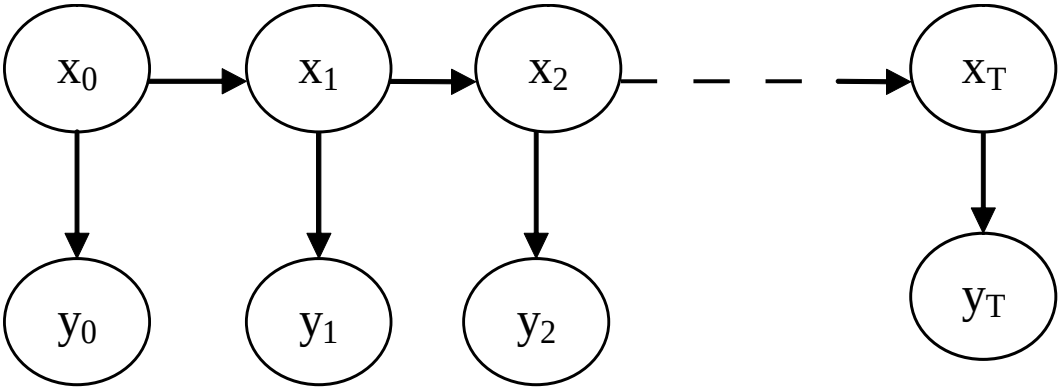

Figure 2.2: Markov process model.

or, the state estimates that maximize the conditional joint probability of the sequences of states $x_{0:T}$ given the observation sequence $y_{0:T}$ as:

$$\max_{\hat{x}_{0:T}} \{P(x_{0:T}|y_{0:T})\} \tag{2.3}$$

2.2.2 Choice of optimality criteria

It is obvious that the solution to the estimation problems of Eqs. (2.2) and (2.3) is not unique as the optimality of the obtained states depends strongly on the choice or definition of the optimality criteria. There are different factors that can influence the choice of the optimality criteria. Among those factors are:

1. **Minimum variance estimate:** The objective function is defined in such a way that the minimum variance estimate is sought for.

2. **Computational complexity:** Defining an optimum criterion in which all of the hidden states ($x_{0:T}$) are to be estimated given all of the observed outputs ($y_{0:T}$) will pose a more computational difficulty than defining an optimum criterion to estimate an individual state x_k at time k given the observed measurements.

3. **Area of applications:** An optimum criterion definition for a state estimation to be used for a batch system for instance, could be different from the one to be used for a continuous system. Even to estimate state sequence for small set of data for a batch system might require to define a different optimum criterion from when state sequence is to be estimated from a large set of data.

4. **Implementation issues:** Whether the state estimation is to be implemented online or offline could also influence the definition of the optimum criterion.

5. **Desired level of accuracy:** The level of accuracy that can be tolerated will also play a big factor in the choice of the optimum criterium.

2.2.3 Point state estimation

The point state estimation is developed by constructing a conditional probability distribution function of the state x_k given all of the observations up to the current time k as

$$\max_{\hat{x}_k}\{P(x_k|y_{0:k})\} \tag{2.4}$$

A generalized solution for Eq. (2.4), in principle, can be achieved using a Bayesian state estimation approach. State estimation methodology, which is based on Bayesian framework is very powerful because it provides a rigorous approach for estimating the probability distribution of unknown variables by utilizing all of the available knowledge, data, and information about the system [18, 19]. It considers all of the variables to be stochastic and determines the distribution of the variables to be estimated through the combination of prior knowledge of the system with the current measurement information according to the Bayesian theorem as

$$P(x_k|y_{0:k}) = \frac{P(y_k|x_k, y_{0:k-1})P(x_k|y_{0:k-1})}{P(y_k|y_{0:k-1})} \tag{2.5}$$

The priori knowledge about the state is represented by the conditional probability density function (*cpdf*) expressed as $P(x_k|y_{0:k-1})$. Given the measurements information in the form of a likelihood function $P(y_k|x_k, y_{0:k-1})$, the prior knowledge about the unknown state at any time k is modified into a posteriori conditional probability distribution function $P(x_k|y_{0:k})$. The denominator in Eq. (2.5) is a normalizing constant obtained from the evidence provided by the measurements up to time k.

The general state estimation procedure consists of three steps, which are:

- **Prediction step**: The *cpdf* $P(x_k|y_{0:k-1})$ is predicted as:

$$P(x_k|y_{0:k-1}) = \int P(x_k|x_{k-1}, y_{0:k-1})P(x_{k-1}|y_{0:k-1})dx_{k-1}, \tag{2.6}$$

  where $P(x_k|x_{k-1}, y_{0:k-1})$ is evaluated according to the state function in Eq. (2.1).

- **Updating step**: The *cpdf* $P(x_k|y_{0:k-1})$ is updated to $P(x_k|y_{0:k})$ by the current measurements y_k using Bayesian rule expressed in Eq. (2.5).

- **Inference step**: Once the conditional probability density function is known, an optimal inference is typically drawn by computing the maximum of the posterior as expressed in Eq. (2.4).

Although, the theory of Bayesian estimation of dynamic systems has been available in the literature for decades [18, 19, 92] , practical application and implementation of this method to real industrial processes remain challenging because of the

methodological and computational problems. However, for multivariate normal distributions and an unconstrained linear dynamic system, a recursive Bayesian state estimation will simplify to a standard Kalman filter [60].

Kalman filter

Among the several available estimation techniques, a Kalman filter (KF) is the most widely used in state estimation applications [50, 62, 85]. The theory behind KF [50, 85] is well established and its applications have grown significantly in both academia and industry [9, 10, 62]. Kalman filter is known to be the best optimum state estimator for an unconstrained, linear system subject to normally distributed process and measurement noise [50]. If we consider an unconstrained linear dynamic system of the following forms:

$$\begin{aligned} x_k &= Ax_{k-1} + Bu_{k-1} + w_k, \qquad && w_k \sim N(0, \delta_w^2) \\ y_k &= Cx_k + v_k, && v_k \sim N(0, \delta_v^2) \end{aligned} \tag{2.7}$$

The noise sequences have zero mean and second-order statistics described by

$$\begin{aligned} &E[w_k w_j^T] = Q_k \delta_{kj} \\ &E[v_k v_j^T] = R_k \delta_{kj} \\ &E[v_k w_j^T] = 0 \quad for \quad all \quad k, j \end{aligned} \tag{2.8}$$

The Kalman filter algorithm to estimate the optimum state x_k is summarized as follows:

- **Prediction step**:

$$\begin{aligned} &\bar{x}_k = A\hat{x}_{k-1}, \quad with \quad x_0 \sim N(\hat{x}_0, \hat{P}_0), \\ &\bar{y}_k = C\bar{x}_k, \\ &\bar{P}_k = A\hat{P}_{k-1}A^T + Q_k. \end{aligned} \tag{2.9}$$

- **Updating step**:

$$\begin{aligned} &\mathbf{K} = \bar{P}_k C^T (C\bar{P}_k C^T + R_k)^{-1}, \\ &\hat{x}_k = \bar{x}_k + \mathbf{K}(y_k - \bar{y}_k), \\ &\hat{P}_k = (I - KC)\bar{P}_k. \end{aligned} \tag{2.10}$$

In Eqs. (2.9) and (2.10), $\hat{x}_k$ is the estimate of the state at sample time k given all of the output measurements up to time k, while $\bar{x}_k$ is a *priori* estimate at time k given all information up to time $k-1$. A filtered state estimate is produced at time k by correcting the predicted state estimate at the previous sample time $k-1$ through the product of the matrix gain $\mathbf{K}$ with the difference between the measured output y_k and the predicted output $\bar{y}_k$. For linear Gaussian systems, this estimate is also the maximum likelihood estimate [60]. The filter is stable provided (C, A) is detectable, $(C, Q_k^{\frac{1}{2}})$ is stabilizable, R_k is positive definite, and Q_k is nonnegative definite [60].

2.2.4 Full information state estimation

The objective is to estimate all of the state sequences $x_{0:T}$ given all of the observation sequences $y_{0:T}$. To formulate an objective function for a full information state estimation, the following lemmas will be required:

- **Lemma 1.** *For a stochastic system that follows a Markov process*:
  $\max_{\hat{x}_{0:T}}\{P(x_{0:T}|y_{0:T})\} = \max_{\hat{x}_{0:T}}\{P(x_{0:T}, y_{0:T})\}$.

  Proof:

  By applying Bayesian Theorem, Eq. (2.3) can be expanded as

$$\begin{aligned}\max_{\hat{x}_{0:T}}\{P(x_{0:T}|y_{0:T})\} &= \max_{\hat{x}_{0:T}}\{\frac{P(x_{0:T}|y_{0:T-1})P(y_T|x_{0:T}, y_{0:T-1})}{P(y_T|y_{0:T-1})}\},\\ &= \max_{\hat{x}_{0:T}}\{P(x_{0:T-1}|y_{0:T-1})\frac{P(x_T|x_{0:T-1}, y_{0:T-1})P(y_T|x_{0:T}, y_{0:T-1})}{P(y_T|y_{0:T-1})}\},\end{aligned} \tag{2.11}$$

  For a Markov process governed by Eq. (2.1), where $P(x_T|x_{0:T-1}, y_{0:T-1}) = P(x_T|x_{T-1})$ and $P(y_T|x_{0:T}, y_{0:T-1}) = P(y_T|x_T)$, then, Eq. (2.11) can further be formulated as

$$\begin{aligned}\max_{\hat{x}_{0:T}}\{P(x_{0:T}|y_{0:T})\} &= \max_{\hat{x}_{0:T}}\{P(x_{0:T-1}|y_{0:T-1})\frac{P(x_T|x_{T-1})P(y_T|x_T)}{P(y_T|y_{0:T-1})}\},\\ &= \max_{\hat{x}_{0:T}}\{P(x_0)P(y_0|x_0)\prod_{k=1}^{T}\frac{P(x_k|x_{k-1})P(y_k|x_k)}{P(y_k|y_{0:k-1})}\},\\ &= \max_{\hat{x}_{0:T}}\{\frac{1}{P(y_{0:T})}P(x_0)P(y_0|x_0)\prod_{k=1}^{T}P(x_k|x_{k-1})P(y_k|x_k)\},\\ &= \max_{\hat{x}_{0:T}}\{\frac{1}{P(y_{0:T})}P(x_{0:T}, y_{0:T})\},\\ &= \max_{\hat{x}_{0:T}}\{P(x_{0:T}, y_{0:T})\},\end{aligned} \tag{2.12}$$

  where

$$P(x_{0:T}, y_{0:T}) = P(x_0)P(y_0|x_0)\prod_{k=1}^{T}P(x_k|x_{k-1})P(y_k|x_k) \tag{2.13}$$

  Note that the term $\frac{1}{P(y_{0:T})}$ in Eq. (2.12) is independent of the decision variables, $x_{0:T}$, and it has been neglected.

- **Lemma 2.** $\max_{\hat{x}_{0:T}}\{P(x_{0:T}, y_{0:T})\} = \min_{\hat{x}_{0:T}}\{-\log P(x_{0:T}, y_{0:T})\}$.

If we define $J_T = -\log P(x_{0:T}, y_{0:T})$, the optimization problem of Eq. (2.3) can be posed as

$$\min_{\hat{x}_{0:T}}\{J_T\} : J_T = -\log P(x_{0:T}|y_{0:T}). \tag{2.14}$$

By taking the log probability of Eq. (2.13), we have

$$\log P(x_{0:T}, y_{0:T}) = \log P(x_0) + \sum_{k=1}^{T} \log P(x_k|x_{k-1}) + \sum_{k=0}^{T} \log P(y_k|x_k). \tag{2.15}$$

Substituting Eq.(2.15) into the Eq. (2.14), we have

$$\min_{\{\hat{x}_{0:T}\}} J_T : \quad J_T = -\log P(x_0) - \sum_{k=1}^{T} \log P(x_k|x_{k-1}) - \sum_{k=0}^{T} \log P(y_k|x_k). \tag{2.16}$$

Assuming Gaussian distributions, $P(x_0)$, $P(x_k|x_{k-1})$ and $P(y_k|x_k)$ can be respectively formulated as

$$\begin{aligned}
&P(x_0) = (2\pi)^{-\frac{n}{2}} P_{-1}^{-\frac{1}{2}} exp\{-\frac{1}{2}(x_0 - \bar{x}_{-1})P_{-1}^{-1}(x_0 - \bar{x}_{-1})\} \\
&P(x_k|x_{k-1}) = (2\pi)^{-\frac{n}{2}} Q_k^{-\frac{1}{2}} exp\{-\frac{1}{2}(x_k - f(x_{k-1}, u_{k-1}; \theta))Q_k^{-1}(x_k - f(x_{k-1}, u_{k-1}; \theta))\}, \\
&P(y_k|x_k) = (2\pi)^{-\frac{q}{2}} R_k^{-\frac{1}{2}} exp\{-\frac{1}{2}(y_k - g(x_k; \beta))R_k^{-1}(y_k - g(x_k; \beta))\},
\end{aligned} \tag{2.17}$$

$P_k \in \mathbb{R}^{n\times n}$, $Q_k \in \mathbb{R}^{n\times n}$, and $R_k \in \mathbb{R}^{n\times q}$ are symmetric positive definite weighting matrices. They are quantitative measurements of the belief in the prior estimate, state transition model, and the observation equation respectively. If we define $\hat{w}_{-1} := (\hat{x}_0 - \bar{x})$; $\hat{v}_k := y_k - g(\hat{x}_k; \beta)$, and $\hat{w}_{k-1} := \hat{x}_k - f(\hat{x}_{k-1}, u_{k-1}; \theta)$, we can further take the negative logarithms of Eq. (2.17) to give

$$\begin{aligned}
-\log P(x_0) &= K_0 + \frac{1}{2}\hat{w}_{-1}P_0^{-1}\hat{w}_{-1}, \\
-\log P(x_k|x_{k-1}) &= K_w + \frac{1}{2}\hat{w}_{k-1}Q_k^{-1}\hat{w}_{k-1}, \\
-\log P(y_k|x_k) &= K_v + \frac{1}{2}\hat{v}_k R_k^{-1}\hat{v}_k,
\end{aligned} \tag{2.18}$$

where $K_0 = -\log\{(2\pi)^{-\frac{n}{2}} P_{-1}^{-\frac{1}{2}}\}$, $K_w = -\log\{(2\pi)^{-\frac{n}{2}} Q_k^{-\frac{1}{2}}\}$, and $K_v = -\log\{(2\pi)^{-\frac{q}{2}} R_{-1}^{-\frac{1}{2}}\}$. By substituting Eq. (2.18) into the Eq. (2.16), while the constants K_0, K_w, and K_v are neglected, the state estimation problem can be constructed as an optimization problem by estimating $\hat{w}_k$ that minimizes as

$$\min_{\{\hat{w}_{-1},\ldots,\hat{w}_{T-1}\}} J_T : \quad J_T = \hat{w}_{-1}^T P_{-1}^{-1}\hat{w}_{-1} + \sum_{k=0}^{T-1} \hat{w}_k^T Q_k^{-1}\hat{w}_k + \sum_{k=0}^{T} \hat{v}_k^T R_k^{-1}\hat{v}_k \tag{2.19}$$

subject to

$$\begin{aligned}
&\hat{x}_0 = \bar{x}_{-1} + \hat{w}_{-1}, \\
&\hat{x}_k = f(\hat{x}_{k-1}, u_{k-1}; \theta) + \hat{w}_k, \quad k = 1, \ldots, T-1, \\
&\hat{y}_k = g_(\hat{x}_k; \beta), \\
&\hat{v}_k = y_k - \hat{y}_k, \\
&\hat{x} \in \mathbb{X}, \quad \hat{w} \in \mathbb{W} \quad \textit{and} \quad \hat{v} \in \mathbb{V}.
\end{aligned} \tag{2.20}$$

The estimated states from time $k = 0 : T$ are evaluated from

$$\begin{aligned} \hat{x}_0 &= \bar{x}_{-1} + \hat{w}_{-1}^{opt}, \\ \hat{x}_k &= f(\hat{x}_{k-1}, u_{k-1}; \theta) + \hat{w}_k^{opt}, \quad k = 1, ..., T-1, \\ \hat{y}_k &= g_(\hat{x}_k; \beta). \end{aligned} \tag{2.21}$$

The problem with a batch estimation formulation is that its solution becomes computationally intractable even for a small system because the optimization problem to solve grows rapidly with every time step. This computational burden will make it practically difficult if not impossible to make use of a batch state estimation in various process monitoring and control schemes where an online implementation is a necessity. It is therefore obvious that different optimality criteria will have to be sought based on different factors such as the area of application, method of implementations, desired level of accuracy and the computational feasibility.

2.2.5 Moving horizon estimation

Moving horizon estimation (MHE) is one of the most efficient optimization-based approaches to state estimation. It is a technique in which a sequence of unknown states or parameters is estimated based on a weighted least squares cost function over a moving but fixed-size window called horizon. The concept of MHE approach was originally proposed to overcome the limitations of the widely used Kalman filter, which are its inability to incorporate constraints on state, approximating a nonlinear model with a linear model, and the assumptions of Gaussian disturbances.

The basic strategy is to use a moving, but fixed-size window of the observed data to estimate the sequence of states. As shown in Figure 2.3, at every time instance, a new available measurement is added to the window of data, while the oldest observed measurement is removed. The effect of the discarded data on the current states is summarized in what is termed as *arrival cost*. Instead of estimating a single point like in other estimation methods, by denoting the state over horizon length $N \in \mathbb{N}^+$ as $x_{T-N:T}$, the MHE provides the estimate sequence, $\hat{x}_{T-N+1:T}$, through a constrained optimization:

$$\max_{\hat{x}_{T-N:T}} \{P(x_{T-N:T}, y_{0:T})\}. \tag{2.22}$$

This formulation can take constraints into account explicitly, and shape the estimates to form different distributions other than the Gaussian distribution by constraining the disturbances. The arrival cost information of a horizon may be propagated to the subsequent horizon by updating the joint probability density function $P(x_{T-N}, y_{0:T})$.

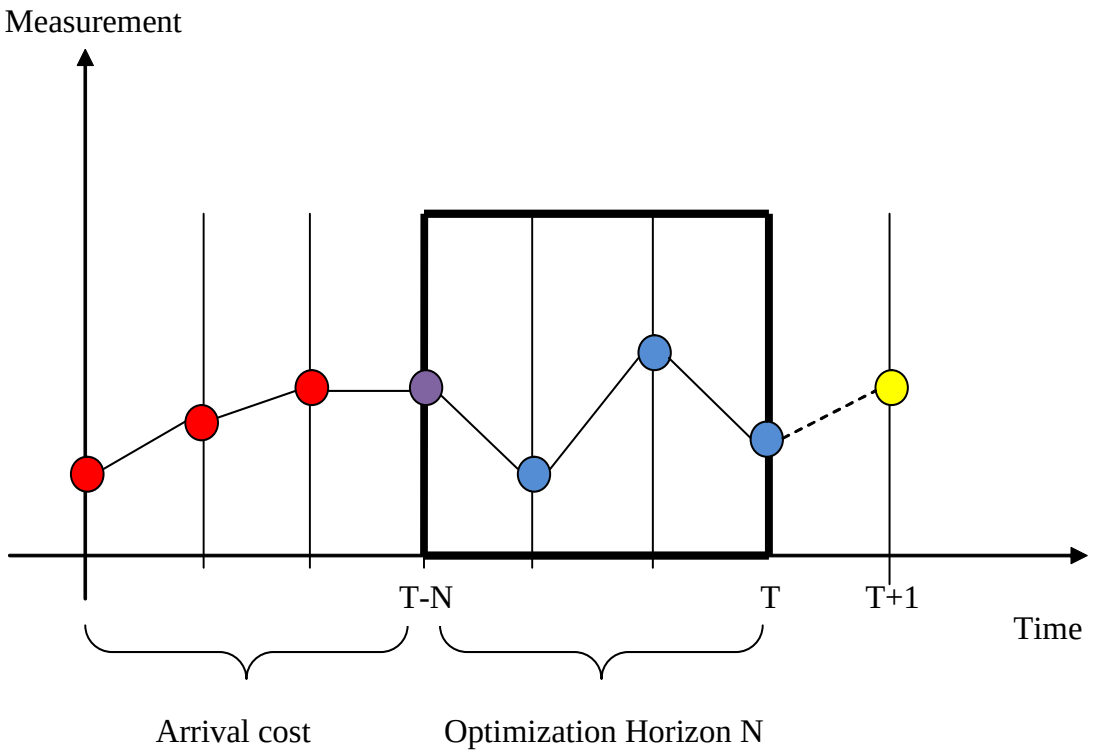

Figure 2.3: Moving horizon scheme.

MHE Review

The idea of moving horizon strategies in state estimation can be traced back to the various works reported from late 60s to early 70s [46, 54, 88]. Since then, significant research works, which spans well over three decades, have surfaced in the literature that discussed the MHE formulation, stability, convergence, robustness, and applications. Findeisen (1997) [27] and Rao (2000) [71] provided a well summarized literature works on a moving horizon estimation method.

The formulation of MHE using a least square methods was given by Muske and Rawlings (1993) [61], while Robertson (1996) [76] discussed MHE development from a probabilistic point of view. Several studies have provided stability proofs for MHE schemes on linear systems [27, 77, 72] as well as nonlinear systems [73]. Rao et al. (2002) [72] investigated the moving horizon approximation for the constrained process monitoring and showed that constrained MHE is an asymptotically stable observer in a nonlinear modeling framework. Rao, et. al. (2002)[72] also presented different arrival costs development options for MHE and discussed their impacts on the stability of moving horizon state estimation with linear models subject to constraints on the estimate.

Convergence and computational time issues in a moving horizon estimation are addressed in the works of [72, 56, 99, 100]. The performances of MHE were compared

to other types of filters [37, 86]. Specifically, Haseltine and Rawlings (2005)[37] critically compared the performance of MHE to an extended Kalman filter(EKF) and concluded that MHE consistently provides improved state estimation and greater robustness to both poor guesses of the initial state and tuning parameters in comparison to the EKF.

Application of a moving horizon estimation to industrial processes have also been studied extensively [81, 52, 89, 97, 98, 86]. Russo and Young (1999) [81] applied a moving horizon estimation to an industrial polymerization process, while Kraus, et. al. (2006) [52] applied a moving horizon state estimation algorithm to the Tennessee Eastman Benchmark process. Gallivan (2007) [97] applied a moving horizon estimation (MHE) technique to estimate thin film growth rate, thickness, and high temperature optical constants in situ monitoring of chemical vapor deposition process. MHE algorithm is shown to provide a better performance in parameters and state estimation of an industrial process fouling than an extended Kalman filter in the work of [86].

MHE formulation

The formulation of a moving horizon estimation from both deterministic and probabilistic point of views is detailed in the literature [61, 71, 72]. Because the objective function for the batch optimization will become computationally expensive and numerically intractable as the T increases, the optimization objective function for a moving horizon estimation method is formulated for a finite horizon length N as:

$$\min_{\{\hat{w}_{T-N-1},\ldots,\hat{w}_{T-1}\}} J_T : \quad J_T = \hat{w}_{T-N-1}^T P_{T-N-1}^{-1} \hat{w}_{T-N-1} + \sum_{k=T-N}^{T-1} \hat{w}_k^T Q_k^{-1} \hat{w}_k + \sum_{k=T-N}^{T} \hat{v}_k^T R_k^{-1} \hat{v}_k, \tag{2.23}$$

subject to

$$\begin{aligned} &\hat{x}_0 = \bar{x}_{-1} + \hat{w}_{T-N-1}, \\ &\hat{x}_k = f(\hat{x}_{k-1}, u_{k-1}; \theta) + \hat{w}_k, \quad k = T-N+1, \ldots, T-1, \\ &\hat{y}_k = g_(\hat{x}_k; \beta), \quad k = T-N+1, \ldots, T-1, \\ &\hat{v}_k = y_k - \hat{y}_k, \quad k = T-N+1, \ldots, T-1, \\ &\hat{x} \in \mathbb{X}, \quad \hat{w} \in \mathbb{W} \quad and \quad \hat{v} \in \mathbb{V} \end{aligned} \tag{2.24}$$

and, the estimated states from time $k = T-N : T$ are evaluated as

$$\begin{aligned} &\hat{x}_{T-N} = \bar{x}_{-1} + \hat{w}_{T-N-1}^{opt}, \\ &\hat{x}_k = f(\hat{x}_{k-1}, u_{k-1}; \theta) + \hat{w}_k^{opt}, \quad k = T-N+1, \ldots, T, \\ &\hat{y}_k = g_(\hat{x}_k; \beta), \quad k = T-N+1, \ldots, T. \end{aligned} \tag{2.25}$$

Note that the first term of Eq. (2.23) represents the arrival cost. The expression in Eq. (2.25) computes the smoothed estimates, $\hat{x}_{T-N:T-1}$, for $k = T-N : T-1$, and

a filtered estimate, $\hat{x}_T$, at the current time $k = T$. When $N = 0$, the MHE objective function reduces to

$$\min_{\hat{w}_{T-1}} J: \quad J_T = \hat{w}_{T-1}^T P_{T-1}^{-1} \hat{w}_{T-1} + \hat{v}_k^T R_k^{-1} \hat{v}_k. \tag{2.26}$$

For a stochastic unconstrained linear system, it is established [72] that when w_k and v_k are independent, zero mean, normally distributed random variables, the solution of Eq. (2.26) is a discrete Kalman filter, which is the optimum or minimum variance estimate of the state.

2.3 Noncontinuum State Estimation

Existing studies on state estimation have almost exclusively been devoted to a continuous-valued system with very few exceptions. In reality, the problem to solve in a system, can also take a discrete-event or noncontinuum forms. Typical examples of noncontinuum form representation problems are stiction versus non-stiction of control valves, multi-mode process operations, and normal versus abnormal conditions in fault detection diagnosis [55]. Even for continuous dynamic systems, the problem to solve may still take a noncontinuum representation such as "desired" or "undesired" operating region, and "good", "bad", or "optimum" in control performance assessment problems. Noncontinuum state also plays a key role in embedded control systems that interact with the physical world. Therefore noncontinuum state estimation deals with the estimation of the discrete-event states (i.e., system mode) from the available measurement data.

The state transition of a switching system can be captured by a Hidden Markov Model (HMM)[29], and the noncontinuum state estimation problem in such system can be posed as an optimization problem in which the set of decision variables takes only a finite set of possible values. Park and Miller (1997) [66] developed an algorithm for realizing optimal maximum a posterior (MAP) estimates of the hidden states associated with a hidden Markov model, given a sequence of observed symbols. Ghahramani (1999) [34] presented a unifying review of linear Gaussian models and shown how the factor analysis, principal component analysis, mixtures of Gaussian clusters, vector quantization, Kalman filter models, and hidden Markov models can all be unified as variations of unsupervised learning under a single basic generative model. In their work, the forward-backward algorithm is used to compute the posterior probabilities of the hidden states in a HMM and therefore formed the basis of the inference required for EM [34].

Doucet and Andrieu (2001) [21] presented both the deterministic and stochastic iterative algorithms for optimal state estimation of jump Markov linear systems. Their algorithms are formulated to obtain the marginal maximum a poste-

riori (MMAP) sequence estimate of the finite state Markov chain. Active mode estimation of switching systems in stochastic set up was studied by Hofbaur and Williams (2002) [38]. The observability and identifiability of a jump linear system are addressed by Vidal, et. al. (2002) [93] and in more recent time, by Baglietto, et. al. [6, 7].

Goodwin and Quevedo (2003) [35] proposed a receding horizon optimization approach for a system where the control input is limited to a small and finite set of scalars and the initial condition is to be estimated. This noncontinuum input optimization approach, which is termed a finite alphabet problem, does not consider time-varying parameter systems neither do switching systems. However, it provides semi-definite programming relaxation methods to yield approximate solutions for receding horizon combinatorial optimization problems. Goodwin and Quevedo (2005) [36] extended their work to include a moving horizon design for discrete coefficient FIR filters.

Schon, et al. (2003) [82] formulated the state estimation problem of HMM in a convex optimization framework. Using a mean square criterium, this approach is shown to be better than formulating HMM in a state space model and employed a Kalman filter algorithm to compute the best possible linear estimate of the Markov states. Domlan (2007) [20] studied the determination of the active mode of switching deterministic systems using only the system's input-output data, and derived the discernability conditions that ensure the uniqueness of the recovered mode. A nonlinear Luenberger hybrid observer for a class of repetitive operation mode process was studied by Aguilar-Lopez and Martinez-Guerra (2007) [1]. The observer was successfully applied to a sequencing batch reactor.

Blackmore and Rajamanoharan [15] designed finite sequences of control inputs that reduce the probability of pruning the true mode sequence while ensuring that a given control task is achieved. The key innovation was to derive a tractable upper bound on the probability of pruning the true mode sequence. Evans and Krishnamurthy (2001) [24] addressed optimal sensor scheduling problems for finite-state hidden Markov models using a stochastic dynamic programming framework. A cost function of estimation errors and measurement costs are minimized to select an optimum measurement scheduling policy.

In the Chapter 3 of the thesis, we will focus exclusively on the development of a noncontinuum state estimator, which is based on a moving horizon approach for switching systems that follow a HMM with either a discrete- or continuous-valued noisy measurements. We will propose a new arrival cost for a moving horizon estimation of noncontinuum state to summarize the effects of the past observed data on the estimation of the states in the current horizon window.

2.4 Continuum and Noncontinuum States Estimation

2.4.1 Hybrid system

The term hybrid is generally used to represent the coexistence of a continuous subsystem (i.e., describing a continuous-valued dynamics) and a discrete subsystem (i.e., describing discrete-valued dynamics), while the concept of a hybrid dynamical system represents a dynamical system where the behavior of interest is governed by the interacting continuous and discrete dynamics. A hybrid system generates mixed states, some of which take values from a continuous set (e.g., the set of real numbers) and are termed *continuum states*, while others take values from a discrete set (e.g., the set of symbols) and are referred to as *noncontinuum states*. Furthermore, these continuum or noncontinuum states usually depend on one or more independent variables such as time. In some other cases, some of the signals from a hybrid system could be time-driven while others could be event-driven.

Over the past few decades, there have been significant research interests in hybrid systems and their applications cutting across mathematics, control engineering, and computer science. A detailed summary of the recent work on the development, modeling, and application of a hybrid system can be found in the work of Antsklis (2000) [5].

The behavior of a hybrid dynamic system may be described via different models. The complexity of modeling a hybrid system is largely dependent on the level of interaction between the coexisting continuum and noncontinuum dynamics. Thus, the nature of a hybrid model considered depends on what the model is intended to be used for. In this thesis, we consider two general forms of dynamic modeling, which are the state space model described by differential or difference equation to represent continuum state, and a Hidden Markov Model (HMM) described by state transition probabilities to represent noncontinuum state. Therefore, the hybrid system of the following dynamic stochastic models

$$\begin{aligned} &m_k = \eta(m_{k-1}; \lambda), \\ &x_k = f_{m_k}\{x_{k-1}, u_{k-1}; \theta\} + w_{k-1}, \\ &y_k = g_{m_k}(x_k; \beta) + v_k, \\ &m_k \in \mathbb{M}: \quad \mathbb{M} = \{1, ..., M\}, \end{aligned} \tag{2.27}$$

are considered. m_k is noncontinuum state governed by a hidden Markov model, η and λ represent the noncontinuum transition function and the HMM parameter respectively.

2.4.2 Hybrid state estimation

State estimation of a hybrid system is a significant and challenging problem for process monitoring[16, 40], feedback control[8, 58, 23], and model-based fault diagnosis and isolation[12]. There are basically two approaches (i.e., sequential and simultaneous) to a hybrid state estimation development. Sequential approach is a method in which two separate algorithms are combined interactively to estimate both the continuum and noncontinuum states. One distinct feature of this method is the requirement to involve two filters or two objective functions (in the case of optimization based filters), one to estimate the continuum state, while the other to estimate the noncontinuum state [8, 17].

Most of the hybrid state estimation methods that exist in the literature use sequential approach largely because it is intuitively the easier of the two approaches to develop or formulate. Besides, combination of different types of filters can be tried to achieve one form of improvement or the other. However, the major setback of this method is the interaction effects of two filters, especially if there are other external constraints desired to be satisfied by the system [72]. Besides, a hybrid state estimation that uses such an approach often poses different implementation challenges. Another approach to a hybrid state estimation development is called a simultaneous approach, in which a single filter with a single objective function is formulated to simultaneously estimate both the continuum and noncontinuum states. The development of such a filter is non trivial, but it has the advantage of addressing a hybrid state estimation problem in a unified and systematic way. Even though, a majority of research work have concentrated on the continuum state estimation developments and applications, quite a sizable number of works has appeared in the literature that discussed the state estimation problems of hybrid systems.

Alessandri and Coletta (2001, 2003)[3, 4] considered an estimation approach based on Luenberger-like observers for a class of switched continuous and discrete time linear systems with a known operation mode. Boker and Lunze (2002) [17] proposed switching Kalman filters for switched affine systems, where a set of Kalman filters is designed for each dynamics of the hybrid system. An estimation method of combining location observers with Luengerger observers based on known discrete input and output was studied by Balluchi et al. (2003) [8], while Hofbaur and Williams (2004) [39] developed a method based on banks of extended Kalman filters, which only focused on the set of most likely modes. Boers and Driessen (2002) [16] numerically solved an hybrid state estimation problem using the particle filter approach.

The design and stability analysis of hybrid nonlinear control systems for a class

of switched nonlinear systems have also been extensively studied in the literature[23, 58]. El-Farra at. al (2005) [23] addressed nonlinear and constrained control system of switched systems. In their work, a deterministic high gain observer was developed for estimation of unconstrained states. A predictive control framework for the constrained stabilization of switched nonlinear systems was proposed by Mhaskar at. al (2005) [58]. The key achievement in this work is the design of a Lyaounov-based model predictive controller (MPC) that guarantees the stability of the switched closed-loop system. In one of the most recent studies in hybrid state estimation application in control system design and implementation, Hu and El-Farra (2010) [40] explored a technique for fault detection and monitoring of nonlinear hybrid systems with control actuator faults and uncertain mode transitions. The proposed mode observers, which work sequentially with the Lyapunov-based fault detector schemes, are able to identify the active mode without information from the controllers.

A state estimation method, which is based on moving horizon estimation (MHE) scheme is able to overcome most of the existing challenges on state estimation problems because it estimates the desired variables over a finite horizon of time [61, 72]. MHE approach has been employed in the literature for state estimation of hybrid systems. Bemporad et. al. (1999) [12] explored the ideas of receding horizon control to the state estimation and fault detection problem of hybrid systems. Ferrari-Trecate, et al. (2000, 2002) [25, 26] investigated state-estimation for hybrid systems in the mixed logical dynamical (MLD) form and proposed a state-smoothing algorithm for hybrid systems based on moving-horizon estimation (MHE). Sufficient conditions to guarantee asymptotic convergence of the MHE were given. [67] extended MHE method to simultaneous estimation of state and unknown input for hybrid linear systems.

Rowe and Maciejowski (2003) [78] developed a strategy for a min-max moving horizon estimation of a class of uncertain Piecewise Affine systems (PWA) with both continuous valued and logic components. Their work is an extension of the MHE scheme for PWA systems, but without plant uncertainties, as presented in the work of Ferrari-Trecate, et al. (2001, 2003) [25, 26]. Sufficient conditions that guarantee convergence of the MHE scheme on hybrid systems were analyzed. Pina and Botto (2006) [67] extended MHE method to simultaneous estimation of state and unknown input for hybrid linear systems. The MHE method can simultaneously estimate the state and the mode of the system and it is based on a moving fixed-size estimation window, which bounds the size of the optimization problem. In a more recent study, Alessandri, et. al. (2007) [2] used a receding-horizon approach for the estimation of the system mode according to a minimum-distance. In this case, the system and measurement equations of each mode are assumed to be linear and perfectly known, but the current mode of the system is unknown and is regarded as a discrete state

to be estimated at each time instant together with the continuous state vector.

2.4.3 Generalized Bayesian hybrid state estimation

Bayesian formulation of the estimation problem suggests a general solution for all types of systems including linear or nonlinear dynamics, Gaussian or non-Gaussian distributions, bias, constraints, and missing or multirate data [30, 18, 19]. State-estimation methodology which is based on Bayesian framework is powerful because they are rigorously based on the probability axioms and therefore preserve information [92]. Besides, they give the probability density function of the model state conditioned on the available information, which may then be used for any probability-based process monitoring, identification, and reliability analysis.

For simplicity, let us use z_k to denote x_k or m_k or their combination $\{x_k, m_k\}$. By denoting $z_{0:T} = \{z_1, ...z_k, ...z_T\}$, the logarithm of the joint probability mass function (i.e., for noncontinuum state) or joint probability density function (i.e., for continuum state) can be written as:

$$\log P(z_{0:T}, y_{0:T}) = \log P(z_0) + \sum_{k=1}^{T} \log P(z_k|z_{k-1}) + \sum_{k=1}^{T} \log P(y_k|z_k). \tag{2.28}$$

If $z_{0:T}$ is continuum, following the general solution procedure described in Section 2.2.5, the continuum MHE solution provided by Rao and Rawlings (2002) [72] can be adopted. If however, $z_{0:T}$ is noncontinuum, under stationarity and hidden Markov model assumptions, we derive the state estimate sequence by minimizing the negative logarithm form of the joint probability $P(z_{0:T}, y_{0:T})$ subject to constraints on input, output, or state, using the maximum a posteriori estimate based on the measurements $y_{0:T}$. If $z_{0:T}$ is a mixture of continuum and noncontinuum states, i.e. $z_{0:T} = \{x_{0:T}, m_{0:T}\}$, one can use the joint probability density function $P(x_{0:T}, m_{0:T})$ to represent the distribution of mixed continuum and noncontinuum states. As we will show in the next chapters, the problem is solved by obtaining the joint distribution of continuum state and noncontinuum state as a summation of logarithm of marginal densities.

2.5 Distillation Processes

Distillation is defined as a process in which liquid or vapor mixture of two or more substances is separated into its component fractions of desired purity, by the application and removal of heat. Distillation is based on the fact that the vapor of a boiling mixture will be richer in the components that have lower boiling points, therefore when this vapor is cooled and condensed, the condensate will contain more volatile components. At the same time, the original mixture will contain more of the

less volatile material. There are many types of distillation column, each designed to perform specific types of separation, and each differs in terms of complexity.

1. **Batch distillation column:** In batch operation, the feed to the column is introduced batch-wise. The column is charged with a 'batch' and then the distillation process is carried out. When the desired task is achieved, a next batch of feed is introduced.

2. **Continuous distillation column:** In contrast to batch distillation, a continuous distillation column processes a continuous feed stream. No interruptions occur unless there is a problem with the column or surrounding process unit. They are capable of handling high throughputs, and they can either design as a tray column or as a packed column.

3. **Binary distillation column:** Feed contains only two components.

4. **Multi-component distillation column:** Feed contains more than two components.

5. **Tray distillation column (internal):** Trays of various designs are used to hold up the liquid to provide better contract between vapor and liquid

6. **Packed distillation column:** Instead of trays, 'packings' are used to enhance contact between vapor and liquid.

The distillation column is made up of several components, each of which is used either to transfer heat energy or enhance material transfer. A typical distillation contains several major components, which are:

- A vertical column where the separation of fluid components is carried out.
- Column internals such as trays or packings, which are used to enhance components separation.
- A reboiler to provide the necessary vaporization for the distillation process.
- A condenser to cool and condense the vapor leaving the top of the column.
- A reflux drums to hold the condensed liquid from the top of the column so that reflux can be recycle back to the column.

2.5.1 State estimation in distillation processes

The development and application of state estimation to distillation processes have a long history in the literature. After the pioneering work of Joseph and Brosilow (1978) [48] who applied optimal estimators to a multicomponent distillation column, several studies have been devoted to the development of estimators for both batch [62, 69] and continuous distillation columns [9, 10, 53, 80]. Lang and Gilles (1991) [53] developed a full-order nonlinear observer for distillation columns. The performance of the observer was tested through numerical simulation and it was found to be very robust toward model errors, wrong parameters and uncertain inputs.

Quintero-Marmol et al.(1991) [69] applied an extended Luenberger observer (ELO) to predict composition in multicomponent batch distillation from temperature measurements, while Ruokang et al. (1991) [80] presented a strategy for fault detection and diagnosis in a closed-loop nonlinear distillation system using an extended Kalman filter. Oisiovici et al. (2000) [62] developed a discrete extended Kalman filter (DEKF) for binary and multicomponent distillation systems. The developed DEKF algorithm provides reliable and real-time column composition profiles from few temperature measurements. Unlike off-line design of the extended Luenberger observer proposed by Quintero-Marmol et al. (1991) [69], the gains of DEKF are calculated and updated online. State estimation techniques have also been recently extended to determine the unmeasurable composition profiles in a more complex reactive distillation column [59, 63].

Among several studies on the application of state estimation to distillation processes, only a few papers tested their results using actual experimental data [9, 10, 57]. Mejdell and Skogestad (1999) [57] implemented a static partial least-square regression estimator for product compositions on a high-purity pilot-plant distillation column. An experimentally based estimator, with logarithmically transformed temperatures and compositions, was reported to give excellent performance over a wide range of operating points. Baratti et al. (1995) [9] developed a nonlinear extended Kalman filter (EKF), which predicts the composition of the outlet streams of a binary distillation column from the temperature measurements. The performance of the estimator was evaluated by comparison with data obtained from the several transient experiments performed in a pilot plant. The EKF estimator was found to be robust with respect to model errors. They extended their work to the multicomponent distillation column and concluded that a more rigorous vapor-liquid equilibrium description is required for composition estimation in multicomponent system [10].

The handful state estimation techniques developed and verified experimentally [9, 10, 57] are limited to the estimation of the column composition as continuum

states. However, due to the advancement in the simultaneous process monitoring, fault detection and control of complex chemical systems such as distillation columns, there is need to experimentally investigate the practical reliability of advanced filters such as hybrid state estimators where the interest will not only be in estimating the process states, but also in the determining the operating mode, detecting the fault in the system and estimating uncertain disturbance inputs simultaneously.

2.5.2 Hybrid state estimation in distillation process with switching dynamics

In a typical industrial distillation process, the state estimation problems to solve often involve the continuum state, noncontinuum state or the combination of both. A common example of continuum state estimation problem is the column composition estimation using the online state observer, while a typical example of noncontinuum form representation of interest is to determine if there is a change (either desirably or undesirably) in the operating mode of a distillation process.

Using several illustrating examples, Jacobsen and Skogestad (1994) [45] showed that two-product distillation columns, operating with reflux and boilup as independent inputs, might have multiple steady-state solutions, even in the ideal binary case. The issue of steady state multiplicities has also been widely reported in reactive distillation processes [87]. A hybrid state estimator, which has the capability to estimate unmeasurable states under switching operating modes, will provide new direction in achieving a more effective monitoring of such unstable distillation processes.

Besides, the operational procedure of a typical industrial distillation process involves switching from one mode into the other, notably from the start-up to the steady-state operation, and to the process shut-down. Under the distillation start-up operation, the determination of an optimum switching time from one operating mode into the other will be a key factor to energy consumption minimization [31]. Other forms of undesirable mode changes are also common in distillation operation. Common examples are operational mode changes due to system malfunctions (i.e., fault) as well as feed input quality change, which is usually being dictated from the upstream [64].

With several other evidences of an industrially operated distillation column exhibiting unstable operating regions [44, 45, 51], the development of advanced filters for distillation processes modeled as hybrid systems will help to address some of the outstanding process monitoring problems such as simultaneous composition estimation, operational mode change determination, fault detection and isolation [80], as well as unknown disturbance input estimation in a unified and systematic way.

Chapter 3

Online Composition Estimation and Experiment Validation of Distillation Processes with Switching Dynamics

3.1 Introduction

[1] This chapter explores both the theoretical and experimental investigations of applying a sequential continuum and noncontinuum state estimator to composition estimation in a distillation process with switching dynamics. At present, the most widely used approximate nonlinear filter in the process monitoring and control of distillation columns is the extended Kalman filters (EKF) [9, 10, 62]. However, it has the disadvantage that the covariance propagation and update are carried out through linearization around some operating regions, and this suggests that the region of stability may be small since nonlinearities in the system dynamics are not fully accounted for. Therefore, it is necessary to investigate new and more advanced nonlinear filters and demonstrate their practical reliability by conducting both the theoretical and experimental investigations on an industrial-type distillation column.

Apart from EKF, other advanced observers (i.e., geometric observers, particle filtering, a moving horizon estimation) have been proposed in the literature. However, a composition estimation problem in a distillation process will require a state observer that can handle system constraints. A moving horizon estimation (MHE) approach is known for its ability to handle constraints on state and parameter estimates. This is particularly needed when designing an observer for a distillation process where the composition (to be estimated) is bounded.

This study aims at developing a sequential continuum and noncontinuum state

1. *This chapter has been published as "M.J. Olanrewaju, B. Huang, and A. Afacan. Online composition estimation and experiment validation of distillation processes with switching dynamics. Chem. Eng. Sci., 2010, 65: 1597-1608."*

estimator for composition estimation in the distillation processes under switching dynamics by using the available temperature measurements. For state estimation purposes, a distillation process will be modeled as a hybrid nonlinear system with column composition as continuum states and operating modes as noncontinuum states. A sequential hybrid moving horizon estimator (SHMHE) is developed for both continuum and noncontinuum states estimation. The performance of SHMHE will be compared to that of an extended Kalman filter in handling distillation process with switching dynamics, physical constraints, measurement noise and plant-model mismatch. For some situations where the system operating mode transition is unknown (i.e., occurs unexpectedly), a new approach to hybrid state estimation under unknown operating mode transition function is proposed and verified by conducting both the simulation on a batch distillation and experiment on a continuous distillation process.

3.2 Hybrid Distillation Process Modeling

A rigorous dynamic model for a typical distillation column shown in Figure 3.1 consists of a large number of nonlinear differential equations and demands much information such as system compositions, vapor and liquid flow rates, liquid hold up in all stages at every instant, tray hydraulics, energy balances and vapor-liquid equilibrium data. However, modeling distillation process as a hybrid nonlinear system depends largely on a particular problem to address and the factors that cause changes in system operating modes. Different scenarios under which a distillation model can be modeled as a hybrid system as well as the system's variables that can be represented as noncontinuum states are highlighted as follows:

- **Scenario 1:** Change in operating modes due to different scheduled industrial operational procedures. Common examples are:

    1. The change in distillation dynamics due to the scheduled operation from "the start-up" to "steady-state operation", and to "shut-down". The system variables that can be modeled as noncontinuum states to achieve such a task are switch in reflux ratio (RR), reflux flow rate (R) distillate flow rate (D), bottoms flow rate (B) and vapor boilup (V).
    2. The switching of operating pressure (P_i) in azeotropic distillation processes [11].

- **Scenario 2:** Steady state multiplicity and the existence of instability regions with respect to the manipulated input variables transformation in distillation processes [44, 45, 51]. Jacobsen and Skogestad (1991,1994) [44, 45] reported

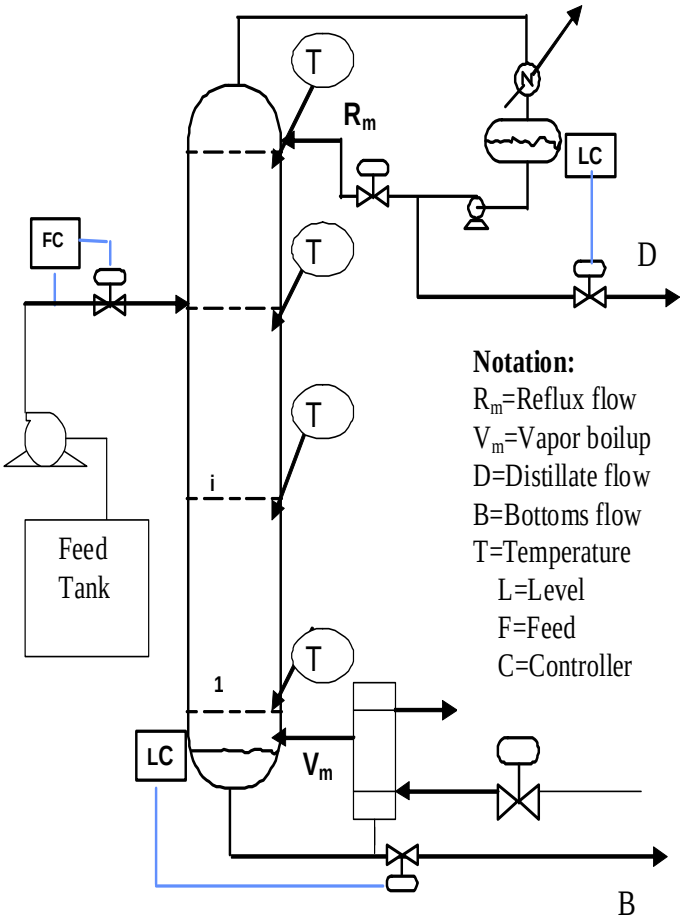

Figure 3.1: A pilot-scale distillation column.

the existence of multiple steady state solutions corresponding to different operating regions for mass or volume input flows (i.e., R and V).

- **Scenario 3:** An unexpected switch in operating modes due to unknown input disturbances from the feed flow rate (F) and feed composition (z) as well as change in the tray efficiency (E_{mv}) due to fouling for instance [45].

- **Scenario 4:** Operating mode changes due to system faults and malfunctions [80]. It will be difficult to achieve a predefined set of reliable modes for a partial fault or malfunction in a system. However, with respect to determining whether the system is operating at normal operating mode, or is at a total fault, it is possible to use past system data to predefine the modes. For instance, the operator might just be interested in quantifying, for instance, input reflux ratio (RR) and heat duty (Q_R) as "too high", "too low" or "normal".

In summary, we have laid out different scenarios under which a distillation process can be modeled as a hybrid system. However, we make no claims that all of

these scenarios listed are addressed in this work. Specifically, change in operating mode due to disturbance inputs is not addressed in this work.

The hybrid nonlinear model of distillation processes can be summarized as follows:

$$\begin{aligned} &\frac{dx_{i,j}}{dt} = f_m(x_{i,j}, y_{i,j}, V_m, R_m, F_m, z_m, E_{mv}; \theta), \\ &Y_i = g_m(x_{i,j}; \beta), \\ &0 \leq x_{i,j} \leq 1, \\ &m \in \mathbb{M}: \quad \mathbb{M} = \{1, ..., M\} \quad i = \{1, ..., N_s\}, \quad j = \{1, ..., Nc - 1\}, \end{aligned} \tag{3.1}$$

By defining the following new variables:

$$\begin{aligned} &X := \{x_{i,j}\}, \quad i = \{1, ..., N\}, \quad j = \{1, ..., Nc - 1\}, \\ &u := \{V_m, R_m, D_m, B_m, F_m, z_m, E_{mv}\}, \end{aligned} \tag{3.2}$$

and by selecting a suitable sampling time, the hybrid dynamic model of a distillation process can be discretized and expressed in a more compact state space equation of the form:

$$\begin{aligned} &m_k = \eta(m_{k-1}, u_{k-1}), \\ &X_{k+1} = f_{m_k}(X_k, u_k; \theta) + w_k, \\ &Y_k = g_{m_k}(X_k; \beta) + v_k, \\ &X \in \mathbb{X}, \quad w \in \mathbb{W}, \quad m \in \mathbb{M}, \end{aligned} \tag{3.3}$$

where X, the liquid composition in the column, represents the continuum state of the system and $m \in \mathbb{M}$, the system operating modes, represents the noncontinuum states. N_s is the total number of column stages including a reboiler and a condenser, N_c represents the number of components to be separated. $y_{i,j}$ is the vapor composition of component j on a stage i, while θ and β are system parameters. m_k is the operating mode at time k, while η is an unknown mode transition function. Y_k represents the noisy output measurements at time k. $w_k \sim N(0, \delta_w^2)$ and $v_k \sim N(0, \delta_v^2)$ are additive process noise and measurement noise respectively.

Modeling a distillation process as a hybrid system will help to address some of the outstanding process monitoring problems such as simultaneous composition estimation, fault detection through operating mode determination as well as unmeasurable disturbance input estimation in a unified and systematic way. If a distillation system operating mode is known, a conventional state estimator can be developed to infer the column composition profiles from the available temperature measurements. In a situation where the system operating mode changes, and in most cases undesirably (i.e. due to system fault or unknown disturbance input), then, an accurate continuum state estimation will also depend strongly on the ability to identify the functioning operating mode correctly at any given point in time.

3.3 Sequential State Estimation of Continuum and Noncontinuum states

Several state estimation algorithms are available in the literature. The most popular among them are the Kalman filter (KF), moving horizon estimator (MHE), and particle filter [74]. In this study, we consider a moving horizon estimation technique largely because of its optimality and ability to handle constraints. Besides, a state estimation method based on MHE is able to overcome most of the existing challenges on state estimation problems because it estimates the desired variables using multiple output data over a horizon. These challenges include formulating the state estimation that can take constraints into account and shape the estimates to form different distributions other than the Gaussian distribution. However, few papers have considered the application of the MHE method to hybrid systems [12, 26].

3.3.1 Estimation under known switching functions

Switching in distillation dynamics occurs when the system operation changes from one mode into the another. This switching in operating mode can either be desirable or undesirable. The change in system operating mode is said to be desirable when the switch of operation follows a specified operational schedule or policy (e.g **Scenario 1** discussed in Section 3.2). In this case, the mode transition function is said to be known and the information on the switching criteria is available to both the real process and the estimator as shown in Figure 3.2.

In the case of a known switching mode criterium (i.e., $m_k = l$), the hybrid process model of Eq. (3.3) becomes:

$$\begin{aligned} X_{k+1} &= f_l(X_k, u_k; \theta) + w_k, \\ Y_k &= g_l(X_k; \beta) + v_k, \end{aligned} \tag{3.4}$$

and the hybrid state estimator model will be of the form:

$$\begin{aligned} \hat{X}_{k+1} &= f_l(\hat{X}_k, u_k; \theta) + \hat{w}_k, \\ \hat{Y}_k &= g_l(\hat{X}_k; \beta), \end{aligned} \tag{3.5}$$

Using MHE algorithm, an optimum sequence of $\hat{w}_k$ can be obtained by constructing a quadratic cost function (Φ_k) as:

$$\begin{aligned} \min_{\{\hat{w}_{k-N-1},\ldots,\hat{w}_{k-1}\}} \Phi_k : \quad \Phi_k = \hat{w}_{k-N-1}^T Q_{k-N-1}^{-1} \hat{w}_{k-N-1} \\ + \sum_{j=k-N}^{k-1} \hat{w}_j^T Q^{-1} \hat{w}_j + \sum_{j=k-N}^{k} \hat{v}_j^T \mathcal{R}^{-1} \hat{v}_j, \end{aligned} \tag{3.6}$$

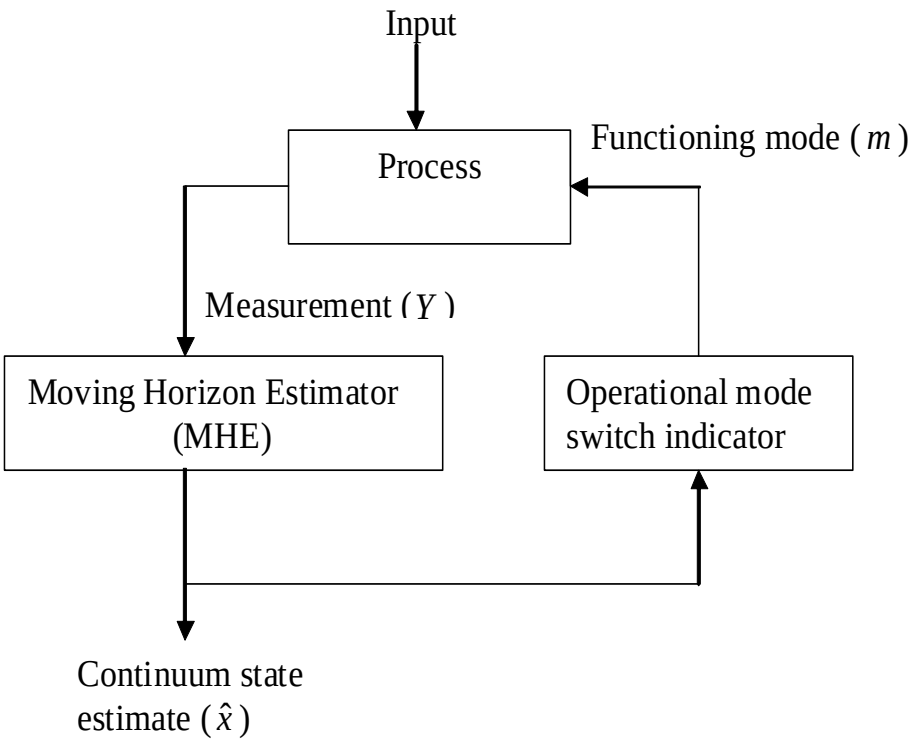

Figure 3.2: The flowchart of a state estimation with known switching transition function.

subject to the following constraints:

$$\begin{aligned}
&\hat{X}_{k-N} = \bar{X}_{k-N} + \hat{w}_{k-N-1}, \\
&\bar{X}_{k-N} = f_l(\hat{X}_{k-N-1}, \hat{u}_{k-N-1}; \theta), \\
&\hat{X}_{j+1} = f_l(\hat{X}_j, \hat{u}_j; \theta) + \hat{w}_j, \quad j = k-N, ..., k-1, \\
&\hat{Y}_j = g_l(\hat{X}_j; \beta), \\
&\hat{v}_j = Y_j - \hat{Y}_j, \\
&\hat{X} \in \mathbb{X}, \quad \hat{w} \in \mathbb{W},
\end{aligned} \tag{3.7}$$

where Q and $\mathcal{R}$ are the weighting matrices and treated as tuning parameters to achieve the best results.

3.3.2 Estimation under unknown switching functions

In this section, a hybrid state estimation is developed for a switching system where the transition between modes is not characterized a priori. By considering a hybrid system model given in Eq. (3.3) with a finite discrete mode set (i.e., $m \in \mathbb{M}$) but with unknown mode transition function, the main objective is to estimate the continuous state x_k as well as the discrete operating mode m_k given the sequences of continuous input and output. The hybrid state estimator proposed comprises three components, which are the moving horizon estimator (MHE) for continuum

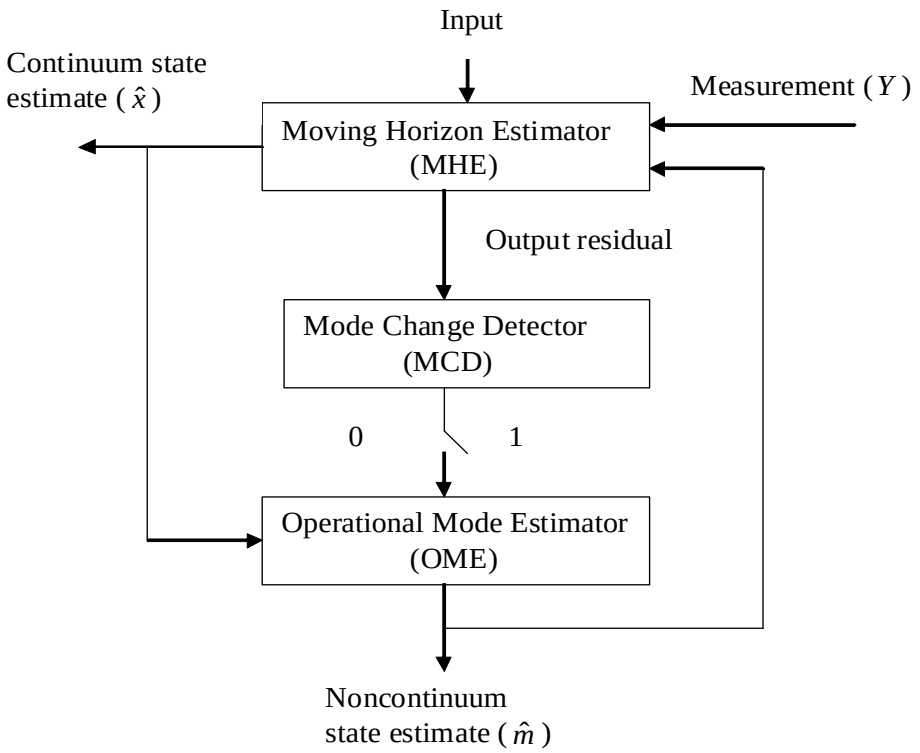

Figure 3.3: The flowchart of a hybrid state estimation implementation.

state estimation, a mode change detector (MCD) to detect a change in operating mode and an operating mode estimator (OME) to estimate the functioning operating mode. Figure 3.3 shows the flowchart of the proposed continuum and noncontinuum state estimator.

In this case of an unknown transition mode, the hybrid process model will be of the form defined in Eq. (3.3). Given an output data of horizon N, we can consider a hybrid time trajectory defined as follows:

- $k_i :=$ The time at which change in the operating mode is detected to occur. For illustration purposes, we assume (in this formulation) that from the time k_{i-1} to the time k_i, the operating mode is detected to change and we also assume without loss of generality that the mode change is from $m_{k_{i-1}} = m_1$ to $m_{k_i} = m_2$.

- $k_{i+b} :=$ The time at which a correct operating mode is identified. For instance, $b = 1$ means the mode estimator is able to identify a new mode after one sample delay of the time the mode change being detected.

A sequential hybrid moving horizon estimator is formulated as

$$\hat{m}_k = \eta(\hat{m}_{k-1}, \hat{u}_{k-1}), \tag{3.8}$$

$$\hat{X}_{k+1} = f_{\hat{m}_k}(\hat{X}_k, \hat{u}_k; \theta) + \hat{w}_{\hat{m},k}, \tag{3.9}$$

$$\hat{Y}_k = g_{\hat{m}_k}(\hat{X}_k; \beta) + \hat{v}_{\hat{m},k}, \tag{3.10}$$

$$\hat{X} \in \mathbb{X}, \quad \hat{w} \in \mathbb{W}, \quad \hat{m} \in \mathbb{M}, \tag{3.11}$$

while the optimum sequence of $\hat{w}_{m,k}$ and mode $\hat{m}_k$ at time k can be obtained from:

$$\begin{aligned} &\min_{\{\hat{w}_{m_1,k-N-1}, \hat{w}_{m_1,k-N}, ..., \hat{w}_{m_1,k_{i+b-1}}, \hat{w}_{m_2,k_{i+b}}, ..., \hat{w}_{m_2,k-1}\}} \Phi_k : \\ &\Phi_k = \hat{w}^T_{m_1,k-N-1} Q^{-1}_{k-N-1} \hat{w}_{m_1,k-N-1} + \sum_{j=k-N}^{k_{i+b-1}} \hat{w}^T_{m_1,j} Q^{-1} \hat{w}_{m_1,j} \quad + \\ &\sum_{j=k_{i+b}}^{k-1} \hat{w}^T_{m_2,j} Q^{-1} \hat{w}_{m_2,j} + \sum_{j=k-N}^{i+b-1} \hat{v}^T_{m_1,j} \mathcal{R}^{-1} \hat{v}_{m_1,j} + \sum_{j=i+b}^{k} \hat{v}^T_{m_2,j} \mathcal{R}^{-1} \hat{v}_{m_2,j}, \end{aligned} \tag{3.12}$$

subject to the following constraints:

$$\begin{aligned} &\hat{m}_k = \eta(\hat{m}_{k-1}, \hat{u}_{k-1}), \\ &\hat{X}_{k-N} = \bar{X}_{k-N} + \hat{w}_{\hat{m},k-N-1}, \\ &\bar{X}_{k-N} = f_{\hat{m}_k}(\hat{X}_{k-N-1}, \hat{u}_{k-N-1}; \theta), \\ &\hat{X}_{j+1} = f_{\hat{m}_k}(\hat{X}_j, \hat{u}_j; \theta) + \hat{w}_{\hat{m},j}, \quad j = k-N, ..., k-1, \\ &\hat{Y}_j = g_{\hat{m}_k}(\hat{X}_j; \beta), \\ &\hat{v}_{\hat{m},j} = Y_j - \hat{Y}_j, \\ &\hat{X} \in \mathbb{X}, \quad \hat{w} \in \mathbb{W}, \hat{m} \in \mathbb{M}. \end{aligned} \tag{3.13}$$

Mode Change Detector (MCD)

To be able to find solution to the sequential hybrid moving horizon estimator of Eqs. (3.12) and (3.13), we need to determine the time k_i and k_{i+b}. Given the output measurement vector $Y_k \in \mathbb{R}^p$ and the estimated output vector $\hat{Y}_k \in \mathbb{R}^p$ obtained from the hybrid moving horizon estimator, the output measurement residual will be

$$r_k = (Y_k - \hat{Y}_k). \tag{3.14}$$

With the availability of the output measurement residual r_k, a mode change index $\varepsilon(k)$ can be defined as:

$$\varepsilon(k) = \|r_k\|^2_{E_k^{-1}}, \tag{3.15}$$

where E_k is the output prediction error covariance matrix. Without change in the system operating mode, $\varepsilon(k)$ will follow a central chi-square distribution with p degree of freedom as

$$\varepsilon(k) \sim \chi^2(p). \tag{3.16}$$

Instead of relying on one single index $\varepsilon(k)$, we monitor a window of $\varepsilon(k)$ with the window size of N_y, as illustrated in Figure 3.4. At a given time step k, by

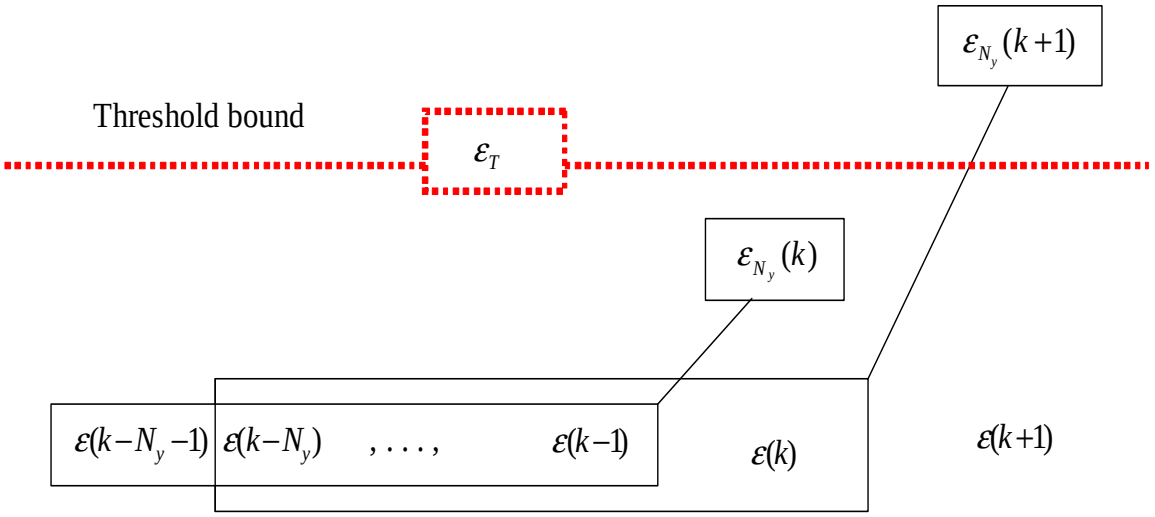

Figure 3.4: A moving horizon mode change index.

considering the last N_y (i.e., $N_y \geq N$) of the mode change indexes (see Figure 3.4), a moving horizon mode change index $\varepsilon_{N_y}(k)$ defined as

$$\varepsilon_{N_y}(k) = \sum_{j=k-N_y+1}^{k} \varepsilon(j), \tag{3.17}$$

is also a chi-square distribution with degree of freedom $p \times Ny$. However, when a change in the system operating mode occurs, $\varepsilon_{N_y}(k)$ will no longer follow a central chi-square distribution. Therefore, a Mode Change Detector (MCD) can be defined such that a moving average mode change index $\varepsilon_{N_y}(k)$ at any given time k is compared with a pre-determined threshold bound $\varepsilon_T(k)$ such that

$$MCD := \begin{cases} 0 & if \quad \varepsilon_{N_y}(k) < \varepsilon_T(k) \\ & \\ 1 & otherwise \end{cases}. \tag{3.18}$$

The pre-determined threshold bound $\varepsilon_T(k) \sim \chi^2_\alpha\{p \times N_y\}$ is evaluated at a selected significance level α from the chi-square table (e.g. $\alpha = 95\%$).

Operation mode estimator (OME)

Based on the information from the mode change detector (MCD), operating mode estimator (OME) will identify and isolate the functioning operating mode, which minimizes the 2-norm of the output prediction errors at any given point in time. Note that the OME is the mathematical formulation of mode transition function expressed in Eq. (3.8). At any given time, operating mode estimator (OME) is either active (i.e. when $MCD = 1$) or inactive (i.e. when $MCD = 0$). Let us assume that

at time $\bar{k}$, an operating mode estimator is active as a result of the $MCD = 1$. The functioning operating mode can be estimated by solving the following optimization problem:

$$\hat{m}_{\bar{k}} =: \min_{\hat{m} \in \mathbb{M}} \|Y_{\bar{k}} - g_{\hat{m}_k}(\hat{X}_{\bar{k}-1}; \beta)\|, \tag{3.19}$$

subject to

$$\hat{X}_{\bar{k}} = f_{\hat{m}_k}(\hat{X}_{\bar{k}-1}, u_{\bar{k}-1}; \theta) + \hat{w}_{\hat{m},\bar{k}-1}, \tag{3.20}$$

and

$$w_{lo} < \hat{w}_{\hat{m}_k,\bar{k}} < w_{up}. \tag{3.21}$$

At any other time when the result from a mode change detector is zero (i.e., $MCD = 0$,), the estimated noncontinuum state $\hat{m}_k$ will simply be equal to $\hat{m}_{k-1}$.

3.4 Simulation Study: A Batch Distillation Process

Batch distillation is one of the most important separation processes used in many chemical industries, especially those related to the production of fine chemicals. This is due to the low scale production and the flexibility in purifying different mixtures under a variety of operating conditions. In order to meet the purity specifications, a batch column has to be operated as precisely as possible. If the current composition profiles of the batch column are known, they can form a basis for improving the process performance through an effective operating decision making. In this section, the objective is to apply the developed hybrid state estimator to estimate the column composition in a batch distillation process with a switching dynamics using the available temperature measurements as shown in Figure 3.5. In this study, we investigate two forms of operating mode changes that can occur in batch distillation process. They are (1) composition estimation under a known mode transition function and (2) composition estimation under an unknown mode transition function.

3.4.1 Hybrid process model

The batch distillation under consideration is a ternary system. The schematic diagram of the batch distillation column with the proposed composition monitoring through a moving horizon estimation scheme is shown in Figure 3.5. In this study, we extended the process model developed by Quintero-Marmol et al.(1991) [69] for batch distillation column to allow modeling the switching operating modes as well as the presence of measurement noise and plant-model mismatch. Based on the

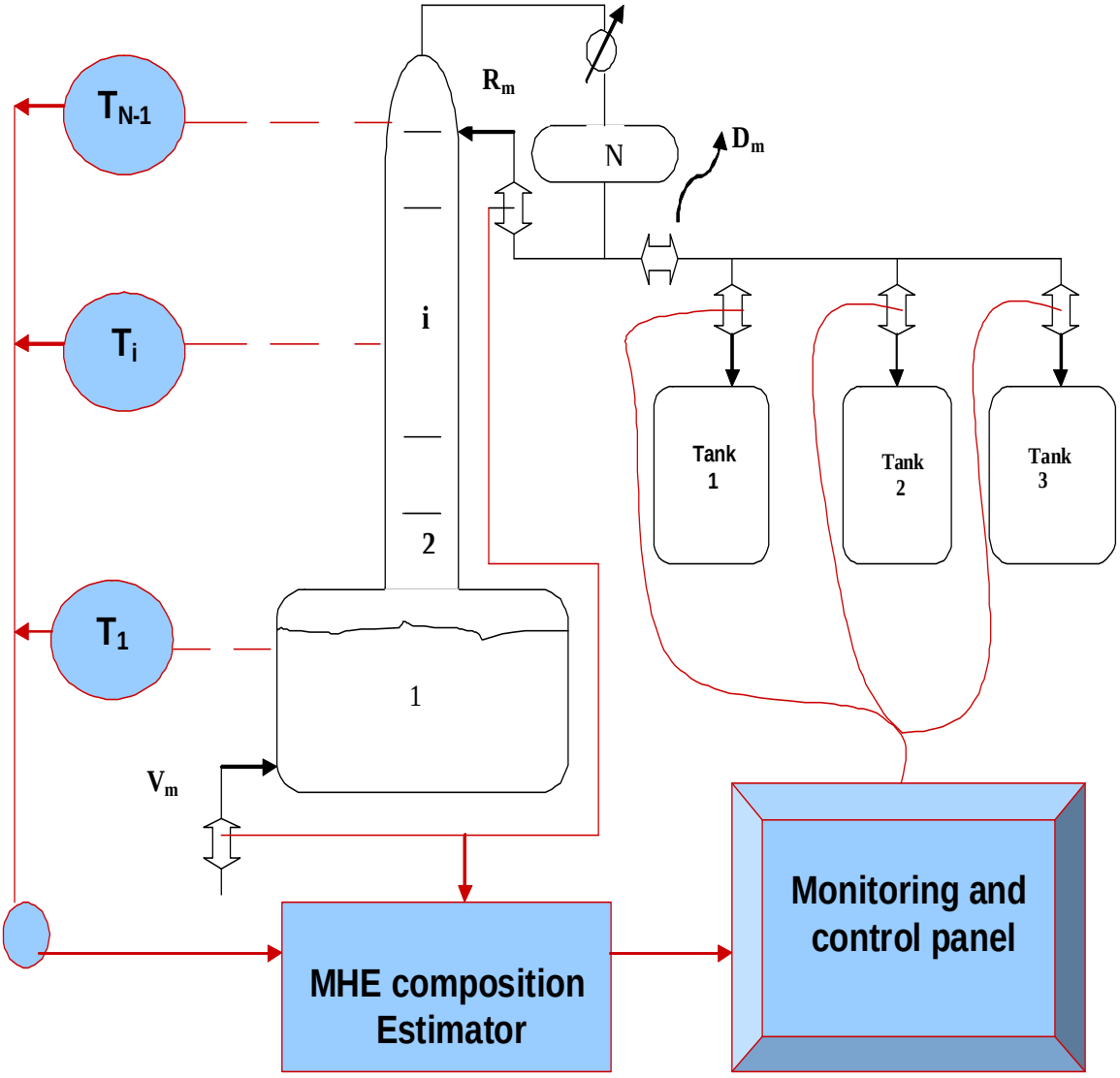

Figure 3.5: Composition estimation of a batch distillation column.

assumptions of equimolar overflow, constant tray and reflux drum holdups and constant relative volatilities, the process model of the system is summarized as follows:

$$\frac{dx_{1,j}}{dt} = R_m(x_{2,j} - x_{1,j}) + V_m(x_{1,j} - y_{1,j})]/H_1, \quad i = 1 : N_S - 1, j = 1 : Nc, \quad (3.22)$$

$$\frac{dx_{i,j}}{dt} = R_m(x_{i+1,j} - x_{i,j}) + V_m(y_{i-1,j} - y_{i,j})]/H_i, \quad i = 1 : N_S - 1, j = 1 : Nc, \quad (3.23)$$

$$\frac{dx_{N_S,j}}{dt} = V_m(y_{N_S-1,j} - x_{N_S,j})]/H_{N_S}, \quad i = 1 : N_S - 1, j = 1 : Nc, \quad (3.24)$$

$$\frac{dH_1}{dt} = -D_m, \quad D_m = V_m - R_m, \quad (3.25)$$

$$y_{i,j} = \alpha_j x_{i,j} / \sum_{l=1}^{Nc} x_{i,l}, \quad i = 1 : N_S - 1, j = 1 : Nc, \quad (3.26)$$

with constraint on composition as

$$0 \leq x_{i,j} \leq 1. \quad (3.27)$$

The output temperature measurement is modeled as:

$$T_i = B_{vp,j}/[A_{vp,j} - \ln(\alpha_j P / \sum_{l=1}^{Nc} \alpha_k x_{i,l})], \quad (3.28)$$

where α is the relative volatility, while $B_{vp,j}$ and $A_{vp,j}$ are the vapor pressure parameters for component j.

3.4.2 Composition estimation under a known mode transition function

The main switching criteria is the purity specification of the distillate product. In this case, the following three different types of operating modes are considered:

- Mode 1: This mode represents the startup dynamics when the column is operated at total reflux (i.e., $RR = \infty$) until the concentration of the lightest component in the distillate, $x_{D,1}$, reaches the specified purity, x_{sp}. The time at which this occurs is defined as $t_1(x_{D,1} = x_{sp})$.

- Mode 2: This represents system mode when the column is being operated at the specified reflux ratio (RR_{sp}) to meet the desired product composition specification. This mode naturally follows Mode 1 when the time t_1 is reached.

- Mode 3: This mode is defined to represent the system operating mode when the column is operated at a specified minimum reflux ratio (RR_{min}) such that $RR_{min} \ll RR_{sp}$. For simulation studies, the switch to this operation mode is designed to occur at time $t_2(x_{D,1} < x_{sp})$.

Table 3.1: Different operating modes for a batch distillation system.

Variables	Mode 1	Mode 2	Mode 3
Number of stages	6	6	6
Number of states	18	18	18
Number of components	3	3	3
R (mol/hr)	100	60	20
D (mol/hr)	0	40	80
RR (D/R)	Infinite	1.2	0.25
$x_{i,1}$	0.45	0.45	0.45
$x_{i,2}$	0.25	0.25	0.25
$x_{i,3}$	0.30	0.30	0.30

The switching functions for operating modes are given as:

$$0 \leq t < t_1(x_{D,1} = x_{sp}), \quad RR = \infty, \tag{3.29}$$

$$t_1(x_{D,1} = x_{sp}) \leq t < t_2(x_{D,1} < x_{sp}), \quad RR = RR_{sp}, \tag{3.30}$$

$$t_2(x_{D,1} < x_{sp}) < t \leq t_f, \quad RR = RR_{min}, \tag{3.31}$$

where t_f is the final batch time. The main job of a state estimator in this case, is to use the estimated composition profiles to determine the time (t_i) at which the switching of operation will take place. An accurate estimation of the composition profiles in the distillation column is a necessity for optimum and safe operation of the process because the time (t_i) at which the switching occurs depends on the column compositions. The system parameters, column configuration and the initial conditions for the five-tray ternary batch distillation column under different operating modes are provided in Table 3.1. The column design and operating parameters are obtained from Quintero-Marmol et al.(1991) [69]. The required product quality specification (x_{sp}) is 95% purity of the component 1 in the distillate. Based on the knowledge of the estimated states, the system switches automatically based on the scheduled estimator-based operating mode switching functions of Eqs. (3.29)-(3.31). The performance of the developed MHE in the composition estimation and monitoring of a switching batch distillation process was examined by investigating the effect of process noise (w), measurement noise (v) and switching operating modes. Figure 3.6 shows the compositions of component 1 and 2, both actual and estimated in some selected stages of the ternary batch distillation column. The result shows that MHE is able to estimate the column composition profiles well with a horizon length just $N = 1$ under the scheduled switching dynamics.

In order to access the performance of MHE comparatively with other existing estimation techniques, an EKF algorithm was developed for the same process. By

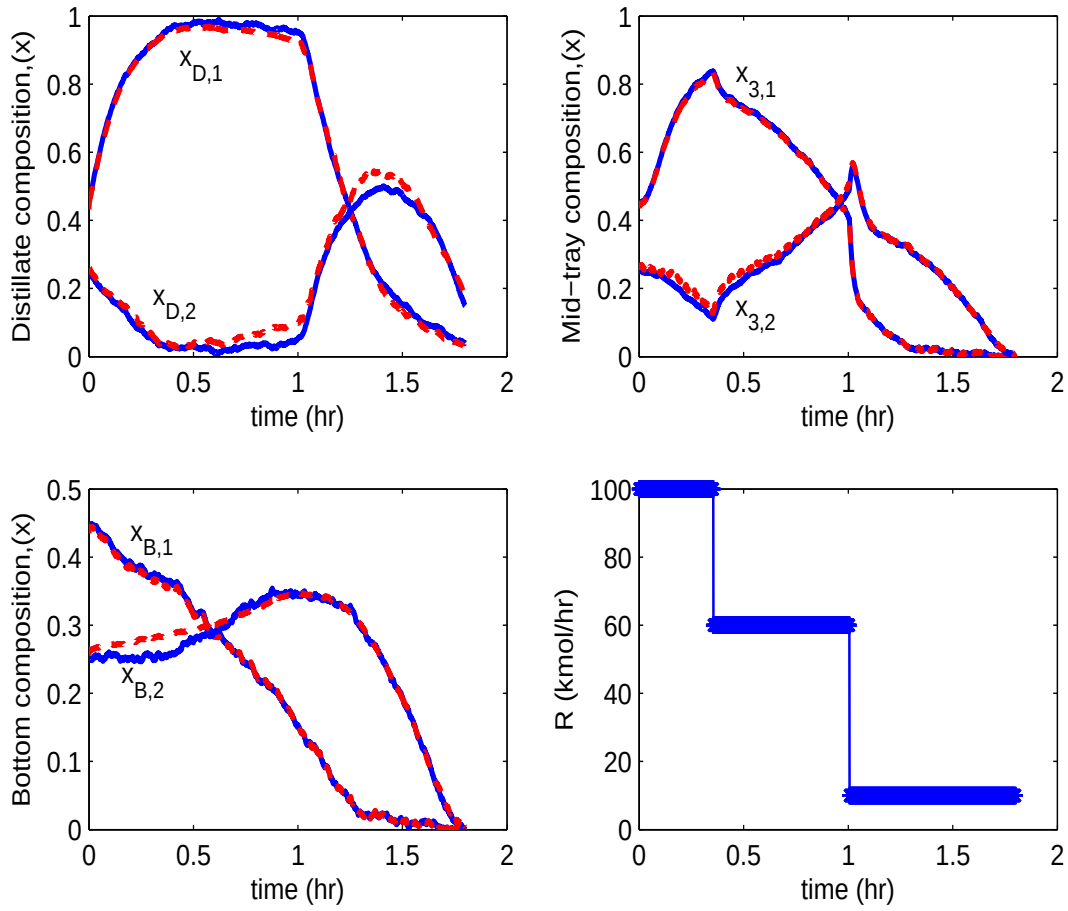

Figure 3.6: Dynamic composition responses of a batch distillation process: measured (dash line); estimated (solid line).

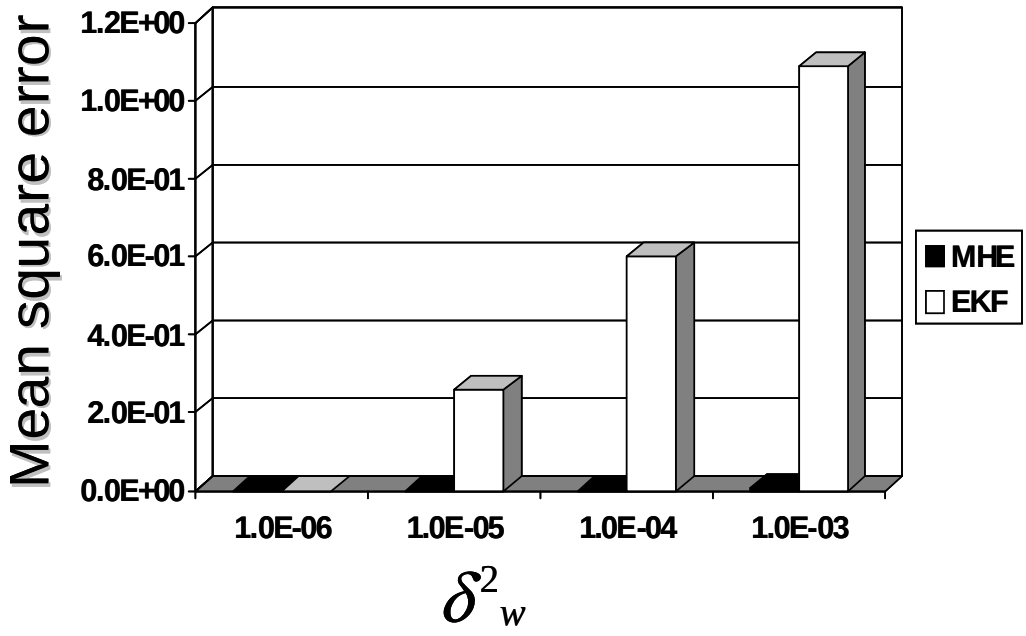

Figure 3.7: MHE and EKF performance comparison using the Mean Square Error (MSE).

fixing the standard deviation of the measurement noise (i.e. $\delta_v^2 = 1 \times 10^{-2}$), the performances of both MHE and EKF with respect to increase in process variability are quantitatively compared through their Mean Square Error (MSE) as shown in Figure 3.7. It is clear that MSE values obtained with MHE algorithm are consistently smaller than that obtained with EKF algorithm with increase in the process noise magnitude. With $\delta_w^2 \geq 1 \times 10^{-4}$, EKF shows divergence in some of the estimated states because some of the set constraints are violated. Figure 3.8 shows that the performance of the MHE can further be improved by increasing the horizon length, though at the expense of the computational time. With a horizon length just $N = 1$, it takes MHE about 10 times as much time as it takes EKF to achieve the same simulation results. In this study, using horizon length of just two is sufficient to give a good composition estimation of the batch distillation column.

3.4.3 Composition estimation under an unknown mode transition function

In this section, the developed continuum and noncontinuum estimator is applied to a batch distillation process to estimate composition profiles as well as tracking the change in system operating mode, which results from an unexpected change in reflux flow rate (i.e., faulty reflux valve). Let us assume that the system has been designed in such that any unforseen changes in the system can only trigger the operating

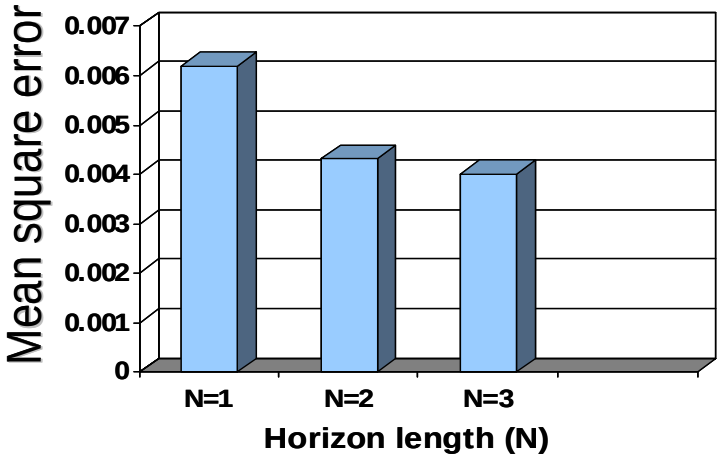

Figure 3.8: MHE performance with different horizon length (N).

mode to change within a finite set of operation mode given in Table 3.1. Because a change in operating mode, as considered in this study, is a result of a faulty valve in the reflux stream, the mode transition function is therefore unknown and the system dynamics can switch randomly from one operating mode into another. Figures 3.9 and 3.10 show the composition estimation in the distillate and mid-tray stage of the column while the sequence of the system operating modes is estimated correctly as shown in Figure 3.11. The mode change detector result shown Figure 3.12 provides a good indication of where the mode changes occur as a function of time. The thick solid lines are the true mode changes detected, while the dash lines are false mode change detected.

It is interesting to compare the result of MCD in Figure 3.12 (i.e., when $\delta_w^2 = 1 \times 10^{-3}$) to that in Figure 3.13, where the process noise variability is reduced to $\delta_w^2 = 1 \times 10^{-4}$. It is obvious that the MCD is able to detect the time at which mode changes occur accurately with no false detection. In general, the effect of a significant plant-model mismatch on the performance of a mode change detector (MCD) is of two folds:

- It may lead to a missed detection, a situation where by the MCD fails to raise alarm when there is indeed a change in the system operating modes. For the duration of time for which MCD fails to raise alarm for a possible change in modes, the operating mode estimator (OME) will fail to identify the correct operating mode on time and the overall performance of the state observer to estimate the continuum state will also be affected.

- The second effect is that it may lead to a false detection, a situation where the MCD raises an alarm when there is indeed no change in the system operating

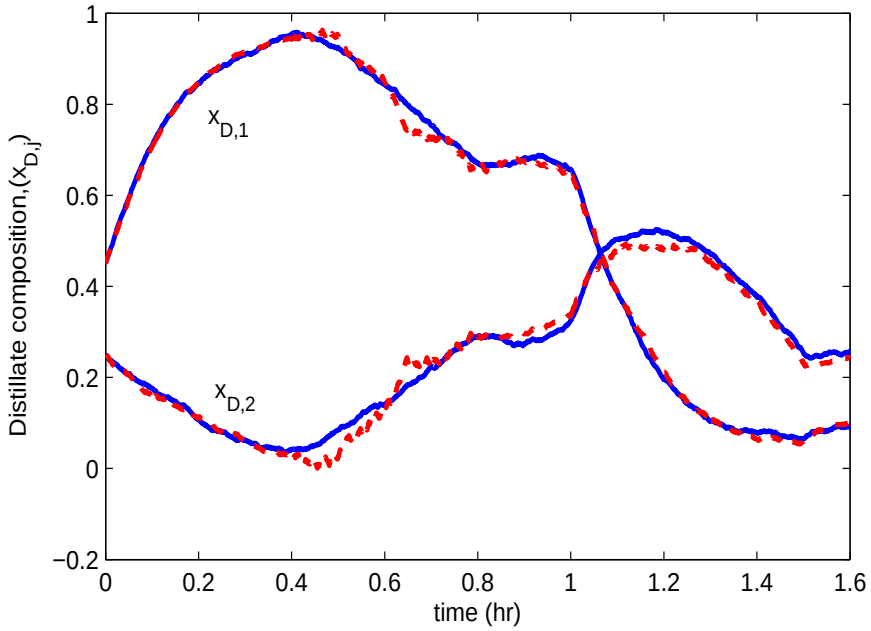

Figure 3.9: Dynamic composition responses at the distillate of a batch distillation process: measured (dash line); estimated (solid line).

modes. In this case, because the operating mode estimator (OME) will be activated to identify the correct operating mode each time there is a detection by MCD, OME will still be able to determine the correct mode. In this way, OME is designed to be robust to false detection. Even though there are some false alarms between the time of 1hr to 1.6hr as shown in Figure 3.12, for instance, the operation mode estimator result presented in Figure 3.11 shows that operating modes within the same time region are correctly identified.

3.5 Experimental Study: A Continuous Distillation Process

Among several studies on the application of state estimation to distillation processes, few papers tested their results using actual experimental data [57, 9, 10]. Mejdell and Skogestad (1991) [57] implemented a static partial least-square regression estimator for product compositions on a high-purity pilot-plant distillation column. An experimentally based estimator, with logarithmically transformed temperatures and compositions, was reported to give excellent performance over a wide range of operating conditions. Baratti et al. (1995) [9] developed a nonlinear extended Kalman filter (EKF), which predicts the composition of the outlet streams of a binary distillation column from the temperature measurements. The performance

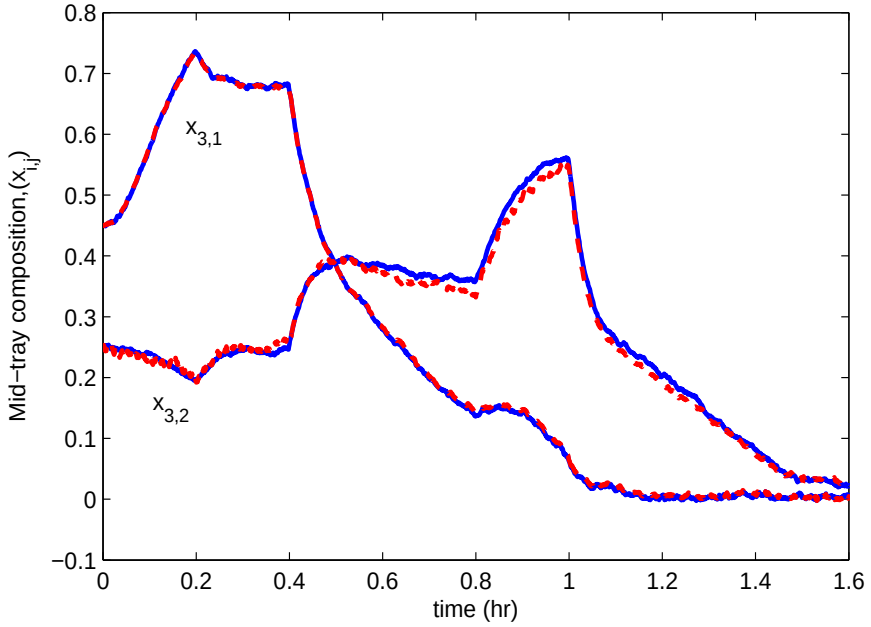

Figure 3.10: Dynamic composition responses at the mid-tray of a batch distillation process: measured (dash line); estimated (solid line).

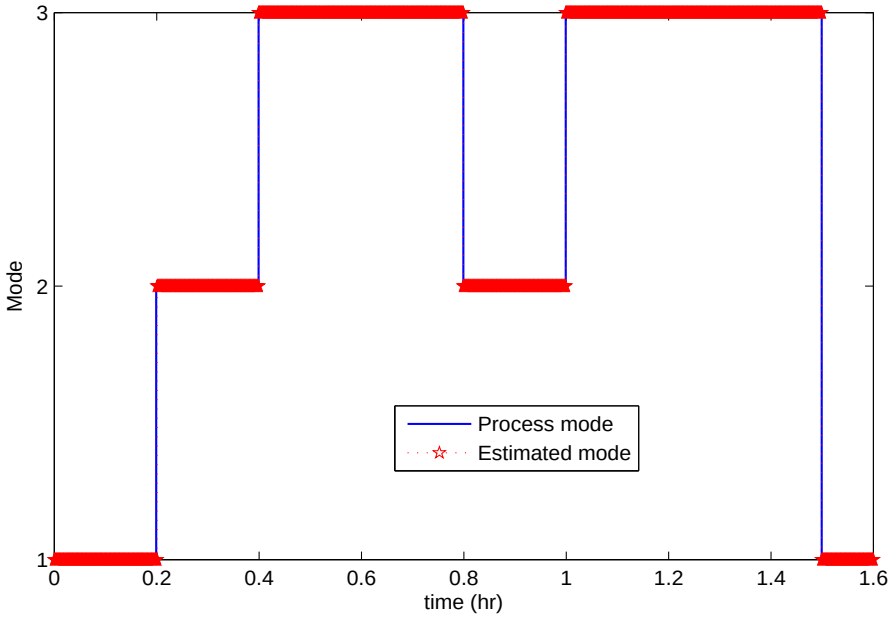

Figure 3.11: Operating mode estimation.

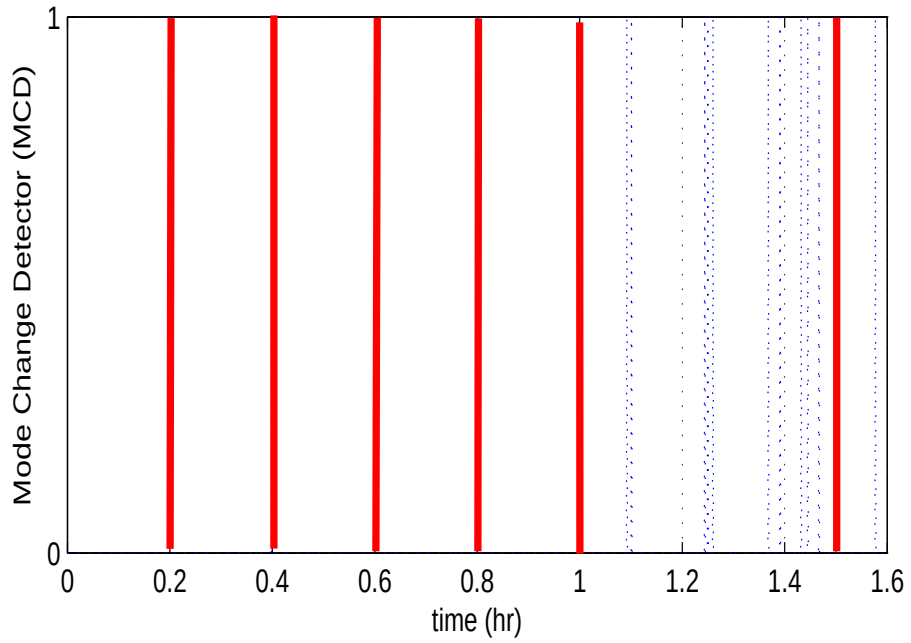

Figure 3.12: Mode Change Detector (MCD) response when $\delta_w^2 = 1 \times 10^{-3}$.

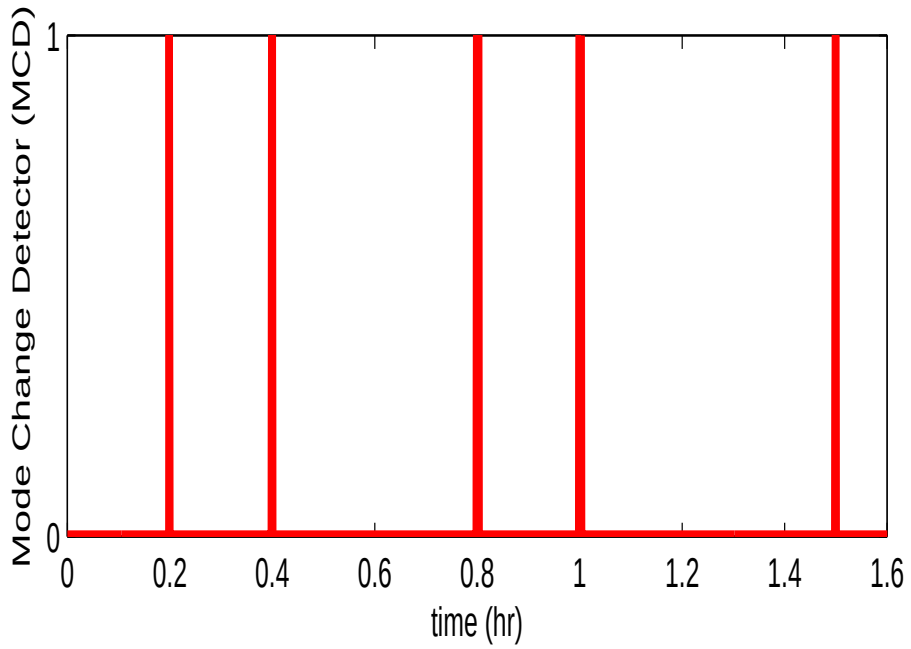

Figure 3.13: Mode Change Detector (MCD) response when $\delta_w^2 = 1 \times 10^{-4}$.

of the estimator was evaluated by comparison with data obtained from the several transient experiments performed in a pilot plant. They extended their work to the multicomponent distillation column and concluded that a more rigorous vapor-liquid equilibrium description is required for composition estimation in multicomponent system [10].

In order to establish the practical reliability of the developed composition estimation technique, we investigate state estimation experimentally on a real distillation column. The experiments were carried out in a 153 mm diameter distillation column operated at ambient pressure to separate methanol (MeoH) from methanol-isopropanol mixture. The flow sheet of the test apparatus is shown in Figure 3.14. The column sections were made of Pyrex glass and contained five identical stainless steel sieve trays spaced 318 mm apart. Each tray was equipped with a thermocouple and two liquid sampling points at the inlet and outlet of the tray. The total pressure drop for the test tray was measured using a differential pressure cell. A total condenser and thermosiphon partial reboiler completed the distillation system. The column was completely instrumented for continuous unattended operation. An Opto-22 process I/O subsystem interface with a personal computer running Lab View (version 7) was used for the process control and data acquisition.

The column was started with total reflux operation and was then switched to the continuous mode (normal operation) by introducing feed to the column and withdrawn two products from top and bottom of the column. When the flow rate and temperature profiles shown by the software (Lab View) remained constant for a period of 60 minutes, steady state conditions were assumed for that particular run. Mass and energy balance calculations were also preformed to ensure that instrumental errors were insignificant (discrepancy $< 5\%$). Triplicate liquid samples were taken and analyzed to minimize the error of measurements using a Hewlett Packard 5790A series II gas chromatograph.

3.5.1 Process modeling and validation

To perform state estimation, a dynamic model of the process is needed. In modeling the distillation column, we consider only RV-configuration in which both the reflux flow rate (R) and vapor boil up (V) are the available independent input variables. For composition estimation purposes, we modeled both the vapor boil up and reflux flow rate as discrete-event states in order to capture the noncontinuum dynamics created by the change in heat input and reflux flow rate. By assuming perfect level controllers at the bottoms and the reflux drum, negligible energy dynamics and a linear pressure drops down the column, the methanol-isopropanol distillation process is modeled based on methanol composition (x) as follows:

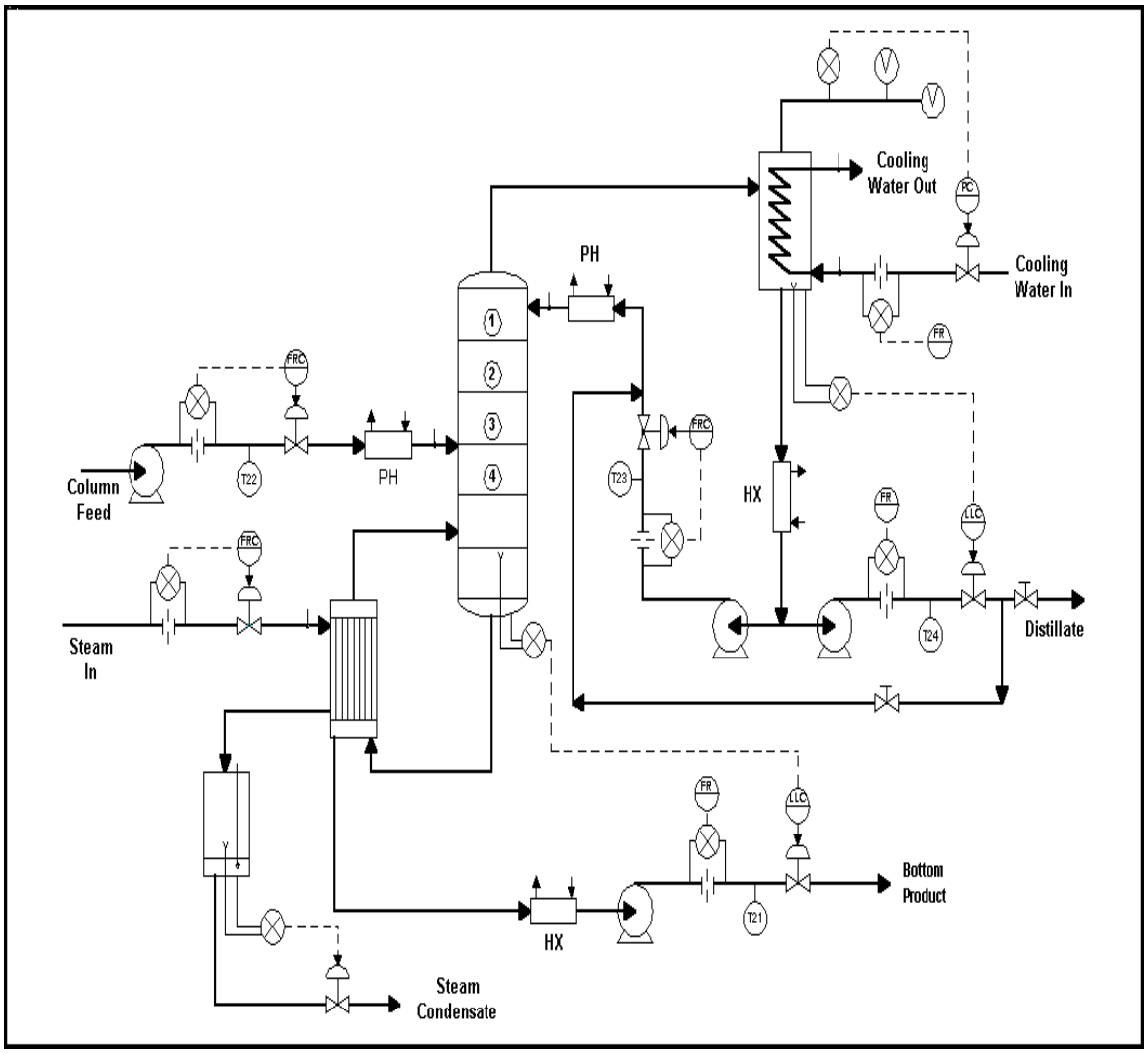

Figure 3.14: A continuous distillation column setup.

Reboiler i=1: subject to the following constraints:

$$\begin{aligned} \frac{d(H_1 x_1)}{dt} &= L_2 x_2 - B_m x_1 - V_m y_1, \\ B_m &= L_2 - V_m, \end{aligned} \tag{3.32}$$

Tray i ($1 \leq i \leq f-1$):

$$\begin{aligned} \frac{d(H_i x_i)}{dt} &= L_{i+1} x_{i+1} - L_i x_i + V_m y_{i-1} - V_m y_i, \\ \frac{dH_i}{dt} &= L_{i+1} - L_i + \delta LR_m + \delta LF_m, \end{aligned} \tag{3.33}$$

Feed tray i=f:

$$\begin{aligned} \frac{d(H_f x_f)}{dt} &= L_{f+1} x_{f+1} - L_f x_f + V_m y_{f-1} - (V_m - \delta LF_m) y_f + F_m z_m, \\ \frac{dH_i}{dt} &= L_{f+1} - L_f + F_m + \delta LR_m + \delta LF_m, \end{aligned} \tag{3.34}$$

Tray i ($f+1 \leq i \leq N_s - 1$):

$$\begin{aligned} \frac{d(H_i x_i)}{dt} &= L_{i+1} x_{i+1} - L_i x_i + (V_m - \delta LF_m) y_{i-1} - V_R y_i, \\ \frac{dH_i}{dt} &= L_{i+1} - L_i + \delta LR_m, \end{aligned} \tag{3.35}$$

Condenser and reflux drum $i = N_s$*:*

$$\begin{aligned} \frac{d(H_{N_s} x_{N_s})}{dt} &= (V_m - \delta LR_m - \delta LF_m) y_{N_s - 1} - R_m x_{N_s} - D_m x_{N_s}, \\ D_m &= (V_m - \delta LR_m - \delta LF_m) - R_m, \end{aligned} \tag{3.36}$$

The liquid flow rate is modeled using the Francis weir formula, while δLR and δLF account for the effect of temperature difference due to incoming reflux flow rate into the top of the column and feed flow rate into the feed tray respectively [9]. The two quantities can be calculated from:

$$\delta LR_m = \frac{C_p R_m (T_{N_T} - T_{N_s})}{\Delta H_{vap}}, \tag{3.37}$$

and

$$\delta LF_m = \frac{C_p R_m (T_f - T_F)}{\Delta H_{vap}}, \tag{3.38}$$

where ΔH_{vap} is the heat of vaporization, T_{N_T} is the top stage temperature, T_{N_s} represents the reflux stream temperature, T_f is the temperature of the feed stream and T_F is the feed tray temperature.

The methanol-isopropanol system properties and equilibrium data were obtained from the work of Ghmeling et al.(1981) [42]. With the vapor-liquid equilibrium equation correlated as

$$y_i^\star = 0.2722827 x_i^4 - 0.4356193 x_i^3 - 0.4627921 x_i^2 + 1.629680 x_i + 3.504611 \times 10^{-5}, \tag{3.39}$$

where $y_i^\star$ is the vapor composition of MeoH that is in equilibrium with the liquid composition (x_i) leaving the tray, the actual vapor composition leaving the tray is calculated using Murphree tray efficiency relation:

$$y_i = y_{i-1} + E_{mv_m}(y_i^\star - y_{i-1}). \tag{3.40}$$

The column temperature (T) on tray i and the reboiler can be obtained from

$$T_i = B_{vp,j}/[A_{vp,j} - \ln(\frac{y_i P_i}{\gamma_j x_i})], \tag{3.41}$$

where γ_j is the activity co-efficient of the component j on tray i.

By defining the following new variables,

$$\begin{array}{l} X := \{x_1, x_1, x_2..., x_{N-1}, x_{N_s}\}, \\ V_m := \{V_1, ..., V_l, ..., V_M\}, \\ R_m := \{R_1, ..., R_l, ..., R_M\}, \\ u := \{V_m, R_m, D_m, B_m\}, \end{array} \tag{3.42}$$

it is straightforward to see that Eqs. (3.32)-(3.42) are of the same form of the Eq. (3.3) presented in Section 3.2.

Figures 3.15 and 3.16 show the steady state composition profiles of methanol (MeoH) at two different operating conditions, while the column composition and temperature dynamics with a step change in the vapor boil up are presented in Figures 3.17 and 3.18. In both figures, the measured compositions are compared with model predictions. It is clear from the figures that the developed model does capture well both the steady state as well as the dynamics of the column.

3.5.2 Hybrid state estimator performance

The developed hybrid state estimation technique was tested online by conducting several experiments. Each of the experiments involve series of operating mode changes to examine how well the estimator can estimate the column composition as well as the change in operating modes. In this study, we considered the change in the system operating mode due to a change in the vapor boilup with a known switching transition function and a change reflux flow rate with an unknown switching function. The operating conditions considered are summarized in Tables 3.2 and 3.3. Measurements of temperature from the thermocouple located on all of the column stages except the condenser are obtained at every minute and feed into the estimator online. The experimental results given in this section are a representative of several online experiments conducted under different types of operating mode changes.

With a known switching transition function, Figure 3.19 shows a comparison of a measured and online composition estimation for various boilup rates. The result

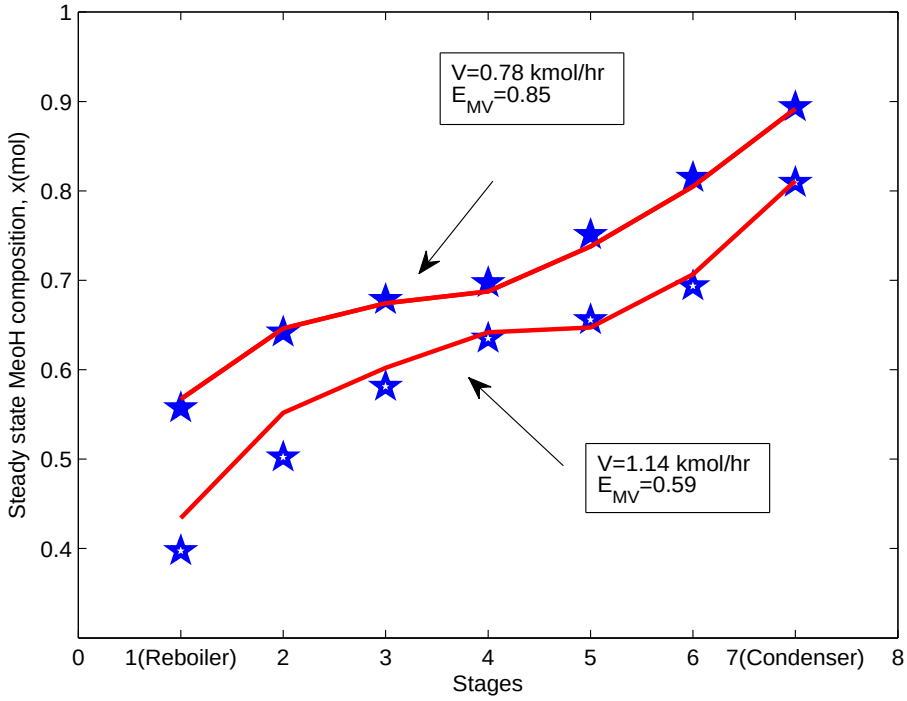

Figure 3.15: Steady state column composition profiles: experiment ($*$); model ($-$).

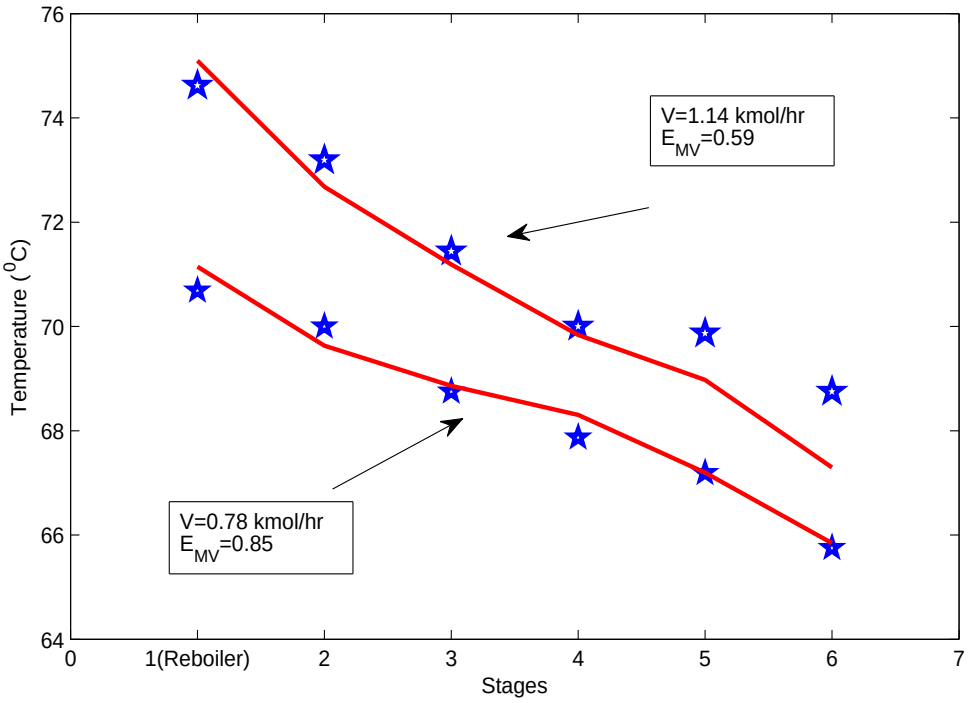

Figure 3.16: Steady state column temperature profiles: experiment ($*$); model ($-$).

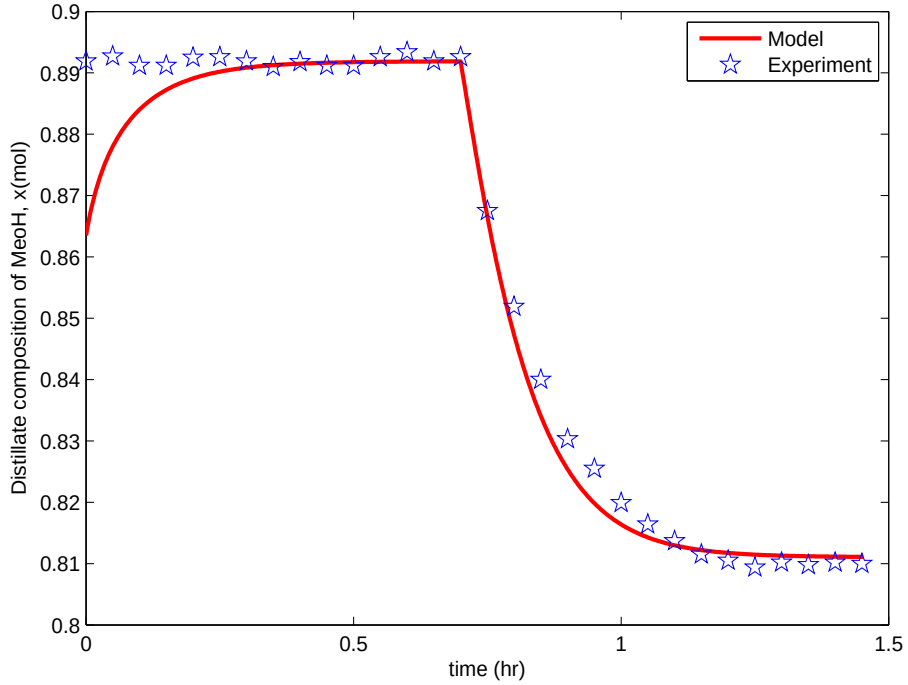

Figure 3.17: Composition dynamics with a step input change in the vapor boilup: experiment ($*$); model ($-$).

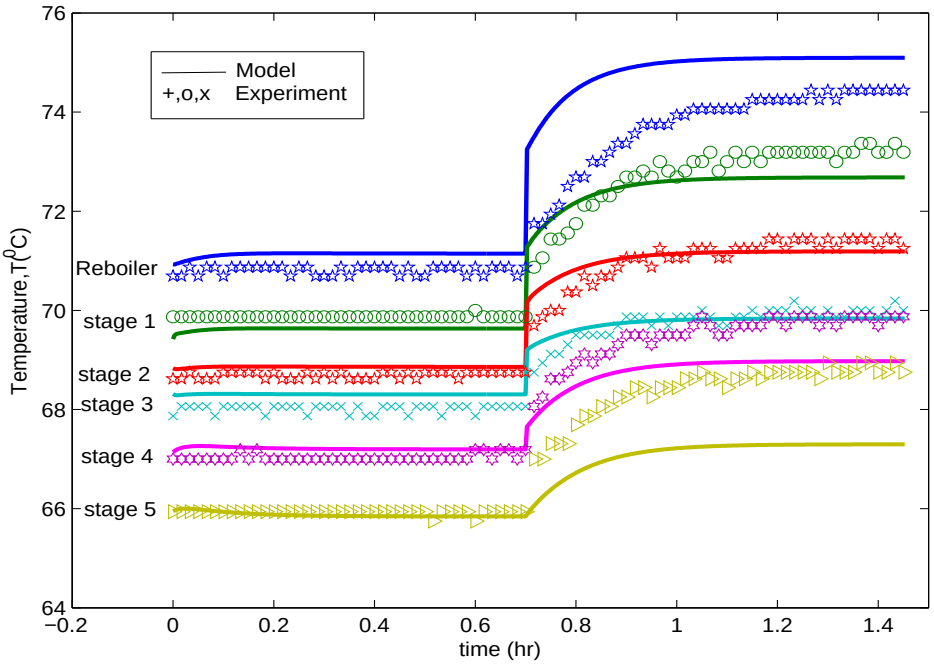

Figure 3.18: Stages temperature dynamics with a step input change in the vapor boilup.

Table 3.2: Operating modes based on different vapor boilup rates.

Variables	Mode I	Mode II	Mode III
Vapor boilup, V(kmol/hr)	0.78	1.14	1.44
Reflux flow rate, R(kmol/hr)	0.35	0.35	0.35
Feed flow rate, F(kmol/hr),	1.19	1.19	1.19
Distillate composition, x	0.8920	0.8091	0.7146
Feed composition, z	0.5613	0.5613	0.5613
Tray efficiency, E_{mv}	0.85	0.59	0.55

Table 3.3: Operating modes based on different reflux flow rates.

Variables	Mode I	Mode II	Mode III
Vapor boilup, V(kmol/hr)	1.16	1.16	1.16
Reflux flow rate, R(kmol/hr)	0.35	0.51	0.64
Feed flow rate, F(kmol/hr),	1.19	1.19	1.19
Distillate composition, x	0.8102	0.8532	0.8854
Feed composition, z	0.5613	0.5613	0.5613
Tray efficiency, E_{mv}	0.72	0.68	0.60

clearly shows that the online estimator is able to estimate the composition profile well under different operating modes. In the result shown in Figure 3.19, the reflux flow rate is set constant, thus making the main source of operating mode changes to be the vapor boilup rate. The estimator performance was also tested when the source of the operating mode changes is a switch in the reflux flow rate created by a faulty reflux valve (i.e., the noncontinuum state is unknown). The results are summarized in Figure 3.20. The estimator performance is consistent in estimating the column composition under different switching dynamics.

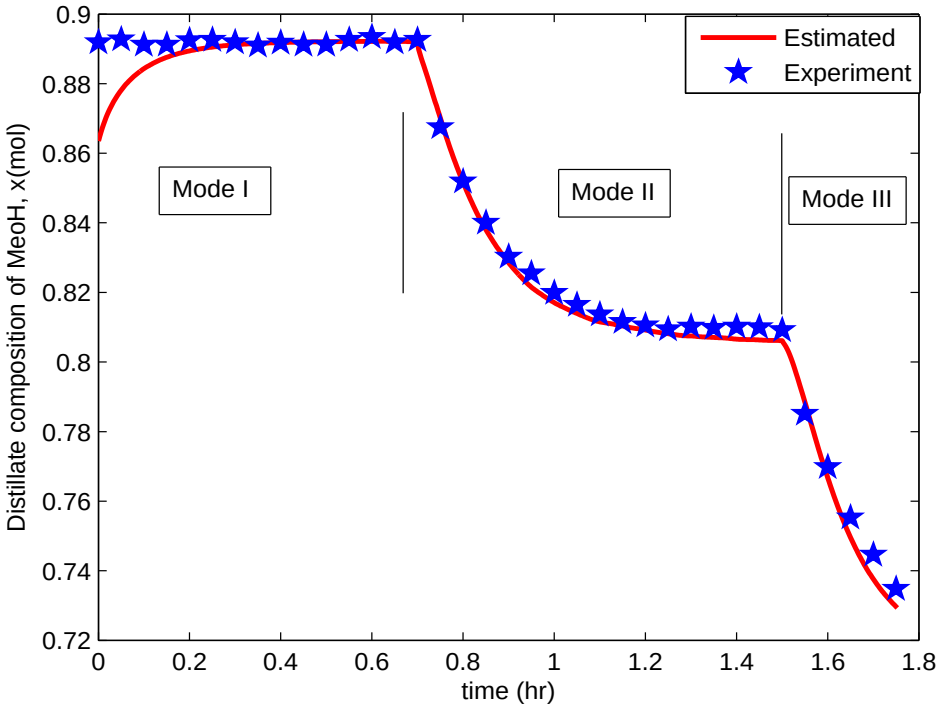

Figure 3.19: State estimator performance under switch in vapor boilup rate (V).

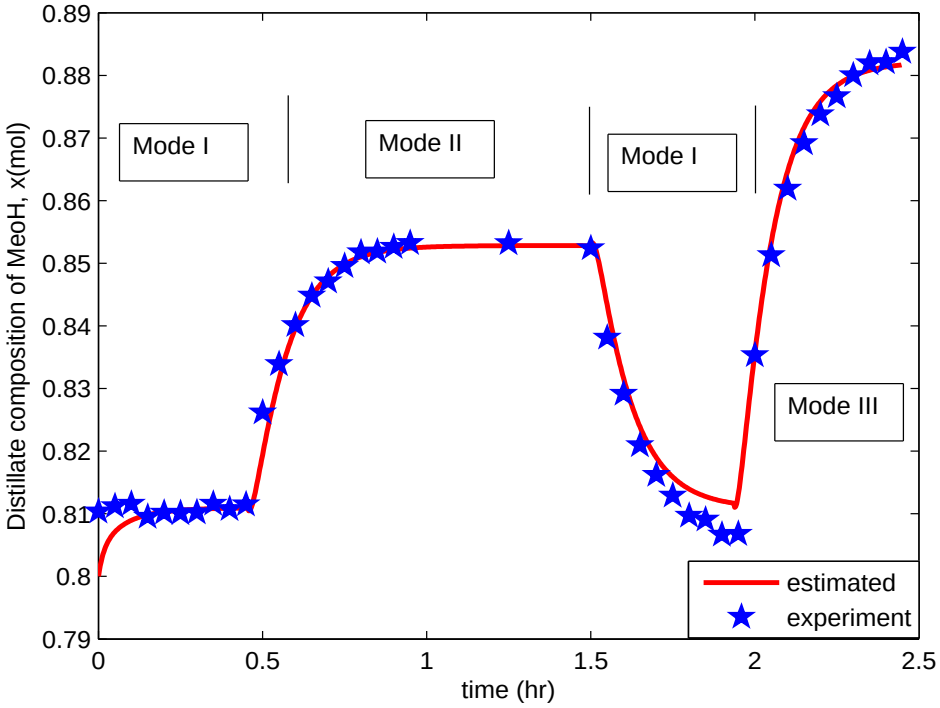

Figure 3.20: State estimator performance under switch in reflux flow rate (R).

3.6 Conclusion

A state estimation technique, which has the capability to monitor composition profiles of a distillation process under switching dynamics using the available temperature measurements, is investigated. A distillation process is modeled as a hybrid nonlinear system with the column compositions considered as continuum states, while the operating modes are modeled as noncontinuum states. A moving horizon estimation algorithm is extended to incorporate a mode change detector and an operating mode estimator in order to estimate the column compositions as well as determine if and when there is a change (either desirably or undesirably) in the system operating mode. The proposed method is shown to be effective by testing it using both the simulation on a switching batch distillation process and the experiment on a lab-scale methanol-isopropanol continuous distillation system.

Chapter 4

A Moving Horizon Approach to a Noncontinuum State Estimation

4.1 Introduction

Existing studies on state estimation have almost exclusively been devoted to a continuous-valued system with very few exceptions. Many problems of academic and industrial interests such as operating mode switching, feed quality change, process fault diagnosis, and phase change analysis in a chemical process either take a noncontinuum form, or can be represented by a discrete-valued state and be readily solved. The state transition of a switching system can be captured by a hidden Markov model (HMM)[29], and the noncontinuum state estimation problem in such system can be posed as an optimization problem in which the set of decision variables takes only a finite set of possible values [66, 35, 82].

This chapter focuses on the development of a noncontinuum state estimator, which is based on a moving horizon approach for switching systems that follow a HMM with either a discrete- or continuous-valued noisy measurements. We propose an arrival cost for a moving horizon estimation of noncontinuum state. The performance of the proposed method is analyzed by addressing a mode estimation problem in a reactor and leakage detection in a water tank system.

4.2 Preliminaries

4.2.1 Hidden Markov model

A hidden Markov model (HMM) shown in Figure 4.1 is a statistical model in which the system being modeled is assumed to be a Markov process. The hidden noncontinuum state sequence, $m_{0:T} = \{m_0, ..., m_k, ..., m_T\}$, and the observation sequence, $y_{0:T} = \{y_0, ...y_k, ..., y_T\}$, are modeled by assuming that each observation depends on the corresponding hidden noncontinuum state and that state at time k is condition-

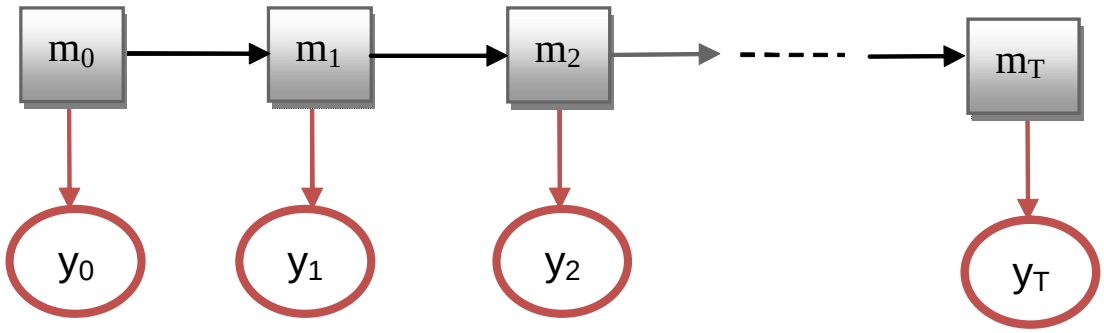

Figure 4.1: Hidden Markov model.

ally dependent only on the state at time $k-1$. Let us consider a HMM λ defined by

$$\lambda = HMM(\mathbb{P}_{k-1,k}^{(i,j)}, d_j(y_k), p_0), \tag{4.1}$$

where $\mathbb{P}_{k-1,k}^{(i,j)} := P(m_k = j | m_{k-1} = i)$, for $i, j \in M$. $d_j(y_k) := P(y_k | m_k = j)$, is the observation probability, p_0 is the initial distribution, while $m_k \in \mathbb{M} : \mathbb{M} = \{1 : M\}$, and $y_k \in R^q$ (if it is continuous-valued), or $y_k \in \mathbb{D} : \mathbb{D} = \{1 : q\}$ (if it is discrete-valued). The main problem is to estimate the hidden state sequence given the observed measurements.

One approach to noncontinuum state estimation is to find the sequence of states, $\hat{m}_{0:T}$, that maximizes the joint probability of the hidden states, $m_{0:T}$, and the measurements, $y_{0:T}$, or simply that solves the optimization problem of the form:

$$\arg\min_{\hat{m}_{0:T}} \{\phi_{0:T}\} : \phi_{0:T} = -\log P(m_{0:T}, y_{0:T}), \tag{4.2}$$

where $P(m_{0:T}, y_{0:T})$ can be expanded as

$$P(m_{0:T}, y_{0:T}) = P(m_0)P(y_0|m_0) \prod_{k=1}^{T} P(m_k|m_{k-1})P(y_k|m_k). \tag{4.3}$$

Therefore,

$$-\log P(m_{0:T}, y_{0:T}) = -[\log P(m_0) + \sum_{k=1}^{T} \log P(m_k|m_{k-1}) + \sum_{k=0}^{T} \log P(y_k|m_k)]. \tag{4.4}$$

By substituting Eq. (4.4) into Eq. (4.2), we have

$$\arg\min_{\hat{m}_{0:T}} \{\phi_{0:T}\} : \phi_{0:T} = -[\log P(m_0) + \sum_{k=1}^{T} \log P(m_k|m_{k-1}) + \sum_{k=0}^{T} \log P(y_k|m_k)]. \tag{4.5}$$

To parameterize the objective function of Eq. (4.5), each term on the right side of Eq. (4.4) will have to be defined, interpreted and expressed as follows:

1. $\log P(m_0)$: This term is called the initial cost (at time $k = 0$) associated with the initial probability distribution of state $m_0 = l$ and it is expressed as

$$\log P(m_0 = l) = \sum_{j=1}^{M} \log \alpha_0^{(j)} p_0^{(j)}, \tag{4.6}$$

where $p_0^{(j)}$ is the j^{th} element of p_0 and $\alpha_k^{(j)}$ is defined by

$$\alpha_k^{(j)} = \begin{cases} 1 & \text{if } \ j=m_k \\ \\ 0 & \text{if } \ j\neq m_k \end{cases}. \tag{4.7}$$

2. $\log P(m_k = l|m_{k-1} = s)$: This term represents the transition cost of a system mode m transiting from state s at time time $k-1$ to state l at the time k. If we define a one-step transition probability by

$$\mathbb{P}_{k-1,k}^{(s,l)} := P(m_k = l|m_{k-1} = s), \quad \text{for} \quad s, l \in M, \tag{4.8}$$

then, the transition cost from a state s at time $k-1$ into a state l at time k can be formulated as

$$\log P(m_k = l|m_{k-1} = s) = \sum_{i=1}^{M} \sum_{j=1}^{M} \log \gamma_{k-1}^{(i)} \alpha_k^{(j)} \mathbb{P}_{k-1,k}^{(i,j)}, \tag{4.9}$$

where $\gamma_{k-1}^{(i)}$ is defined as

$$\gamma_{k-1}^{(i)} = \begin{cases} 1 & \text{if } \ i=m_{k-1} \\ \\ 0 & \text{if } \ i\neq m_{k-1} \end{cases}. \tag{4.10}$$

3. $\log P(y_k|m_k)$: This is termed as the observation cost, which is the cost associated with the uncertainties in the observation data and it can be defined using the conditional distribution of observation y_k given the state m_k as

$$\log P(y_k|m_k = l) = \log d_l(y_k). \tag{4.11}$$

The exact form of $d_l(y_k)$ depends on whether the observation sequence is discrete or continuous.

By substituting Eqs. (4.8)-(4.11) into Eq. (4.5), then, the generalized objective function can be formulated as

$$\begin{aligned} \arg\min_{\hat{m}_{0:T}} \{\phi_{0:T}\} : \phi_{0:T} \quad = \quad & -\sum_{j=1}^{M} \alpha_0^{(j)} \log p_0^{(j)} - \sum_{k=1}^{T} \sum_{i=1}^{M} \sum_{j=1}^{M} \gamma_{k-1}^{(i)} \alpha_k^{(j)} \log \mathbb{P}_{k-1,k}^{(i,j)} \\ & - \sum_{k=0}^{T} \sum_{j=1}^{M} \alpha_k^{(j)} \log d_j(y_k), \end{aligned} \tag{4.12}$$

subject to:

$$\begin{aligned}
\gamma_{k-1}^{(i)} &= \begin{cases} 1 & \text{if} \quad i=\hat{m}_{k-1} \\ \\ 0 & \text{if} \quad i\neq\hat{m}_{k-1} \end{cases}, \\
\alpha_{k}^{(j)} &= \begin{cases} 1 & \text{if} \quad j=\hat{m}_{k} \\ \\ 0 & \text{if} \quad j\neq\hat{m}_{k} \end{cases}, \\
\hat{m}_k &\in \{1, ..., M\}, \qquad k = 0:T.
\end{aligned} \tag{4.13}$$

It is obvious that Eqs. (4.12) and (4.13) constitute a batch optimization problem and will become computationally expensive and numerically intractable as time T increases. Besides, the total number of all possible trajectories of the noncontinuum state sequences will increase with increase in time T according to the following relation

$$\upsilon_{0:T} = M^{T+1}. \tag{4.14}$$

For instance, if $M = 10$ and $T = 10$, then total number of all possible trajectories will be $\upsilon_{0:10} = 10^{11}$. Given a discrete observation sequence, an approximate recursive solution to estimate a discrete state sequence has been provided by a famous Viterbi algorithm (VA) [29]. In the sections that follow, a brief description of a VA algorithm will be provided with the expectation to provide a necessary background to our work as well as to elucidate the similarities and the differences between the VA algorithm and our proposed method.

4.2.2 Viterbi algorithm (VA)

The Viterbi algorithm is typically an application of dynamic programming, which is widely used for estimation and detection of a discrete-event problems in signal processing, digital communication as well as character recognitions [70]. Given a set of observation sequence $y_{0:T}$, VA is an inductive and recursive algorithm, which attempts to find the most likely state sequence $\hat{m}_{0:T}$ in a given hidden Markov process and the accumulated corresponding likelihood scores [70]. Based on the different area of applications and method of implementations, there are generally two types of VA algorithm that exist in the literature, which are offline VA algorithm [70] and online VA algorithm [29]. In this section, the two algorithms are summarized.

Offline Viterbi algorithm

An offline VA algorithm uses a dynamic programming method to provide a recursive solution to the optimization problem of the following form:

$$\arg\min_{m_{0:T}} \{-\log P(m_{0:T}, y_{0:T})\}, \tag{4.15}$$

under the following conditions:

- The observations are noncontinuum states represented with generated symbols.
- All of the observation sequences must be available up to time T.
- The algorithm is implemented offline for a finite sequence of the observed data.

If we define $\delta_k(l)$, the accumulated cost along a single path, which accounts for the first k observed data with final optimum state $\hat{m}_k = l$ at a time k, by

$$\delta_k(l) := \min_{\hat{m}_{0:k}} \{-\log P(m_{0:k}, y_{0:k})\}, \tag{4.16}$$

then, the complete procedure of the offline Viterbi algorithm as adapted from the work of [70] is summarized as follows:

1. Given observation sequence:

$$y_{0:T} = \{y_0, y_1, ..., y_T\}. \tag{4.17}$$

2. Initialization at time $k = 0$ and for $i \in \{1 : M\}$:

$$\delta_0(i) = -\log p_0^{(i)} - \log d_i(y_0), \tag{4.18}$$

$$\psi_0(i) = 0, \tag{4.19}$$

   where $\psi_k(i)$ denotes the state at time $k-1$, which has the lowest cost corresponding to the mode transition to state i at time k.

3. Recursion: For $k \in \{1 : T\}$ and for $l \in \{1 : M\}$:

$$\delta_k(l) = \min_{i \in \{1:M\}} \{\delta_{k-1}(i) - \log \mathbb{P}_{k-1,k}^{(i,l)} - \log d_i(y_k)\}, \tag{4.20}$$

$$\psi_k(l) = \arg \min_{i \in \{1:M\}} \{\delta_{k-1}(i) - \log \mathbb{P}_{k-1,k}^{(i,l)}\}, \tag{4.21}$$

4. Termination:

$$\hat{J} = \min_{i \in \{1:M\}} \{\delta_T\}, \tag{4.22}$$

$$\hat{m}_T = \arg \min_{i \in \{1:M\}} \{\delta_T\}, \tag{4.23}$$

   where $\hat{J}$ and $\hat{m}_T$ are the optimum accumulated cost and state at the final time T respectively.

5. Back tracking the optimal state sequence for $k = T-1, T-2, ..., 0$ as:

$$\hat{m}_k = \psi_{k+1}(\hat{m}_{k+1}). \tag{4.24}$$

It is obvious that the implementation of the VA algorithm summarized in Eqs. (4.16)-(4.24) is offline. However, many process monitoring and control applications will demand a state estimation that can be implemented online. Besides, this algorithm can only be applied to estimate a noncontinuum state sequence from the offline data obtained from a batch system, or from a continuous system with the observed data obtained and analyzed in batch mode. Even if VA is to be used for a batch system, a large memory will be required for storage (i.e., as shown through the Eq. (4.14) given a large observed data sequence.

Online Viterbi algorithm

Given the observation y_k at any given time k, the online Viterbi algorithm provides a recursive optimal solution to the problem of estimating the noncontinuum state m_k based on the smallest cumulative cost $\delta_k(m_k)$ among the M surviving costs up to time k. Therefore, the online Viterbi algorithm provides a recursive solution to the integer optimization problem of the following form:

$$\arg\min_{m_k}\{-\log P(m_k, y_{0:k})\}, \tag{4.25}$$

If we define $\delta_k(\hat{m}_k)$ such that

$$\delta_k(\hat{m}_k) := \min_{\hat{m}_k}\{-\log P(m_k, y_{0:k})\}, \tag{4.26}$$

then, the online VA algorithm is summarized as follows:

1. Initialization at time $k = 0$ and for $i \in \{1 : M\}$:

$$\delta_0(i) = -\log p_0^{(i)} - \log d_i(y_0), \tag{4.27}$$

$$\hat{m}_0 = \arg\min_{i\in\{1:M\}}\{\delta_0(i)\} \tag{4.28}$$

2. Recursion: For $k \in \{1 : T\}$ and for $l \in \{1 : M\}$:

$$\delta_k(l) = \min_{i\in\{1:M\}}\{\delta_{k-1}(i) - \log \mathbb{P}_{k-1,k}^{(i,l)} - \log d_i(y_k)\}, \tag{4.29}$$

$$\hat{m}_k = \arg\min_{i\in\{1:M\}}\{\delta_k(i)\}, \tag{4.30}$$

Even though, the On-VA is a viable option for a real-time implementation, we will later demonstrate through simulation studies that the On-VA is less accurate than the Off-VA as expected. In the next section, we will develop a new noncontinuum state estimator, which is based on a moving horizon estimation approach that will be shown to be as accurate as the Off-VA, and as efficient as On-VA for online implementation.

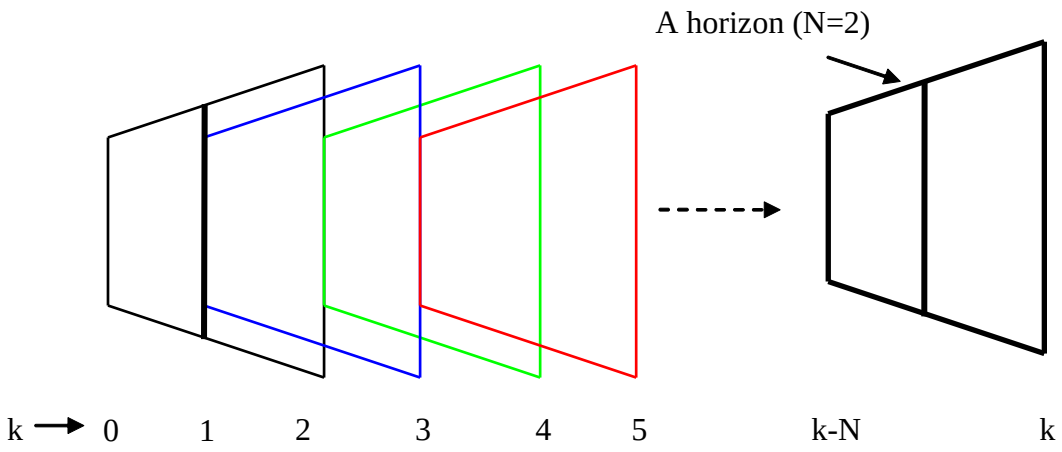

Figure 4.2: Moving horizon scheme.

4.3 Moving Horizon Estimation Approach

In order to develop a state estimator that is computationally feasible to be implemented online, a new optimality criterium for a moving horizon estimation of noncontinuum state (MHENS) is defined as

$$\arg \min_{\hat{m}_{T-N:T}} \{\phi_{MHE}\} : \phi_{MHE} = -\log P(m_{T-N:T}, y_{0:T}). \tag{4.31}$$

In this way, we solve for a finite set of the optimum state sequence over a moving window as shown in Figure 4.2. At each time step, the oldest observation sample will be eliminated upon the arrival of the newest sample, thus keeping a fixed horizon length N with $N+1$ observation samples available at each time T for the estimation.

By making use of Markov properties, ϕ_{MHE} in Eq. (4.31) can be reformulated as follows:

$$\begin{aligned}
\phi_{MHE} &= -\log P(m_{T-N:T}, y_{0:T}), \\
&= -\log[P(m_{T-N}, y_{0:T-N}) P(m_{T-N+1:T}, y_{T-N+1:T}|m_{T-N})], \\
&= -\log[P(m_{T-N}, y_{0:T-N})] - \log[P(m_{T-N+1:T}, y_{T-N+1:T}|m_{T-N})], \\
&= -\log[P(m_{T-N}, y_{0:T-N})] - \sum_{k=T-N+1}^{T} \log P(m_k|m_{k-1}) - \sum_{k=T-N+1}^{T} \log P(y_k|m_k).
\end{aligned} \tag{4.32}$$

If $\phi_{T-N}(j) := -\log[P(m_{T-N} = j, y_{0:T-N})]$, at time T, for which $T \geq N$, the

optimization problem in Eq. (4.31) becomes

$$\begin{aligned}\arg\min_{\hat{m}_{T-N:T}}\{\phi_{MHE}\}:\phi_{MHE} &= \sum_{j=1}^{M}\alpha_{T-N}^{(j)}\phi_{T-N}(j) - \sum_{k=T-N+1}^{T}\sum_{i=1}^{M}\sum_{j=1}^{M}\gamma_{k-1}^{(i)}\alpha_{k}^{(j)}\log\mathbb{P}_{k-1,k}^{(i,j)} \\ &- \sum_{k=T-N+1}^{T}\sum_{j=1}^{M}\alpha_{k}^{(j)}\log d_j(y_k), \end{aligned} \tag{4.33}$$

subject to:

$$\begin{aligned}\gamma_{k-1}^{(i)} &= \begin{cases}1 & \text{if} \quad i=\hat{m}_{k-1} \\ & \\ 0 & \text{if} \quad i\neq\hat{m}_{k-1}\end{cases}, \\ \alpha_{k}^{(j)} &= \begin{cases}1 & \text{if} \quad j=\hat{m}_{k} \\ & \\ 0 & \text{if} \quad j\neq\hat{m}_{k}\end{cases}, \\ \hat{m}_k &\in \{1,...,M\} \qquad k=T-N:T.\end{aligned} \tag{4.34}$$

where $\phi_{T-N}(j)$ is termed *the arrival cost*, which accounts for the cost of arriving at state j at time $T-N$ given all of the past observed data.

4.3.1 Arrival cost development

Arrival cost is important to a moving horizon estimation implementation because it summarizes the effect of the past data on the estimation of the current state [72]. In order to achieve a computationally tractable solution to the optimization problem posed in Eqs. (4.33) and (4.34), we must formulate the arrival cost in a recursive form. Using a forward procedure technique [70], the arrival cost is derived as:

$$\begin{aligned}\phi_{T-N}(j) &= -\log\left[P(m_{T-N}=j, y_{0:T-N})\right], \\ &= -\log\left[\sum_{i=1}^{M}P(y_{T-N}, m_{T-N}=j|y_{T-N-1}\{m_{T-N-1}=i\})P(y_{T-N-1}\{m_{T-N-1}=i\})\right] \\ &= -\log\left[\sum_{i=1}^{M}P(y_{T-N}|m_{T-N}=j, y_{T-N-1}\{m_{T-N-1}=i\})\right. \\ &\quad \left.P(m_{T-N}=j|y_{T-N-1}\{m_{T-N-1}=i\})P(y_{T-N-1}|m_{T-N-1}=i)P(m_{T-N-1}=i)\right] \\ &= -\sum_{i=1}^{M}\log\{P(y_{T-N-1}|m_{T-N-1}=i)P(m_{T-N-1}=i)\} - \\ &\quad \sum_{i=1}^{M}\log P(m_{T-N}=j|m_{T-N-1}=i) - \log P(y_{T-N}|m_{T-N}=j), \\ &= \sum_{i=1}^{M}\left[\phi_{T-N-1}(i) - \log\mathbb{P}_{T-N-1,T-N}^{(i,j)}\right] - \log d_j(y_{T-N}). \end{aligned} \tag{4.35}$$

4.3.2 The MHENS algorithm

Once the arrival cost $\phi_{T-N}(j)$ at time $T-N$ is derived, the final form of a moving horizon estimation for noncontinuum state (MHENS) is obtained by substituting the arrival cost function of Eq. (4.35) into Eq. (4.33) to give

$$\begin{aligned}\arg\min_{\hat{m}_{T-N:T}}\{\phi_{MHE}\}:\phi_{MHE} &= \sum_{j=1}^{M}\sum_{i=1}^{M}\alpha_{T-N}^{(j)}\gamma_{T-N-1}^{(i)}\big[\phi_{T-N-1}(i)-\log\mathbb{P}_{T-N-1,T-N}^{(i,j)}\big]\\ -\sum_{k=T-N+1}^{T}\sum_{i=1}^{M}\sum_{j=1}^{M}\gamma_{k-1}^{(i)}\alpha_{k}^{(j)}\log\mathbb{P}_{k-1,k}^{(i,j)} &- \sum_{k=T-N+1}^{T}\sum_{j=1}^{M}\alpha_{k}^{(j)}\log d_j(y_k),\end{aligned} \tag{4.36}$$

subject to:

$$\begin{aligned}\gamma_{k-1}^{(i)} &= \begin{cases}1 & \text{if } \ i=\hat{m}_{k-1}\\ 0 & \text{if } \ i\neq\hat{m}_{k-1}\end{cases},\\ \alpha_{k}^{(j)} &= \begin{cases}1 & \text{if } \ j=\hat{m}_{k}\\ 0 & \text{if } \ j\neq\hat{m}_{k}\end{cases},\\ \hat{m}_k &\in \{1,...,M\} \qquad k=T-N:T.\end{aligned} \tag{4.37}$$

The objective function of Eqs. (4.36) and (4.37) constitutes an integer optimization problem. In this study, we have employed an enumerative combinatorial optimization method [14] to provide the solution to the integer optimization problem of Eq. (4.36). Combinatorial optimization is an integer-based method in which the set of feasible solutions is discrete or can be reduced to a discrete one, with the objective of finding the best possible solution [14]. Unlike linear programming for a continuous-valued optimization, whose feasible region is a convex set and the optimum solution can be obtained using the calculus-based derivative approaches, in combinatorial problems, one must search a lattice of feasible points or, in the mixed-integer case, a set of disjoint line segments, to find an optimal solution.

When $N=0$, Eqs. (4.36) reduces to

$$\arg\min_{\hat{m}_T}\{\phi_{MHE}\}:\phi_{MHE}=\sum_{j=1}^{M}\sum_{i=1}^{M}\alpha_{T}^{(j)}\gamma_{T-1}^{(i)}\big[\phi_{T-1}(i)-\log\mathbb{P}_{T-1,T}^{(i,j)}\big]-\sum_{j=1}^{M}\alpha_{T}^{(j)}\log d_j(y_T), \tag{4.38}$$

subject to Eq. (4.37). It is interesting to note from Eq. (4.37)) that when $N=0$, the MHENS reduces directly to a point estimation problem, the solution of which is the same as that provided by online Viterbi algorithm (On-VA).

MHENS for a discrete-event system

In this section, we consider a hidden Markov process in which the measurements are discrete symbols. In this case, the observation can only take on a set of finite obser-

vation symbols (i.e., $y_k = z$ such that $z \in \{1, ..., q\}$). The probability distribution can be characterized by observation matrix D such that

$$P(y_k = z|m_k = j) = D_{j,z} \quad \text{for} \quad z \in \{1, ..., q\} \quad \text{and} \quad j \in \{1, ..., M\}. \tag{4.39}$$

Therefore, Eq. (4.39) can be substituted into Eq. (4.36) to give a simplified integer optimization problem of the form:

$$\begin{aligned} \arg \min_{\hat{m}_{T-N:T}} \{\phi_{MHE}\} : \phi_{MHE} \quad = \quad & \sum_{i=1}^{M} \sum_{j=1}^{M} \gamma_{T-N-1}^{(i)} \alpha_{T-N}^{(j)} \left[\phi_{T-N-1}(i) - \log \mathbb{P}_{T-N-1,T-N}^{(i,j)}\right] \\ & - \sum_{k=T-N+1}^{T} \sum_{i=1}^{M} \sum_{j=1}^{M} \gamma_{k-1}^{(i)} \alpha_{k}^{(j)} \log \mathbb{P}_{k-1,k}^{(i,j)} \\ & - \sum_{k=T-N}^{T} \sum_{j=1}^{M} \sum_{z=1}^{q} \sigma_{k}^{(j,z)} \log D_{j,z}, \end{aligned} \tag{4.40}$$

subject to:

$$\begin{aligned} & \gamma_{k-1}^{(i)} = \begin{cases} 1 & if \quad i = \hat{m}_{k-1} \\ & \\ 0 & if \quad i \neq \hat{m}_{k-1} \end{cases}, \\ & \alpha_{k}^{(j)} = \begin{cases} 1 & if \quad j = \hat{m}_{k} \\ & \\ 0 & if \quad j \neq \hat{m}_{k} \end{cases}, \\ & \sigma_{k}^{(j,z)} = \begin{cases} 1 & if \quad j = \hat{m}_{k}, \quad z = y_k \\ & \\ 0 & if \quad j \neq \hat{m}_{k}, \quad z \neq y_k \end{cases}, \\ & \hat{m}_k \in \{1, ..., M\}. \end{aligned} \tag{4.41}$$

MHENS for a stochastic continuous dynamic system

Let us consider a switching discrete-time linear system given as

$$\begin{aligned} & x_k = F^{(m_k)} x_{k-1} + B^{(m_k)} u_{k-1} + w_{k-1}, \quad && w_k \in N(0, Q_k), \\ & y_k = H^{(m_k)} x_k + v_k, && v_k \in N(0, R_k), \\ & m_k = \eta(m_{k-1}, \lambda) \end{aligned} \tag{4.42}$$

where $x_k \in R^n$, $u_k \in R^p$, $y_k \in R^q$ denote state, input, and observation vectors respectively. Both the additive process noise, w_k, and measurement noise, v_k, are assumed to be Gaussian with the covariance matrices of Q_k and R_k respectively. Therefore the continuous observation density function $d_j(y_k) = P(y_k|m_k = j)$ follows a Gaussian distribution with the mean of $H^{(m_k)} x_k$ and covariance matrix R_k. If we express $P(y_k|m_k)$ as

$$P(y_k|m_k = j) = (2/\pi)^{-\frac{q}{2}} R_k^{-\frac{1}{2}} \exp\{-\frac{1}{2} v_k^T R_k^{-1} v_k\}, \tag{4.43}$$

where $v_k = y_k - H^{(m_k=j)}$, the MHENS algorithm for a stochastic dynamic system with a continuous observation function is derived as

$$\begin{aligned}\arg\min_{\hat{m}_{T-N:T}} \{\phi_{MHE}\} : \phi_{MHE} \;=\; & \sum_{i=1}^{M}\sum_{j=1}^{M} \gamma_{T-N-1}^{(i)} \alpha_{T-N}^{(j)} \left[\phi_{T-N-1}(i) - \log \mathbb{P}_{T-N-1,T-N}^{(i,j)}\right] \\ & - \sum_{k=T-N+1}^{T} \sum_{i=1}^{M}\sum_{j=1}^{M} \gamma_{k-1}^{(i)} \alpha_{k}^{(j)} \log \mathbb{P}_{k-1,k}^{(i,j)} \\ & + \frac{1}{2} \sum_{k=T-N}^{T} \sum_{j=1}^{M} \alpha_k^{(j)} \hat{v}_k^T R_k^{-1} \hat{v}_k, \end{aligned} \tag{4.44}$$

subject to:

$$\begin{aligned} & \hat{v}_k^{(\hat{m}_k)} = y_k - H^{(\hat{m}_k)} x_k, \\ & \gamma_{k-1}^{(i)} = \begin{cases} 1 & if \quad i=\hat{m}_{k-1} \\ & \\ 0 & if \quad i\neq\hat{m}_{k-1} \end{cases}, \\ & \alpha_k^{(j)} = \begin{cases} 1 & if \quad j=\hat{m}_k \\ & \\ 0 & if \quad j\neq\hat{m}_k \end{cases}, \\ & \hat{m}_k \in \{1, ..., M\}. \end{aligned} \tag{4.45}$$

The MHENS is designed to estimate the sequence, $\hat{m}_{k-N:T}$. Therefore, at any given time T, the estimates comprise both the smoothing part (i.e., $\hat{m}_{k-N:T-1}$) and the filtering part (i.e., $\hat{m}_T$). For online implementation, only $\hat{m}_T$ is used. However, the estimated $\hat{m}_T$ depends on the most updated smoothing estimates. In order to solve for $\hat{m}_{T-N:T}$ from Eqs. (4.44) and (4.45), we need to know the continuum state sequence $x_{T-N:T}$ a priori. If these continuum states are not measurable or they can only be measured with some degree of uncertainties, The MHENS algorithm will have to be combined sequentially with an optimum continuous-valued filter, i.e., a Kalman filter [85], to provide the continuum state estimates. For a hybrid linear system, a switching Kalman filter of the following form

$$\begin{aligned} & \bar{x}_k = F^{(\hat{m}_k)} \hat{x}_{k-1} + B^{(\hat{m}_k)} u_{k-1}, \\ & \bar{y}_k = H^{(\hat{m}_k)} \bar{x}_k, \\ & P_k = F^{(\hat{m}_{k-1})} P_{k-1} (F^{(\hat{m}_{k-1})})^T + Q_k, \\ & K_k = P_k (H^{(\hat{m}_k)})^T \{H^{(\hat{m}_k)} P_k (H^{(\hat{m}_k)})^T + R_k\}^{-1}, \\ & \hat{x}_k = \bar{x}_k + K_k (y_k - \bar{y}_k), \end{aligned} \tag{4.46}$$

can be constructed and embedded as an intermediate step to provide the continuum state estimate.

Constraint handling in noncontinuum state estimation

A moving horizon estimator has the natural ability to handle constraints. Constraints are typically required when modeling bounded variables (i.e., state, input

or disturbance). Besides, other additional information about a system can be easily casted in the form of constraints to aid a state estimator performance. Constraint handling on a continuum state estimation through a moving horizon optimization has been well studied [12, 72]. In this work, we demonstrate that additional information about a system measured input can be used to constrain the system operating mode space (i.e., noncontinuum state space). For illustration purposes, we consider the following additional constraints based on the available information about the system inputs:

$$u_k \in \mathbb{U}, \quad M_i = f(u_k), \quad m_k \in \{1, ..., M_i\}. \tag{4.47}$$

In this case, the system operating mode space M_i is time varying as its value at any given time k depends on the control input u_k. Therefore, the combination of Eqs. (4.44) - (4.46) with Eq. (4.47) completes a MHENS formulation for a constrained stochastic dynamic system.

4.3.3 Performance index

In this study, the performance of MHENS will be analyzed by using a Monte Carlo simulation method [79] with the following defined performance index:

$$\text{Missing Rate (MR)} = \frac{\text{\# of false estimation}}{\text{\# of sampling instants}}\%. \tag{4.48}$$

Missing rate (MR) quantifies the MHENS performance, in term of percentage, how well the noncontinuum state sequence is estimated. For instance, a MR of 0% means we have a perfect estimation with no missing point, while a MR of 100% implies all of the states are incorrectly estimated.

4.4 Case Studies

4.4.1 Case study I: Leakage detection in a water tank system

Let us consider a storage water tank system with water level indicators installed on it as shown in Figure 4.3. The water level indicator readings are characterized as discrete symbols chosen from a finite set of alphabets (i.e., $\{a, b, c\}$, which indicate different height (m) of water in the tank as shown in Figure 4.3). The aim is to determine if there is a leakage from the tank given the water level indicator readings. In this case, we cast the problem as two discrete-event states such that state "1" represents "leakage", while state "2" represents "No leakage". This problem can be represented by using a hidden Markov model as shown in Figure 4.4. We have assumed that the hidden Markov parameters given in Figure 4.4 are available as

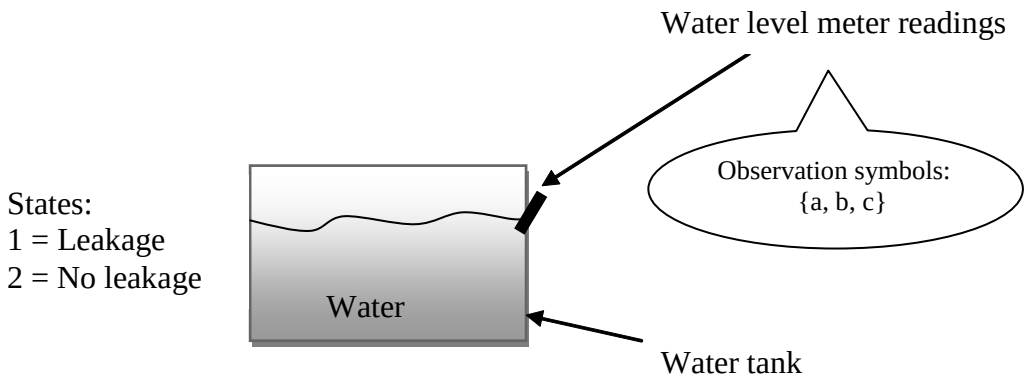

Figure 4.3: Leakage detection in a storage water tank system.

these can be obtained using different system identification methods [70] from the historical observation data of the system.

Using the performance index defined in Section (4.3.3), we compare the performances of the three algorithms, which are the offline Viterbi algorithm (Off-VA) [70], the online Viterbi algorithm (On-VA), and our proposed method, the moving horizon estimation for noncontinuum state (MHENS). Note that only the On-VA and MHENS can be implemented online, while Off-VA can only be implemented offline and it is considered for a performance assessment analysis only.

Figure 4.5 compares the performance of the online MHENS with those of the offline Viterbi algorithm (Off-VA) and the online Viterbi algorithm (On-VA). The results show that MHENS has the same level of accuracy with the Off-VA with the missing rate MR = 3%, while MHENS is implemented online in the same way with On-VA, which has a lower estimation accuracy (i.e., MR = 10%).

In order to see the effect of the horizon length N on the performance of the MHENS, we have used a Monte Carlo simulation analysis [79] to simulate $10,000$ random samples with 100 iterations in each case studied. This analysis is repeated for a varying horizon length N and the results are shown in Figure 4.6. The MR for Off-VA and On-VA remain fairly constant at 5.84% and 10.45% respectively since they are independent of horizon length N. However, it is interesting to see from Figure 4.6, how the MR of the MHENS decreases rapidly as the horizon length increases and then converges to the MR of the Off-VA from the point when $N = 5$.

4.4.2 Case study II: Continuous stirred tank reactor

The continuous stirred tank reactor (CSTR) shown in Figure 4.7 is one of the most common and important chemical processes, which often exhibits complex behavior such as steady-state multiplicities. The possibility of steady-state multiplicity im-

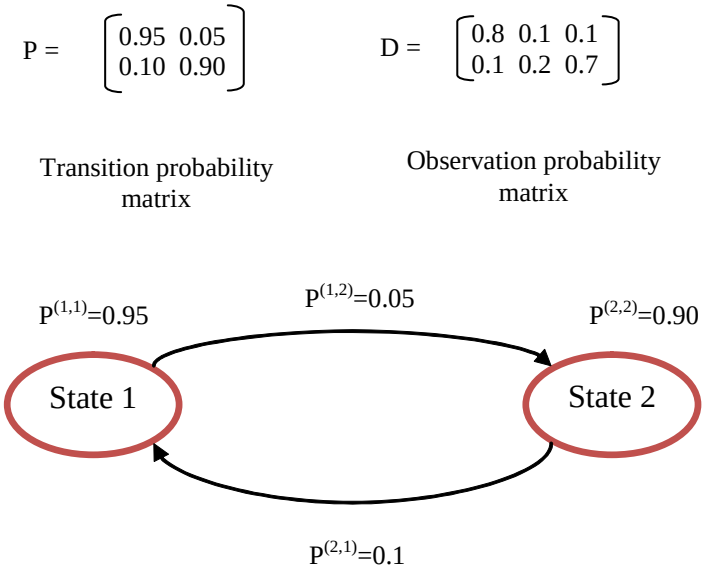

Figure 4.4: Hidden Markov model and parameters for a leakage detection in a storage water tank system.

plies that the process dynamics can easily switch between multiple operating regions at the slightest change in the system conditions either due to process fault or an undesirable disturbance input [83].

To achieve an effective operation, monitoring, and control of such system, which has tendency to switch in between multiple operating regions,a state estimator that has the capability to estimate a real-time operating mode is required. Besides, safety analysis of CSTR towards undesirable changes in operating conditions will demand a noncontinuum state estimator that will be able to estimate the active system operating mode based on the available measurement data.

A CSTR model

Different types of models with various levels of complexities have been developed for CSTR in the literature. In this work, we consider a CSTR model presented in Senthil et al. (2006) [83]. The process involves an irreversible, exothermic reaction $A \rightarrow B$, which occurs in a constant volume reactor cooled by a coolant stream q. The process dynamics equations are summarized as follows:

$$\frac{dC_A}{dt} = \frac{q}{V}(C_{A0} - C_A) - k_0 C_A e^{-E/RT}, \tag{4.49}$$

$$\frac{dT}{dt} = \frac{q}{V}(T_0 - T) - \frac{(-\Delta H C_A k_0)}{\rho C_p} e^{-E/RT} + \frac{\rho_c C_{pc} q_c}{\rho C_p V}[1 - e^{-hA/q_c \rho C_p}]\{T_{c0} - T\}, \tag{4.50}$$

where C_A, q and T are the concentration (mol/L), flow rate (L/min), and temperature (K) inside the reactor respectively. V is the reactor volume, k_0 is the reaction

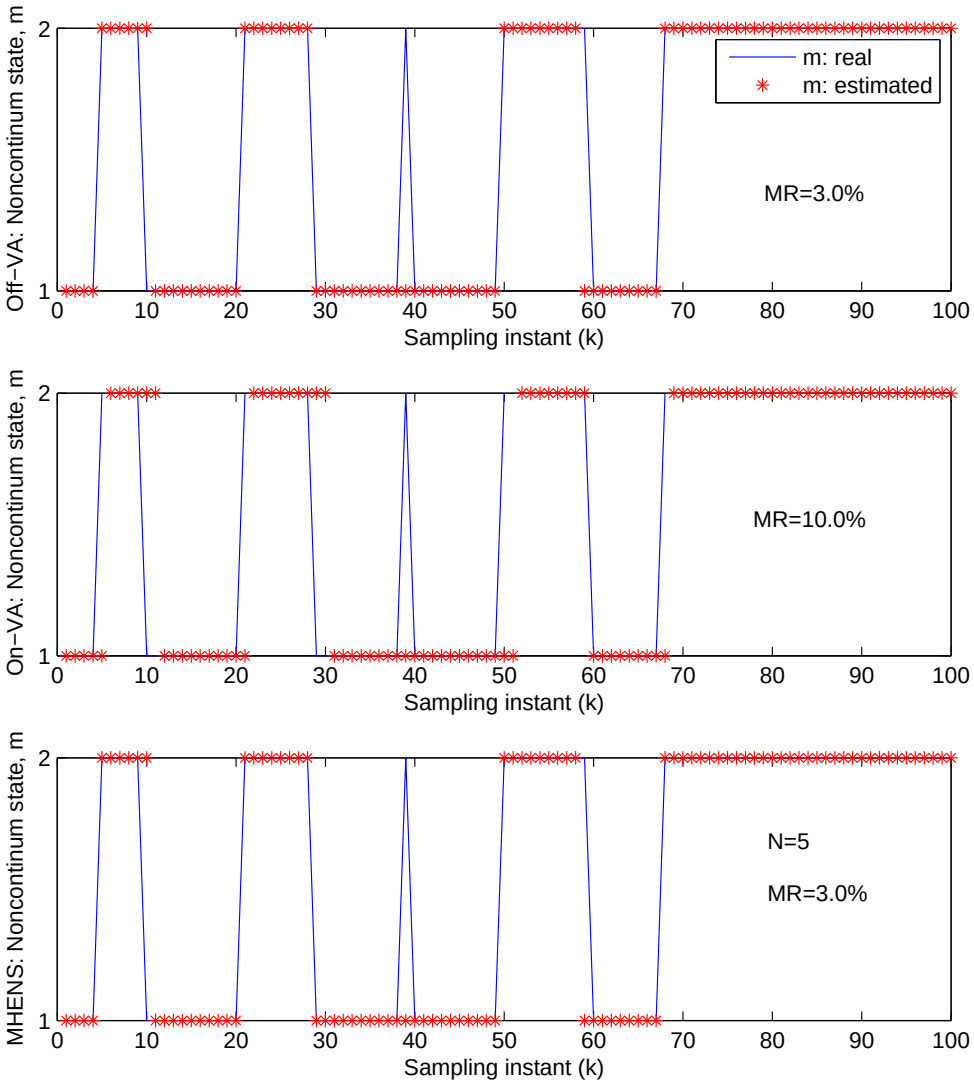

Figure 4.5: Noncontinuum state estimation in a water tank system.

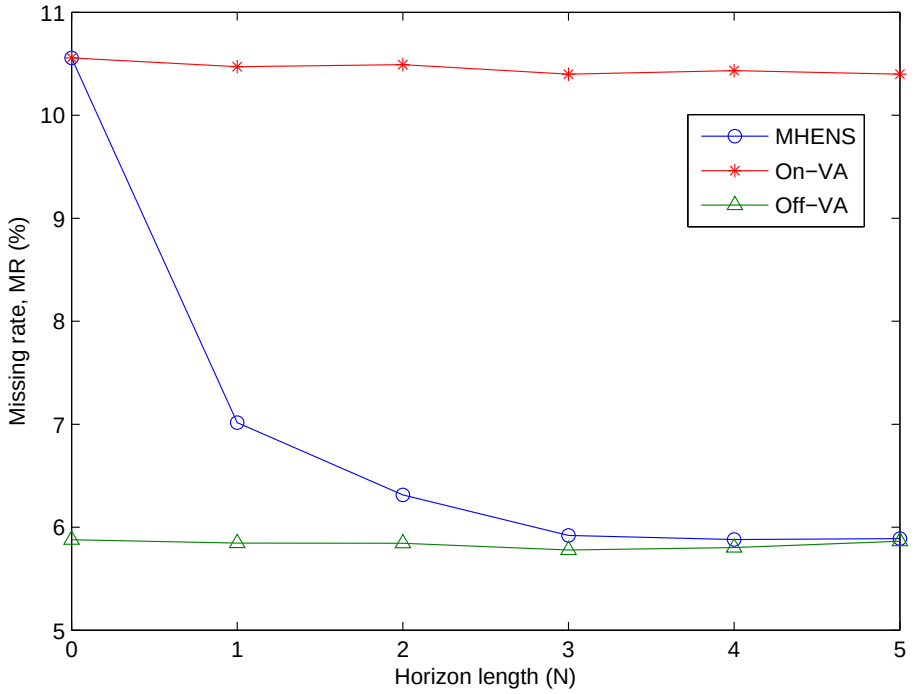

Figure 4.6: Effect of the horizon length N on the MHENS performance.

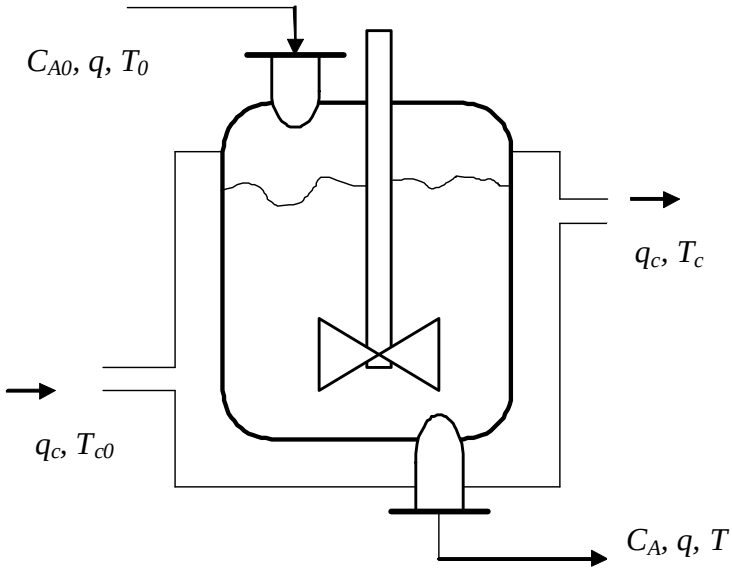

Figure 4.7: A continuous stirred tank reactor (CSTR).

Table 4.1: System parameters

Parameters, (units)	Values
Reactor volume, V (L)	100
Specific heats, C_p, C_{pc} (cal/gK)	1
Heat of reaction, $-\Delta H$ (cal/mol)	-2×10^5
Activation energy term, E/R (K)	1×10^4
Reaction rate constant, k_0 (min^{-1})	7.2×10^{10}
Heat transfer term, hA $(cal/minK)$	7×10^5
Liquid density, ρ_c, ρ (g/L)	1×10^3

Table 4.2: Multiple operating modes

Process variables, (units)	1	2	3	4	5
Reactor conc., $C_A(mol/L)$	0.0795	0.0885	0.0989	0.1110	0.1254
Reactor temp.,, $T(K)$	443.46	441.15	438.78	436.31	433.69
Coolant flowrate, $q_c(L/min)$	97	100	103	106	109
Feed conc., $C_{A0}(mol/L)$	1	1	1	1	1
Feed temp., $T_0(K)$	350	350	350	350	350
Coolant temp., $T_{c0}(K)$	350	350	350	350	350
Process flowrate, $q(L/min)$	100	100	100	100	100
Damping factor, DF,	0.661	0.540	0.416	0.285	0.141
Frequency, $Fr(rad/s)$	3.93	3.64	3.34	3.03	2.71

rate, ΔH is the reaction heat, ρ is the density, C_p is the specific heat, while U and A are the effective heat transfer coefficient and area respectively.

If we define $x := [C_A, T]^T$ as the continuum states; $u = q$ as the controlled input variable; $e = q_c$ as the disturbance variable, and by denoting the operating mode at time k as $(m_k \in M)$, then the nonlinear CSTR model of Eqs. (4.49) and (4.50) can be discretized and linearized around different set of operating conditions to conform to the switching linear system of Eq. (4.42)

The system parameters as well as the five sets of operating modes considered in this work as summarized in Tables 4.1 and 4.2 are obtained from the work of Senthil et al. (2006) [83]. The switch in system operating modes is based on the variation of the coolant flow rate (q_c). The switching transition function that defines the changes from one operating mode into the other is not known a priori, but it follows a hidden Markov model (HMM).

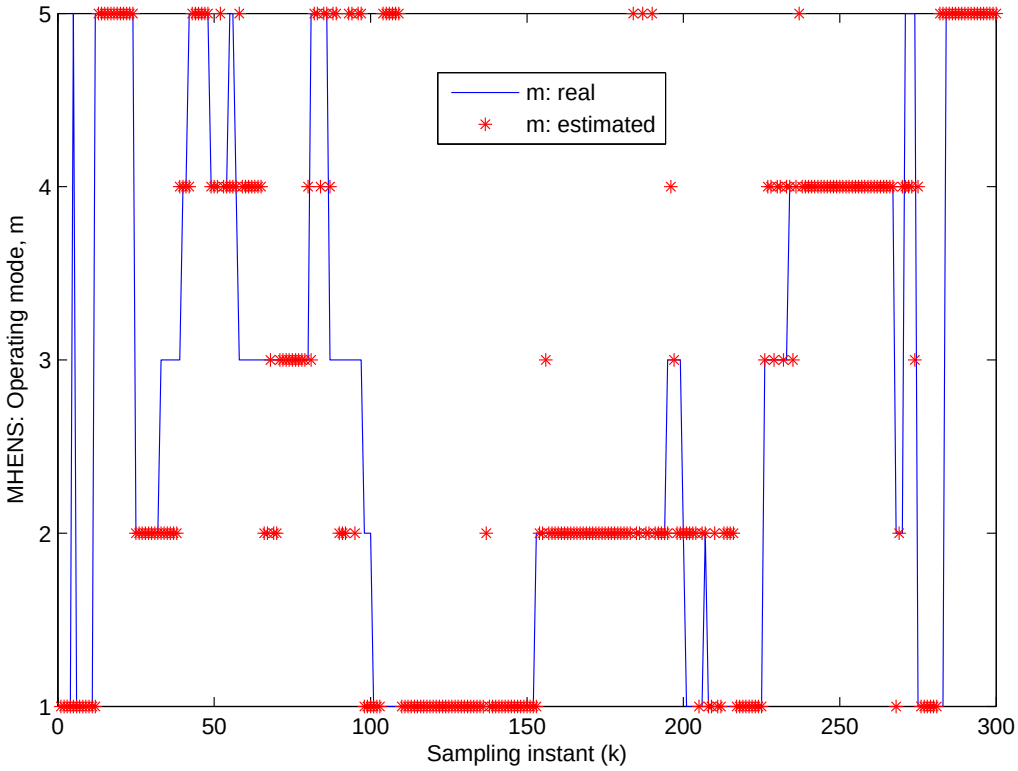

Figure 4.8: Operating mode estimation: m.

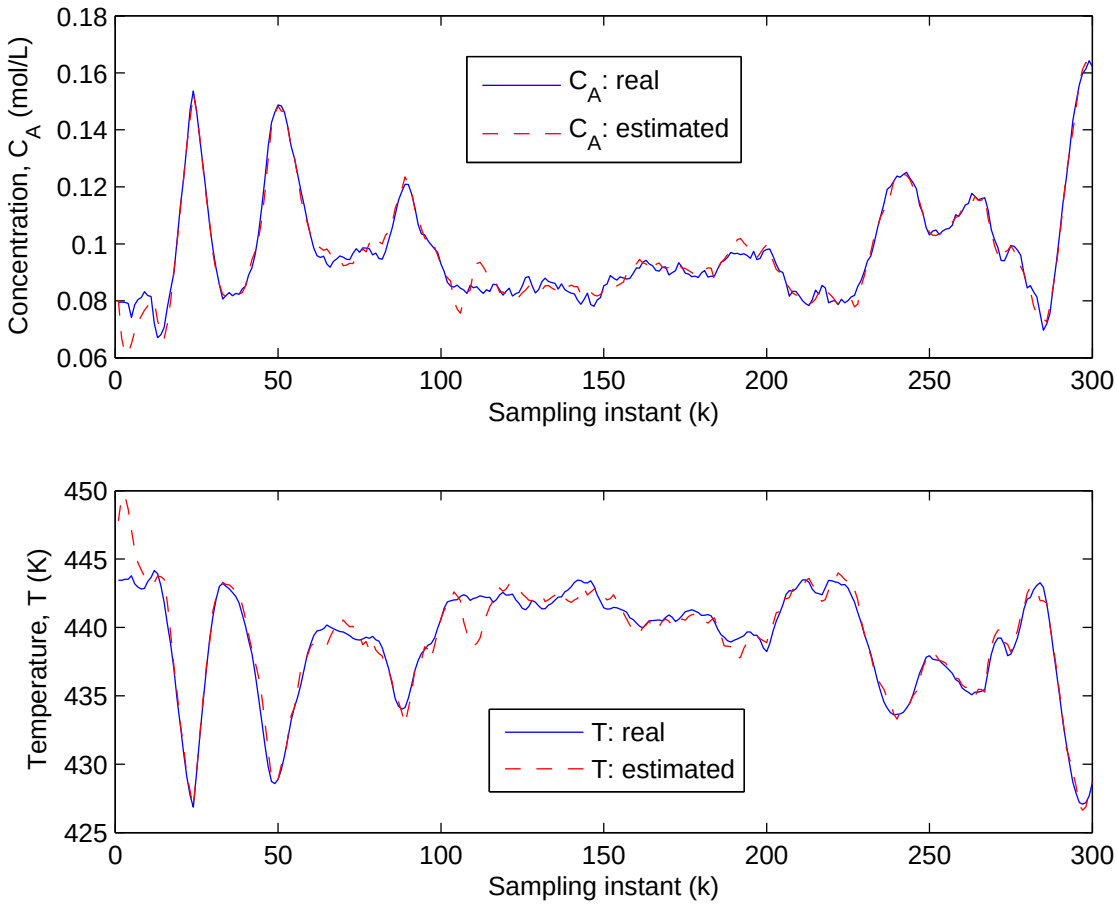

Figure 4.9: Concentration and temperature estimates.

Table 4.3: Effect of the horizon length (N) and the incorporating constraints

No Constraint	MR	CPU time (sec)
N=1	17.67%	5.89
N=2	16.67%	27.17
N=3	14.50%	176.49
Constraint	MR (%)	CPU time (sec)
N=1	17.00%	5.21
N=2	16.67%	22.15
N=3	13.67%	117.40

Noisy temperature and concentration measurements

In this section, we will assume that both the temperature and concentration are measurable, but with some degree of uncertainties. The process and measurement noise covariance matrices are assumed to be

$$Q_k = \begin{pmatrix} 0.001^2 & 0 \\ 0 & 0.1^2 \end{pmatrix}, \quad R_k = \begin{pmatrix} 0.005^2 & 0 \\ 0 & 1.50^2 \end{pmatrix}. \tag{4.51}$$

The errors in initial conditions for both temperature and concentration are assumed to be 1% of their true values. The simulation results of the operating mode estimation as well as estimated temperature and concentration dynamics are shown in Figure 4.8 and Figure 4.9. It can be seen from Figure 4.8 that the estimator is able to estimate well the operating mode. The results clearly demonstrate that the developed state estimator can be effective in estimating the switching operating modes as a function of time.

Effect of the horizon length and incorporating constraints

Among several advantages of a state estimator development, which is based on a moving horizon approach is the ability to use horizon length (N) as an additional degree of freedom to improve state estimation accuracy and the effectiveness in handling system constraints. As shown in Table 4.3, increasing the horizon length, while keeping other factor constant, will lead to a lower missing rate (MR) for noncontinuum state estimation. However, as shown in Table 4.3, the computational time can be rapidly increased with increase in the horizon length.

By observing critically an unconstrained noncontinuum state estimation shown in Figure 4.8, one can easily see that from time $k = 100$ to $k = 200$, the real noncontinuum state m switches only between operating mode 1 to 3. This observation occurs, each time when the change in the control input signal is positive. This additional information from the control input can be casted as constraints to improve

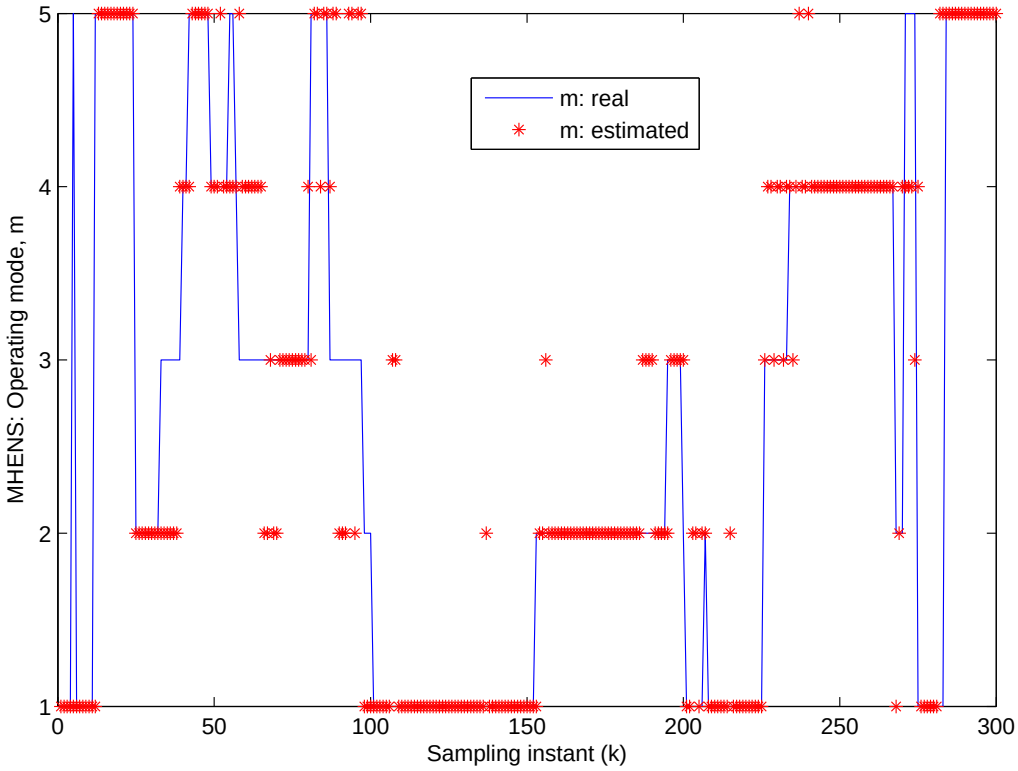

Figure 4.10: Operating mode estimation with constraints: m.

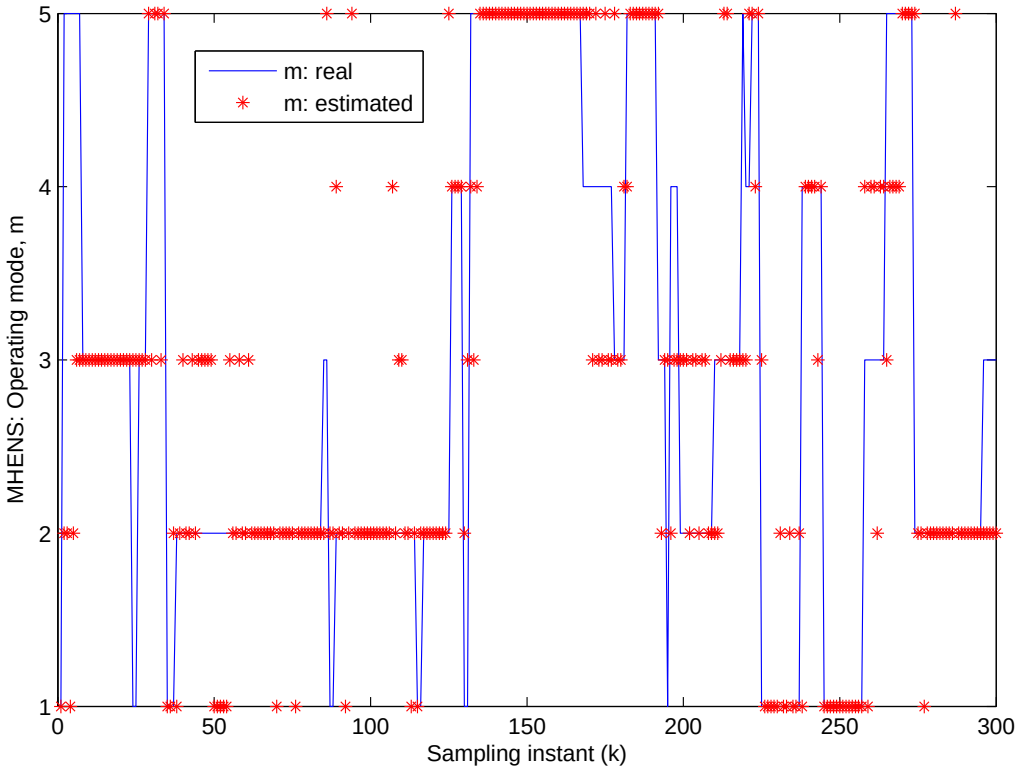

Figure 4.11: Operating mode estimation with no constraints: m.

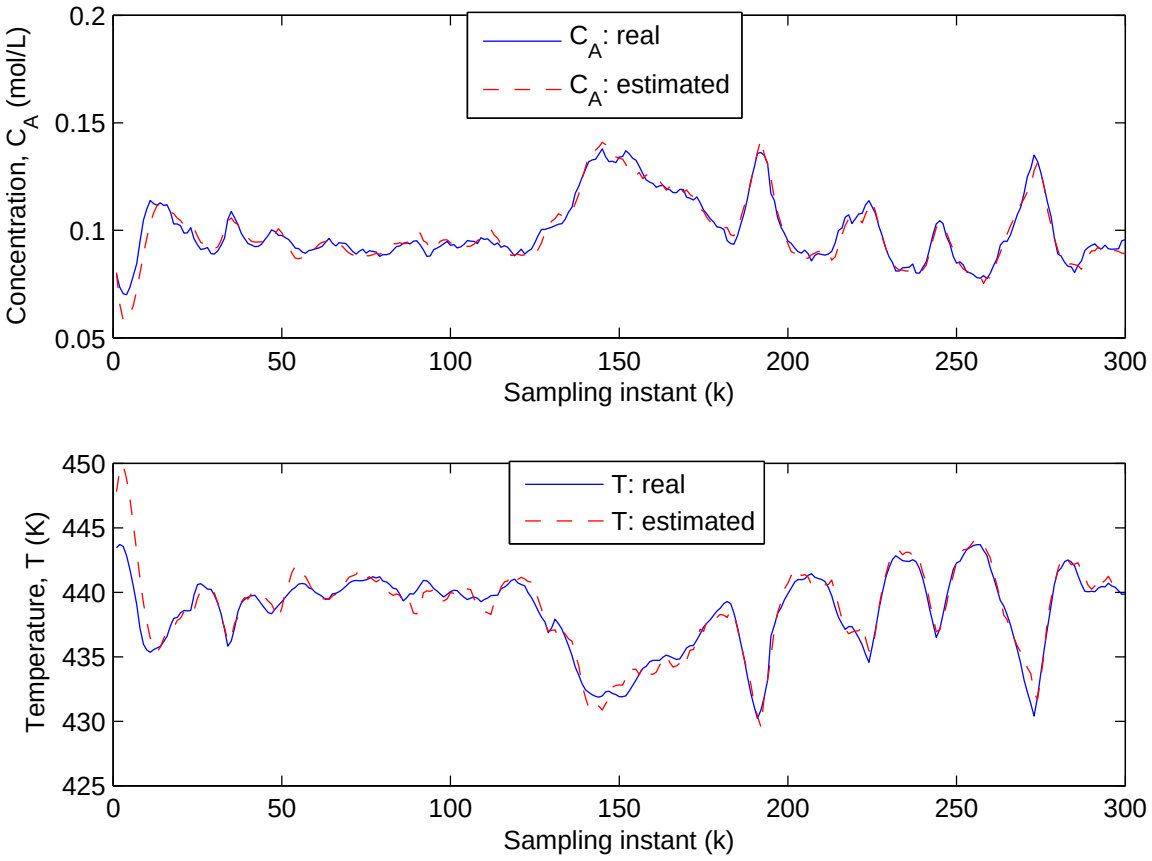

Figure 4.12: Concentration and temperature estimates.

the MHENS performance. In order to assess the performance of the MHENS when this information is taken into consideration, the following constraints are considered and incorporated in the MHENS algorithm:

$$\Delta u_k > 0, \qquad m_k \in M_i : \quad M_i = 3, \tag{4.52}$$

$$\Delta u_k \leq 0, \qquad m_k \in M_i : \quad M_i = 5. \tag{4.53}$$

Δu_k is the change in input at time k and M_i denote sets of operating conditions. Figure 4.10 shows a real-time performance of MHENS in estimating the system operating mode when the constraints are included. The MHENS makes use of the additional information provided by the constraints to improve the estimation. Between the time interval, $k = 100 : 233$, during which $\Delta u_k > 0$, the MHENS imposes the constraints as defined in the Eqs. (4.52)-(4.53) to limit the noncontinuum state domain (i.e., $M_i = 3$). If we quantitatively compare the state estimation results when there are no constraints with those when the constraints are imposed as summarized in Table 4.3, we can clearly see that the missing rate (MR), as well as the computational time, is much lower when the constraints are imposed. This indicates that the switching operating mode has been better estimated with less computational time.

Effect of using noisy temperature measurement only

In a practical situation, the online measurement of the reactor concentration is often difficult, while the measurement of temperature is relatively easy and available. In this section, the performance of the developed state estimator is tested when the only observation available is a noisy temperature measurement. In this case, the standard deviation of the temperature measurement noise is assumed to be $\delta_{v,1} = 1.50K$. The state estimator performances in estimating the switching operating mode as well as the reactor concentration and the temperature are shown in the Figure 4.11 and Figure 4.12. If the constraints given in the form of Eqs. (4.52)-(4.53) are imposed, Figure 4.13 and Figure 4.14 show that switching operating mode as well as the reactor concentration and the temperature are better estimated.

4.5 Conclusion

An online noncontinuum state estimation, which is based on a moving horizon approach for switching systems that follow a HMM with either a discrete- or continuous-valued noisy measurements, is proposed in this study. The arrival cost, which summarizes the effect of past and *a prior* information on the current states, is developed. The effects of horizon length as well as constraints handling on MHENS performance

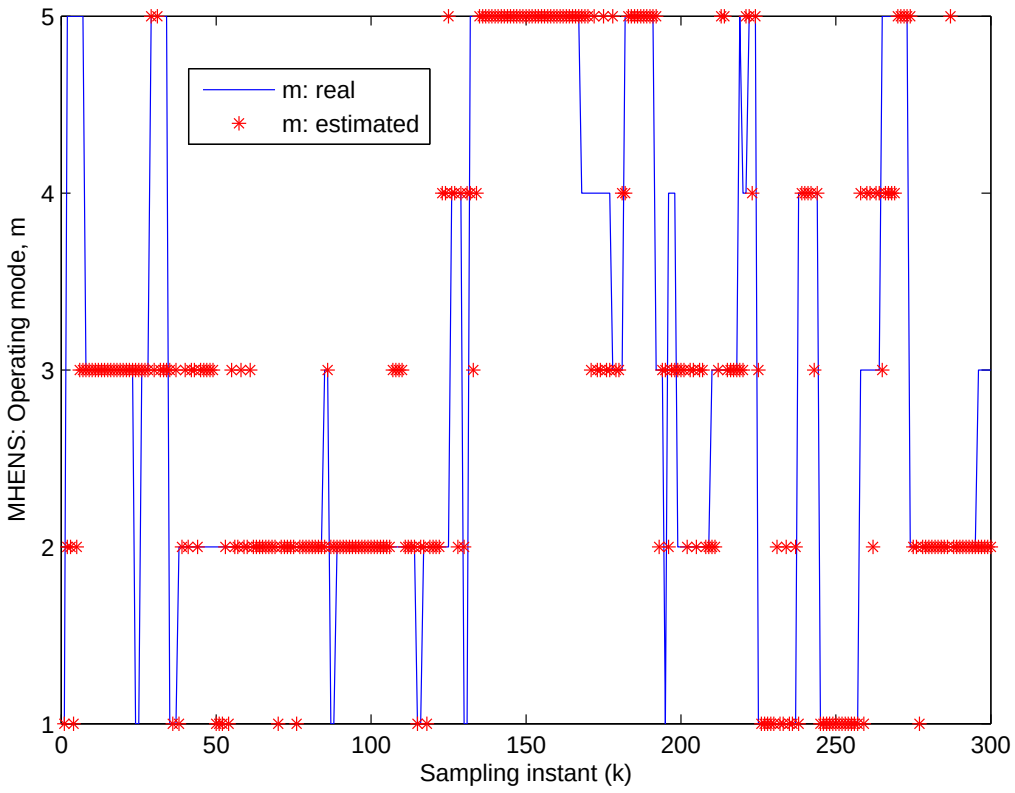

Figure 4.13: Operating mode estimation with constraints: m.

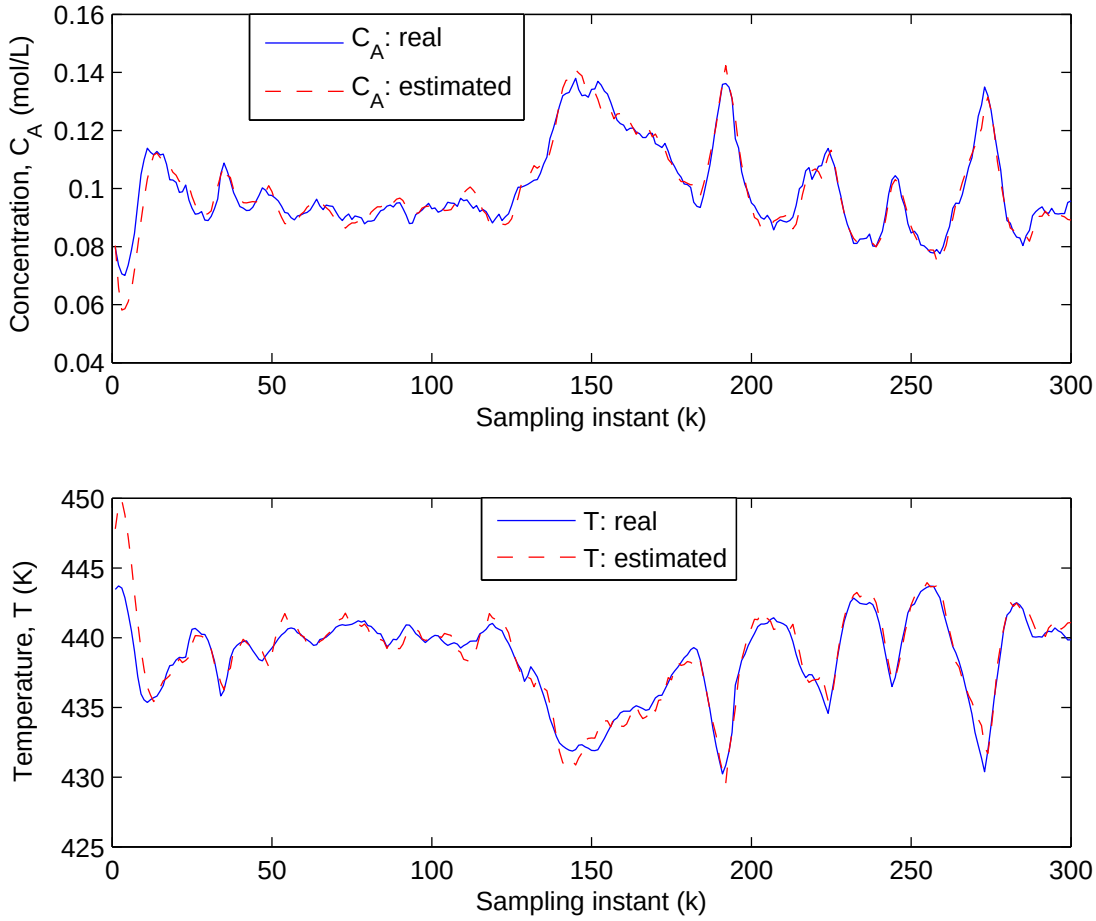

Figure 4.14: Concentration and temperature estimates.

are quantitatively analyzed. The simulation studies on a water tank system for a leakage detection problem as well as on a continuous stirred tank reactor for an operating mode estimation problem have shown that the developed noncontinuum state estimator is effective.

Chapter 5

Development of a Simultaneous Continuum and Noncontinuum States Estimator

5.1 Introduction

[1]Most of the hybrid state estimation methods that exist in the literature use sequential approach largely because it is intuitively the easier of the two approaches to develop or formulate. Besides, combination of different types of filters can be tried to achieve one form of improvement or the other. However, the major setback of this method is the interaction effects of two filters, especially if there are other external constraints desired to be satisfied by the system [72]. Besides, a hybrid state estimation that uses such an approach often poses different implementation challenges. Another approach to a hybrid state estimation development is called a simultaneous approach, in which a single filter with a single objective function is formulated to simultaneously estimate both the continuum and noncontinuum states. The development of such a filter is non trivial, but it has the advantage of addressing a hybrid state estimation problem in a unified and systematic way. The work presented in this chapter belongs to the simultaneous approach. A moving horizon estimation (MHE) is one of the few methods, which provides a platform to develop a simultaneous continuum and noncontinuum states estimation largely because a state estimation problem can be casted as an optimization problem and be readily solved [72, 12, 25, 26, 67].

Although, a moving horizon estimation reduces the computational burden of solving a full information estimation problem by considering a finite horizon of the measurement data, however, the process of summarizing and updating the prior

1. *This chapter has been published as "M.J. Olanrewaju, B. Huang, and A. Afacan. Development of a simultaneous continuum and noncontinuum state estimator with application on a distillation process, AIChE Journal, 2011, DOI 10.1002/aic, Vol.00, No. 0."*

information from the past data (i.e., arrival cost), is non-trivial [72, 68, 91]. The problem of the arrival cost development will surely be further complicated by the presence of noncontinuum states. This is because the arrival cost for a hybrid moving horizon estimator must not only summarize the past data based on the continuum state evolution, but also must be able to account for the past history of the system mode transition trajectory. In Chapter 4, a moving horizon estimation method was used to develop noncontinuum state estimator for a class of switching dynamical system. A detailed derivation of an arrival cost for noncontinuum state moving horizon estimation was provided. When applying the noncontinuum state estimator to the switching dynamic system, a Kalman filter is recommended to approximately reproduce the continuum state in order to sequentially estimate the noncontinuum state (i.e., switching sequence).

In this chapter, a generalized hybrid state estimation technique, which is based on a moving horizon approach to achieve a simultaneous estimation of both the continuum and noncontinuum states from a single objective function, is developed. Arrival cost for a hybrid moving horizon estimator (HMHE) will be derived. The effects of constraints, process and measurement noise levels, and a moving horizon length on the simultaneous estimation of both the continuum and noncontinuum states will be studied. To test the practical reliability of the proposed estimation method, a detailed experimental work will be carried out on a distillation process to estimate the top product composition as well as the operating mode change due to the switching dynamics in the vapor boilup using the available noisy temperature measurements.

5.2 A Hybrid Process Model

Consider once again, the following switching discrete process model:

$$\begin{aligned} &m_k = \eta(m_{k-1}; \lambda), \\ &x_k = f_{m_k}\{x_{k-1}, u_{k-1}; \theta\} + w_{k-1}, \\ &y_k = g_{m_k}(x_k; \beta) + v_k, \\ &m_k \in \mathbb{M}: \quad \mathbb{M} = \{1, ..., M\}, \end{aligned} \tag{5.1}$$

where $x_k \in \mathbb{R}^n$ denotes the continuum state, $u_k \in \mathbb{R}^p$ is the input and $y_k \in \mathbb{R}^q$ denotes the observed output from the system. m_k is the noncontinuum state, which denotes the system operating mode. f_{m_k} is a transition function determining the mean of x_k given x_{k-1} and m_k, while g_{m_k} is an output function determining the mean of the y_k given x_k and m_k. $w_k \in N(0, Q_k)$ and $v_k \in N(0, R_k)$ are assumed to be the additive process noise and measurement noise respectively, while the initial condition is also assumed to be Gaussian, i.e., $x_0 \in N(\bar{x}_0, P_0)$. θ and β denote the system parameters. Change in the system operating mode can be due to either a

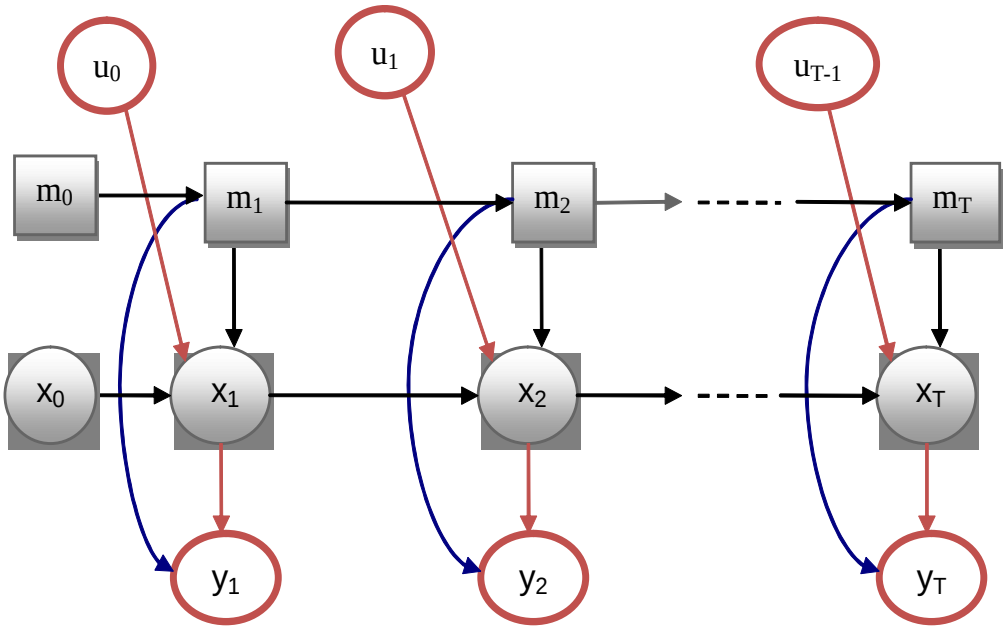

Figure 5.1: A switched dynamic system with continuum and noncontinuum states.

change in the system internal states, a case that is common in chemical systems with steady state multiplicities [43], or an unknown external disturbance input [96]. This work focuses only on state estimation of a switched system given that both the output y and input u are known.

5.3 Hybrid Moving Horizon Estimator (HMHE)

If we define $x_{0:T} = \{x_0, ..., x_T\}$ and $m_{0:T} = \{m_0, ..., m_T\}$, then, a hybrid batch state estimation can be formulated as the optimum sequences of the continuum and non-continuum states for which the conditional joint probability density function (*jpdf*) $P(m_{0:T}, x_{0:T}|y_{0:T})$ is maximized or equivalently, for which the negative logarithm of the *jpdf* $P(m_{0:T}, x_{0:T}, y_{0:T})$ is minimized:

$$\min_{\hat{m}_{0:T},\ \hat{x}_{0:T}} J_T : \quad J_T := -\ln P(m_{0:T}, x_{0:T}, y_{0:T}). \tag{5.2}$$

However, instead of using all of the available measurements $y_{0:T}$ to solve for the optimum state sequence $\hat{m}_{0:T}$ and $\hat{x}_{0:T}$ through a batch optimization, we propose a rigorous formulation of a hybrid moving horizon estimator (HMHE) objective function, which seeks to optimize the negative logarithm of the joint distribution of the states $x_{T-N:T}$ and $m_{T-N:T}$ given all of the measurement data up to time T as

$$\min_{\hat{m}_{T-N:T},\ \hat{x}_{T-N:T}} \{J_T\} : \quad J_T = -\ln\{P(x_{T-N:T}, m_{T-N:T}, y_{0:T})\}. \tag{5.3}$$

J_T can also be expressed as

$$\begin{aligned} J_T &= -\ln\{P(x_{T-N}, m_{T-N}, y_{0:T-N})\} - \\ &\quad \ln\{P(x_{T-N+1:T}, m_{T-N+1:T}, y_{T-N+1:T}|x_{T-N}, m_{T-N}, y_{0:T-N})\}. \end{aligned} \tag{5.4}$$

However, given the fact that $x_{T-N+1:T}, m_{T-N+1:T}$ and $y_{T-N+1:T}$ are conditionally independent on $y_{0:T-N}$, given x_{T-N} and m_{T-N} (see Figure 5.1, and using the Markov property), Eq. (5.4) can be reduced to

$$\begin{aligned} J_T &= -\ln\{P(x_{T-N}, m_{T-N}, y_{0:T-N})\} - \\ &\quad \ln\{P(x_{T-N+1:T}, m_{T-N+1:T}, y_{T-N+1:T}|x_{T-N}, m_{T-N}). \end{aligned} \tag{5.5}$$

If we define each term of Eq. (5.5) as follows:

$$\phi_{T-N} = -\ln(P(x_{T-N}, m_{T-N}, y_{0:T-N}), \tag{5.6}$$

and

$$J_{T-N+1:T} = -\ln\{P(x_{T-N+1:T}, m_{T-N+1:T}, y_{T-N+1:T}|x_{T-N}, m_{T-N}), \tag{5.7}$$

then, Eq. (5.3) can be simplified to

$$\min_{\hat{m}_{T-N:T},\ \hat{x}_{T-N:T}} \{J_T\} : \quad J_T = \phi_{T-N} + J_{T-N+1:T}, \tag{5.8}$$

Using Markov properties [70], the HMHE objective function can be derived from Eq. (5.8) as shown in Appendix A to give

$$\begin{aligned} \min_{\{\hat{m}_{T-N:T},\ \hat{w}_{T-N:T}\}} J_T : \quad J_T &= \phi_{T-N} - \sum_{k=T-N+1}^{T} \sum_{i=1}^{M} \sum_{j=1}^{M} \gamma_{k-1}^{(i)} \alpha_k^{(j)} \ln \mathbb{P}_{k-1,k}^{(i,j)} \\ + \sum_{k=T-N}^{T-1} \sum_{j=1}^{M} \alpha_k^{(j)} \hat{w}_k^T {Q_k}^{-1} \hat{w}_k &+ \sum_{k=T-N+1}^{T} \sum_{j=1}^{M} \alpha^{(j)} \hat{v}_k^T {R_k}^{-1} \hat{v}_k, \end{aligned} \tag{5.9}$$

subject to:

$$\begin{aligned} &\hat{x}_k = f_{\hat{m}_k}(\hat{x}_{k-1}, u_{k-1}; \theta) + \hat{w}_{k-1}, \quad k = T-N : T-1, \\ &\hat{v}_k = y_k - g_{\hat{m}_k}(\hat{x}_k; \beta), \qquad\qquad k = T-N : T, \\ &\gamma_{k-1}^{(i)} = \begin{cases} 1 \quad if \quad i = \hat{m}_{k-1} \\ \\ 0 \quad if \quad i \neq \hat{m}_{k-1} \end{cases}, \\ &\alpha_k^{(j)} = \begin{cases} 1 \quad if \quad j = \hat{m}_k \\ \\ 0 \quad if \quad j \neq \hat{m}_k \end{cases}, \\ &\hat{m}_k \in \mathbb{M} : \quad \mathbb{M} = \{1, ..., M\}. \end{aligned} \tag{5.10}$$

ϕ_{T-N} in Eq. (5.9) is the cost at time $T-N$, given all of the observations up to time $T-N$. The term ϕ_{T-N} will be referred to as the *the arrival cost*, which means

the cost associated with the uncertainty of continuum and noncontinuum states at time $T-N$, given all the observed outputs up to time $T-N$, the beginning of the horizon phase. By examining Eqs. (5.9) and (5.10), one can interpret a moving horizon estimation as an approach that tries to preserve the old information through the description of the uncertainty in the first term of Eq. (5.9) while using the most recent N+1 measurements over a sliding horizon window as shown in Figure 5.2 to achieve the desired optimum estimation of all the states within the window.

5.3.1 Arrival cost

Arrival cost is important to a moving horizon estimation approach because it summarizes the effect of the past processed data on the estimation of the current states [72]. Intuitively, the arrival cost as defined in Eq. (5.6) accounts for two things: (1) the cost associated in part with the uncertainty in the estimated noncontinuum state $\hat{m}_{T-N}$ being in mode $l \in \{1, ..., M\}$ and (2) the cost associated in part with the uncertainties in the estimated continuum state $\hat{x}_{T-N}$.

The arrival cost in Eq. (5.6) can be expanded as follows:

$$\phi_{T-N} = -\ln[P(x_{T-N}|m_{T-N}, y_{0:T-N})P(m_{T-N}, y_{0:T-N})] = \phi^x_{T-N} + \phi^m_{T-N}, \quad (5.11)$$

where $\phi^x_{T-N} = -\ln P(x_{T-N}|m_{T-N}, y_{0:T-N})$, is the arrival cost in part, due to the uncertainty in the continuum state and $\phi^m_{T-N} = -\ln(P(m_{T-N}, y_{0:T-N})$, is the arrival cost in part, due to the uncertainty in the noncontinuum state at time $T-N$.

Arrival cost: ϕ^m_{T-N}

While various forms of arrival cost of a moving horizon estimation for a continuous-valued system have been well explored in the literature [72, 68, 91], little attention has been given to arrival cost development of a moving horizon based approach to noncontinuum state estimation. In this section, we will present the arrival cost due to the noncontinuum state transition by considering the second term of Eq. (5.11) as follows:

$$\phi^m_{T-N}(j) = -\ln(P(m_{T-N}, y_{0:T-N}), \quad (5.12)$$

where $\phi^m_{T-N}(j)$ is the cost of arriving at state $m_{T-N} = j$ at time $T-N$ given all of the measurements up to time $T-N$. A recursive solution of Eq. (5.12) can be derived using a forward procedure technique as derived in Chapter 4 to obtain

$$\phi^m_{T-N}(j) = \sum_{i=1}^{M} \left[\phi_{T-N-1}(i) - \ln \mathbb{P}^{(i,j)}_{T-N-1,T-N}\right] - \ln P(y_{T-N}|m_{T-N} = j). \quad (5.13)$$

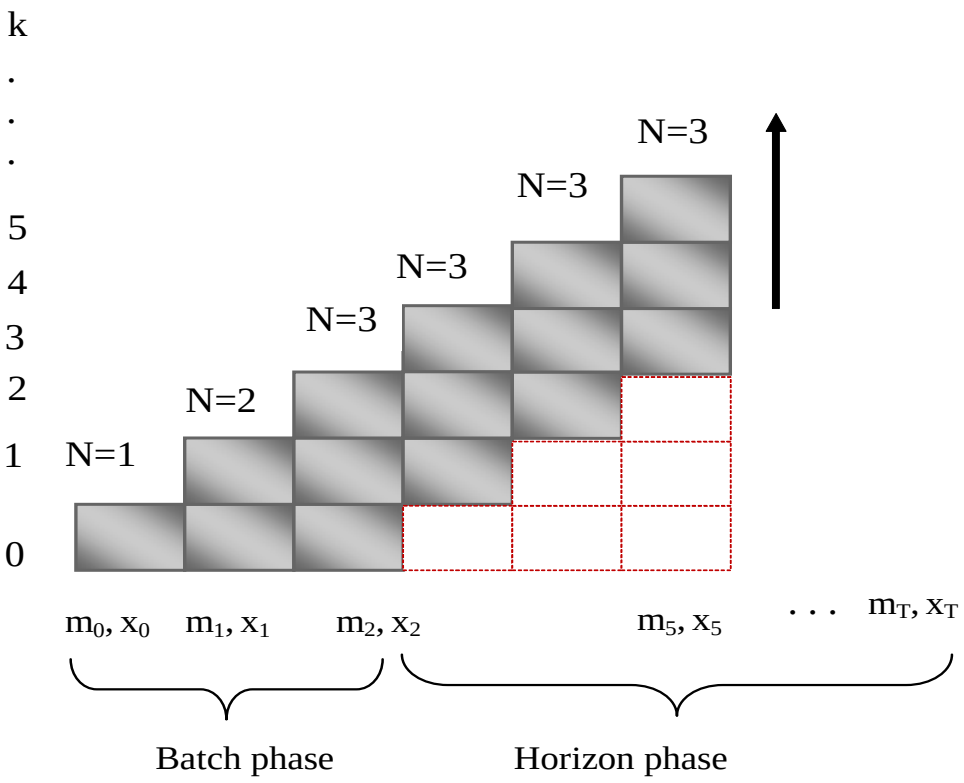

Figure 5.2: Batch and horizon phases.

Under the assumption of a Gaussian distribution, the conditional distribution density function $P(y_{T-N}|m_{T-N}=j)$ from the Eq. (5.13) can be expressed as

$$\begin{aligned} P(y_{T-N}|m_{T-N}) &= (2\pi)^{-\frac{q}{2}} R_{T-N}^{-\frac{1}{2}} \exp\big[-\frac{1}{2}\{y_{T-N}-g_{m_{T-N}}(x_{T-N};\beta)\}^T \\ &\quad R_{T-N}^{-1}\{y_{T-N}-g_{m_{T-N}}(x_{T-N};\beta)\}\big]. \end{aligned} \tag{5.14}$$

Therefore, the last term in Eq. (5.13) will become

$$-\ln P(y_{T-N}|m_{T-N}=j) = \mathcal{C}_{T-N} + \frac{1}{2} v_{T-N}^T R_{T-N}^{-1} v_{T-N}, \tag{5.15}$$

where $\mathcal{C}_{T-N} = -\ln(2\pi)^{-\frac{q}{2}} R_{T-N}^{-\frac{1}{2}}$ and $v_{T-N} = y_{T-N} - g_{m_k}(x_{T-N};\beta)$. By substituting Eq. (5.15) into Eq. (5.13), we have the following cost function:

$$\begin{aligned} \phi_{T-N}^m(j) &= \underbrace{\sum_{i=1}^{M}\big[\phi_{T-N-1}(i) - \ln \mathbb{P}_{T-N-1,T-N}^{(i,j)}\big]}_{\text{Arrival cost based on past data}} + \\ &\quad \underbrace{\frac{1}{2} v_{T-N}^T R_{T-N}^{-1} v_{T-N} + \mathcal{C}_{T-N}}_{\text{Cost based on current data at } T-N}. \end{aligned} \tag{5.16}$$

Arrival cost:ϕ^x_{T-N}

In this section, we shall derive the first term of Eq. (5.11), which is given as follows

$$\phi^x_{T-N} = -\ln P(x_{T-N}|m_{T-N}, y_{0:T-N}). \tag{5.17}$$

The derivation of an equivalent but recursive optimum solution of Eq. (5.17) for a constrained dynamic system is difficult to achieve analytically. However, for an unconstrained hybrid linear system, the recursive form of Eq. (5.17) is a well known switching Kalman filter [17, 72]. Let us first consider an unconstrained switching linear system of the form

$$\begin{aligned} x_k &= F^{(m_k)}x_{k-1} + w_k \qquad w_k \in N(0, Q_k), \\ y_k &= H^{(m_k)}x_k + v_k \qquad v_k \in N(0, R_k). \end{aligned} \tag{5.18}$$

At any given time k and the noncontinuum state m_k, Eq. (5.17) reduces to

$$\phi^x_k = -\ln P(x_k|m_k, y_{0:k}). \tag{5.19}$$

where ϕ^x_k is the cost due to the uncertainties in the continuum state given the observation sequence up to time k. Following the work of Rao and Rawlings (2002) [72], we can derive the cost function of Eq. (5.19) at any given time k as

$$\phi^x_k = \underbrace{\frac{1}{2}\hat{w}^T_{k-1}P^{-1}_k\hat{w}_{k-1}}_{\text{Arrival cost based on past data}} + \underbrace{\frac{1}{2}\hat{v}^T_k R^{-1}_k \hat{v}_k}_{\text{Observation cost at time } k} + \mathcal{E}_k. \tag{5.20}$$

The derivation of Eq. (5.20) from Eq. (5.19) as well as the definition of the parameter $\mathcal{E}_k$ are detailed in Appendix B. For a nonlinear hybrid system, an approximate extended switching Kalman filter has to be employed and the P_k will be evaluated according to the following equations [72]:

$$P_k = F_k P_{k-1} F^T_k + Q_{k-1} - F_k P_{k-1} H_k (H_k P_{k-1} H^T_k + R_k)^{-1} H_k P_{k-1} F^T_k, \tag{5.21}$$

where F_k and H_k are evaluated along the estimated trajectories according to the following equations:

$$F_k = \frac{\partial f_{\hat{m}_k}(\hat{x}_{k-1}, u_{k-1}; \theta)}{\partial x_k}. \tag{5.22}$$

$$H_k = \frac{\partial g_{\hat{m}_k}(\hat{x}_k; \beta)}{\partial x_k}. \tag{5.23}$$

In a similar way, the cost function at the time $T - N$, which is a recursive form of Eq. (5.20) can be written as

$$\phi^x_{T-N} = \underbrace{\frac{1}{2}\hat{w}^T_{T-N-1}P^{-1}_{T-N}\hat{w}_{T-N-1}}_{\text{Arrival cost based on past data}} + \underbrace{\frac{1}{2}\hat{v}^T_{T-N}R^{-1}_{T-N}\hat{v}_{T-N}}_{\text{Observation cost at } k=T-N} + \mathcal{E}_{T-N}, \tag{5.24}$$

5.3.2 A generalized HMHE

By substituting Eqs. (5.16) and (5.24) into the Eq. (5.9), a generalized hybrid moving horizon estimator can be formulated as

$$\begin{aligned}\min_{\{\hat{m}_{T-N:T},\ \hat{w}_{T-N-1:T-1}\}} \quad & J_T : J_T = \sum_{j=1}^{M}\sum_{i=1}^{M} \alpha_{T-N}^{(j)} \gamma_{T-N-1}^{(i)} \left[\phi_{T-N-1}(i) - \log \mathbb{P}_{T-N-1,T-N}^{(i,j)}\right] \\ & + \hat{w}_{k-N-1}^{T} \bar{P}_{k-N}^{-1} \hat{w}_{k-N-1} - \sum_{k=T-N+1}^{T}\sum_{i=1}^{M}\sum_{j=1}^{M} \gamma_{k-1}^{(i)} \alpha_{k}^{(j)} \ln \mathbb{P}_{k-1,k}^{(i,j)} \\ & \sum_{k=T-N}^{T-1}\sum_{j=1}^{M} \alpha_{k}^{(j)} \hat{w}_{k}^{T} \bar{Q}_{k}^{-1} \hat{w}_{k} + \sum_{k=T-N}^{T}\sum_{j=1}^{M} \alpha^{(j)} \hat{v}_{k}^{T} \bar{R}_{k}^{-1} \hat{v}_{k}, \end{aligned} \tag{5.25}$$

subject to:

$$\begin{aligned} & \hat{x}_k = f_{\hat{m}_k}(\hat{x}_{k-1}, u_{k-1}; \theta) + \hat{w}_{k-1}, \quad k = T-N : T-1, \\ & \hat{v}_k = y_k - g_{\hat{m}_k}(\hat{x}_k; \beta), \qquad\qquad k = T-N : T, \\ & \gamma_{k-1}^{(i)} = \begin{cases} 1 & if \quad i = \hat{m}_{k-1} \\ & \\ 0 & if \quad i \neq \hat{m}_{k-1} \end{cases}, \\ & \alpha_{k}^{(j)} = \begin{cases} 1 & if \quad j = \hat{m}_{k} \\ & \\ 0 & if \quad j \neq \hat{m}_{k} \end{cases}, \\ & \hat{m}_k \in \mathbb{M} : \quad \mathbb{M} = \{1, ..., M\}. \end{aligned} \tag{5.26}$$

where $\bar{P}_{k-N}^{-1} = \frac{1}{2} P_{k-N}^{-1}$, $\bar{Q}_{k}^{-1} = \frac{1}{2} Q_{k}^{-1}$ and $\bar{R}_{k}^{-1} = \frac{1}{2} R_{k}^{-1}$. Note that the parameters $\mathcal{C}_{T-N}$ and $\mathcal{E}_{T-N}$ have been neglected in the final form of HMHE in Eq. (5.25) because they are independent of the decision variables in the optimization function. The objective function of Eqs. (5.25) and (5.26) constitutes a mixed integer nonlinear programming (MINLP) problem.

For simplicity, the general form of the MINLP problem can be posed as

$$\min_{x,m} J_T = f(x, m), \tag{5.27}$$

subject to:

$$\begin{aligned} & g(x, m) \leq 0, \\ & x \in \mathbb{X}, \\ & m \in \mathbb{M}, \qquad \text{(Integer)}. \end{aligned} \tag{5.28}$$

The function $f(x, m)$ is a nonlinear objective function and $g(x, m)$ is a nonlinear constraint function. The variables x and m are the decision variables, where m is required to be integer taking discrete values in the space $\mathbb{M} = \{1, ..., M\}$. Any decision variables $\{x, m\}$ satisfying the constraints of Eq. (5.28) is called a feasible point of Eq. (5.27) [28]. Any feasible point, whose objective function value is less than or equal to that of all other feasible points, is called optimal solution. The continuous variables in Eq. (5.27) could, for instance, describe the states (i.e. concentration,

temperature and pressure), flow rates or design parameters of a chemical process. The discrete variables, may be used to describe a change in system operating modes, the existence or non-existence of process faults, and stiction or nonstiction of control valves.

There are different methods that have been developed in the literature to solve MINLP problems. Some of the solution methods include branch-and-bound (B&B) [32], combinatorial mixed-integer optimization [28, 14], outer approximation (OA) [22, 94], extended cutting plane [28], and a generalized benders decomposition (GBD) [33]. Most of these approaches generally rely on the successive solutions of closely related nonlinear problems (NLP) [28]. In this work, we have employed a combinatorial mixed-integer optimization approach [28, 14] to provide the solution for MINLP problem of Eqs. (5.27) and (5.28).

5.3.3 State constraints

One of the major advantages of a moving horizon state estimation formulation is the ability to handle system constraints. Constraints are typically used to model bounded variables (i.e., states, input or disturbance). Besides, other additional information about a system can be easily casted in the form of constraints to improve state estimation performance. Constraint handling on a continuum state estimation through a moving horizon optimization has been well studied. In this work, we demonstrate that additional information about a system can be used to constrain the system operating modes space. For illustration purposes, we consider the following additional constraints as

$$u_k \in \mathbb{U}, \quad M_i = f(u_k), \quad m_k \in \{1, ..., M_i\}, \tag{5.29}$$

$$x_k \in \mathbb{X}, \tag{5.30}$$

$$w_k \in \mathbb{W}. \tag{5.31}$$

In this case, the system operating modes space M_i is time varying as its value at any given time k depends on the control input sequences.

5.3.4 Hybrid state estimator performance index

To quantify the performance and accuracy of the developed HMHE, two different types of error criteria are used, which are:

- Average Missing Rate (AMR): This factor quantifies the performance of the HMHE with respect to noncontinuum state estimation. It expresses, in term

of percentage, how well the state estimation is able to capture the change in system modes. The AMR is defined as

$$\text{Average Missing Rate (AMR)} = \frac{\text{Total number of false estimations}}{\text{Total number of sampling instants}}\%. \tag{5.32}$$

For instance, an AMR of 0% means we have a perfect estimation with no misclassified points, while 100% implies all of the state operating modes at all sampling instances are identified incorrectly.

- Root Mean Square Error (RMSE): This factor quantifies the differences between estimated and the true values of continuum states. The RMSE is defined as

$$RMSE = \sqrt{\frac{\sum_{k=1}^{i=T}(x_k - \hat{x}_k)^2}{T}}. \tag{5.33}$$

5.4 Simulation Studies

5.4.1 A hybrid linear system

In this section, the performance of the developed HMHE will be assessed through a simulation example on a simple linear system switching between two modes as

$$\begin{aligned} &m_k = \eta(m_{k-1}; \lambda), \\ &x_k = F^{(m_k)}x_{k-1} + B^{(m_k)}u_{k-1} + w_k, \qquad && w_k \in N(0, Q_k), \\ &y_k = H^{(m_k)}x_k + v_k, && v_k \in N(0, R_k). \end{aligned} \tag{5.34}$$

The system parameters as well as the hidden Markov parameters are given in the Appendix C. In order to assess the performance of the HMHE in presence of constraints, the following constraints are incorporated:

$$\begin{aligned} &u_k < 0, && m_k \in M_i : \quad M_i = \{1, 2\}, \\ &u_k \geq 0, && m_k \in M_i : \quad M_i = \{1, 2, 3\}, \\ &-L\delta_w \leq w_k \leq L\delta_w. \end{aligned} \tag{5.35}$$

where $L \geq 1$ is a tuning parameter for the continuum state constraint and the last inequality specifies constraint on continuum disturbances.

In this example, the objective is to simultaneously estimate the continuum state $\hat{x}_k$ as well as the noncontinuum state $\hat{m}_k$ given noisy measurements. The measurement noise covariance matrix R_k and state noise covariance matrix Q_k are given as

$$Q_k = \begin{pmatrix} \delta_{w,1}^2 & 0 \\ 0 & \delta_{w,2}^2 \end{pmatrix}, \quad R_k = \begin{pmatrix} \delta_{v,1}^2 & 0 \\ 0 & \delta_{v,2}^2 \end{pmatrix}, \tag{5.36}$$

where $\delta_{w,i}$ and $\delta_{v,i}$ are the standard deviation of the process and measurement noise respectively.

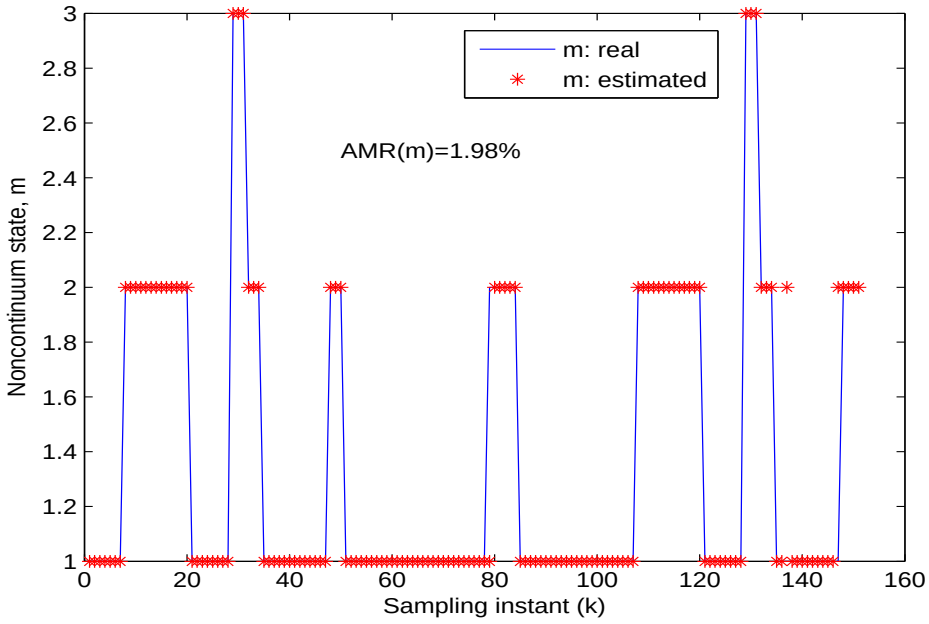

Figure 5.3: Noncontinuum state estimation: m; $\delta_w = [3.0; 3.0]$; $\delta_v = [3.0; 3.0]$, $N = 2$.

The simulated results in Figures 5.3 - 5.6 show the performance of the developed hybrid moving horizon estimator. Figures 5.3 and 5.4 show the estimation performance with both process and measurement noise being the standard deviation of 3, while Figures 5.5 and 5.6 show that the hybrid state estimation performance when the standard deviation of the process is increased from 3 to 10. It can be seen that the state estimator tracks well the continuum state dynamics, while correctly estimating the change in the system operating modes. However, in order to quantitatively assess the performance of a simultaneous continuum and noncontinuum state estimator developed, the effect of the noise level (in both the process and measurements), the horizon length N and the constraints on the noncontinuum state space M_i are further examined.

Using the performance index defined in Eqs. (5.32)-(5.33), the HMHE performances are analyzed and summarized in Table 5.1. The results indicate that using the additional known information of the system to constrain the noncontinuum state space will improve both the accuracy of continuum and noncontinuum states estimation. Besides, we can also see from the results of Table 5.1 that constraining the noncontinuum state space leads to a reduction in the computational time.

A moving horizon estimation naturally offers us one more degree of freedom, which is the availability of the horizon length N as a tuning parameter. From the results in Table 5.1, it is clear that increasing the horizon length will increase the state estimation performance, though it comes at the expense of the computational

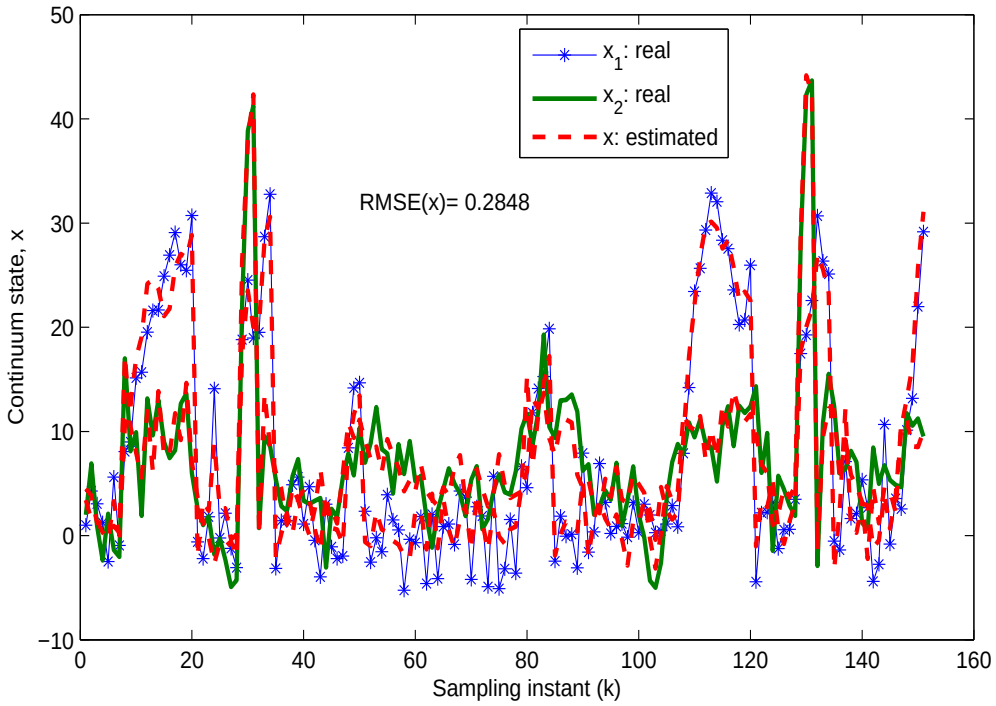

Figure 5.4: Continuum state estimation: x; $\delta_w = [3.0; 3.0]$; $\delta_v = [3.0; 3.0]$, $N = 2$.

Table 5.1: Effects of the noise level, horizon length and constraint handling on the HMHE performance.

	Noise parameters δ_w , δ_v	N=1 AMR, RMSE, Time (%), (x) ,(min)	N=2 AMR, RMSE, Time (%),(x), (min)
Constraint. $\{M_i\}$ is varying	3 , 3	1.987, 0.2848, 0.90	1.987, 0.2848, 3.41
	3 , 10	16.55, 0.7407, 0.76	13.24 , 0.6814, 2.76
	10 , 3	19.86, 0.3604, 1.09	18.54, 0.3602, 4.54
Unconstraint. $\{M_i\}$ is fixed	3 , 3	1.987, 0.2848, 1.08	1.987, 0.2848, 4.32
	3 , 10	18.54, 0.7964, 0.91	14.56, 0.7273, 3.48
	10 , 3	20.53, 0.3566, 1.31	18.55, 0.3562, 5.88

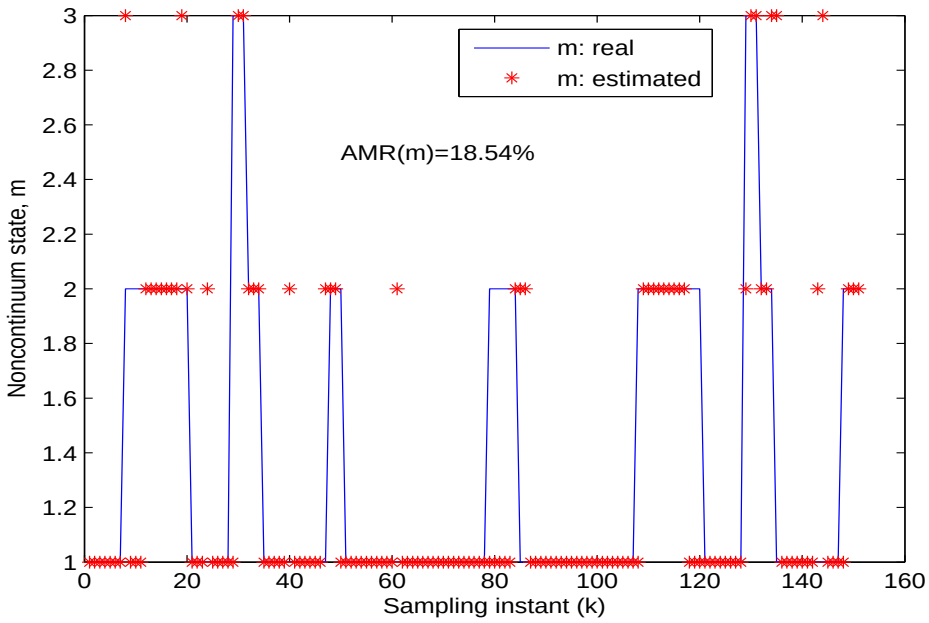

Figure 5.5: Noncontinuum state estimation: m; $\delta_w = [10.0; 10.0]$; $\delta_v = [3.0; 3.0]$, $N = 2$.

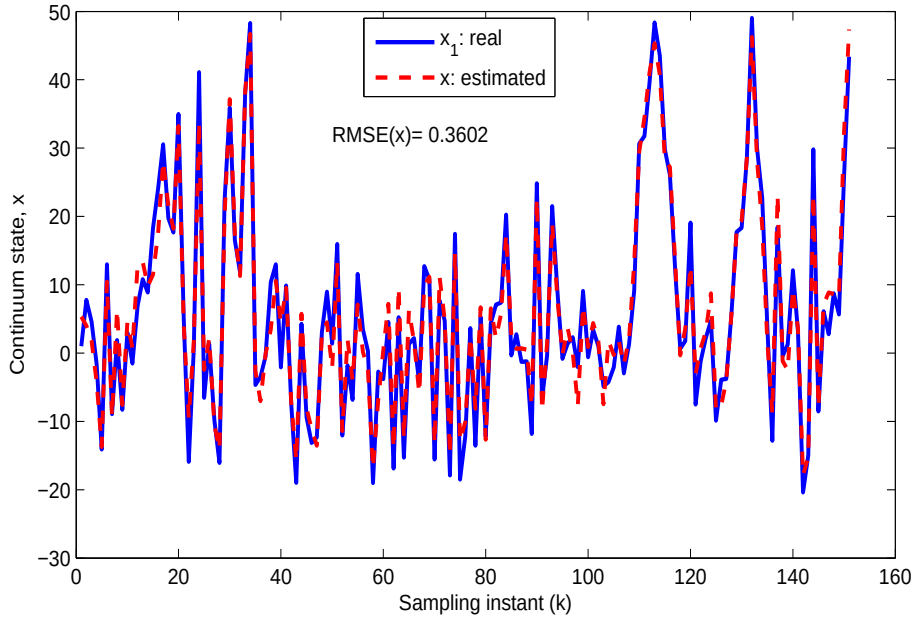

Figure 5.6: Continuum state estimation: x; $\delta_w = [10.0; 10.0]$; $\delta_v = [3.0; 3.0]$, $N = 2$

time. Therefore, a trade-off has to be reached in selecting the horizon length N to give the desired level of state estimation accuracy for which an acceptable computational time is feasible.

5.5 Conclusion

A hybrid moving horizon estimator for simultaneous continuum and noncontinuum state estimation in a constrained switching dynamic system is developed. We have shown that a hybrid state estimator, which is based on a moving horizon optimization technique, is a powerful tool in which further information about the system can be incorporated in estimation through constraints on both the continuum and noncontinuum states. A generalized arrival cost, which accounts for the cost due to the mode transition states as well as due to the continuum state dynamics, is derived for hybrid moving horizon estimator. A series of simulation studies have shown that HMHE performs well in estimating both the continuum and noncontinuum states simultaneously.

Chapter 6

Online State Estimation in a Distillation Process Using a Hybrid Moving Horizon Estimator: Experimental Studies

6.1 Introduction

[1]In order to establish the practical reliability, the capabilities, and limitations of a hybrid moving horizon estimator (HMHE) , it is important test the HMHE performance through a comparison with the actual data measured in an experimental apparatus. State estimation problems can be verified from pilot-scale experiments owing to relatively easy measurement of state variables in pilot scale processes. In this chapter, we study the performance of a hybrid moving horizon estimator (HMHE) for a simultaneous estimation of continuum and noncontinuum states from a distillation process.

There have been a lot of research interests on the application of state estimation to composition monitoring in a distillation process. But only few papers have verified their developed state estimators on the actual experimental data [57, 9, 10, 65]. Besides, the demand in achieving simultaneous estimation of column composition profiles, operating mode change detection, and fault detection and isolation, are among several factors that necessitate the application of advanced hybrid filters to a distillation process monitoring and control. A hybrid state estimator will also provide a better estimates of the key process variables in an industrially operated distillation column with steady state multiplicities [43, 95] and unmeasured disturbance inputs[75].

1. *This chapter is a part of the manuscript that has been published as "M.J. Olanrewaju, B. Huang, and A. Afacan. Development of a simultaneous continuum and noncontinuum state estimator with application on a distillation process, AIChE Journal, 2011, DOI 10.1002/aic, Vol.00, No. 0."*

6.2 Experimental Setup and Operation

In Chapter 3, we conducted an experimental studies to test the practical reliability of applying a sequential moving horizon estimator to infer both the composition dynamics as well as the process operating mode as a function of time in a distillation column with diameter $0.157m$. In this Chapter, we consider a different distillation process set up. It is an industrial type distillation column with $0.300m$ in diameter. A schematic diagram of the experimental setup is shown in Figure 6.1. Unlike the previous distillation column studied in Chapter 3, this column has higher production capacity, and higher tray efficiency, and has about 10 times the energy input. The column contains five identical sieve trays and spaced $0.457m$ apart. Each tray is made of stainless steel and equipped with thermocouple and liquid sampling point at the outlet of the tray. The top two sections of the column are made of Pyrex glass to enable observation of the vapor/liquid phenomena; the rest are made of stainless steel. Detailed dimensions of the column and tray are shown in Table 6.1. The total pressure drop for two trays is measured using a Rosemount differential pressure cell. A total condenser and a thermosiphon partial reboiler complete the distillation system.

The column is instrumented for continuous unattended operation. An Opto-22 process I/O subsystem interface with a personal computer running LabView (Version 7.1) software was used for process control and data acquisition. Multi-loop single-input-single-output (SISO) control structures for input streams, levels, and column pressure in a LabView platform are shown in Figure 6.2. The pressure is controlled by the heat removal from condenser. The assignment of manipulated variables for level controllers is based on the principle of choosing the stream with most direct impact. The base level is controlled by manipulating the bottoms flowrate, while the reflux drum level is controlled by manipulating the distillate flowrate. The controllers are tuned using the Tyreus-Luyben tuning method [90] and the controllers' parameter settings obtained are shown in Figure 6.2. The liquid samples were analyzed using a Hewlett Packard 5790A series II gas chromatograph with a thermal conductivity detector having a column ($3.17mm$ -i.d.) packed with Carbopack.

The column was started with total reflux operation and was then switched to continuous mode by introducing feed to the column and withdrawal of two products from the top and bottom of the column. In this study, a total of three different steady state operating modes were carried out under ambient pressure using methanol-isopropanol mixture. For each operating mode, the reflux flow rate, R_m, feed flow rate, F_m, and methanol composition in the feed, z_m, were kept constant while the only vapor boilup rate was varied. Table 6.2 shows the operating variables for three

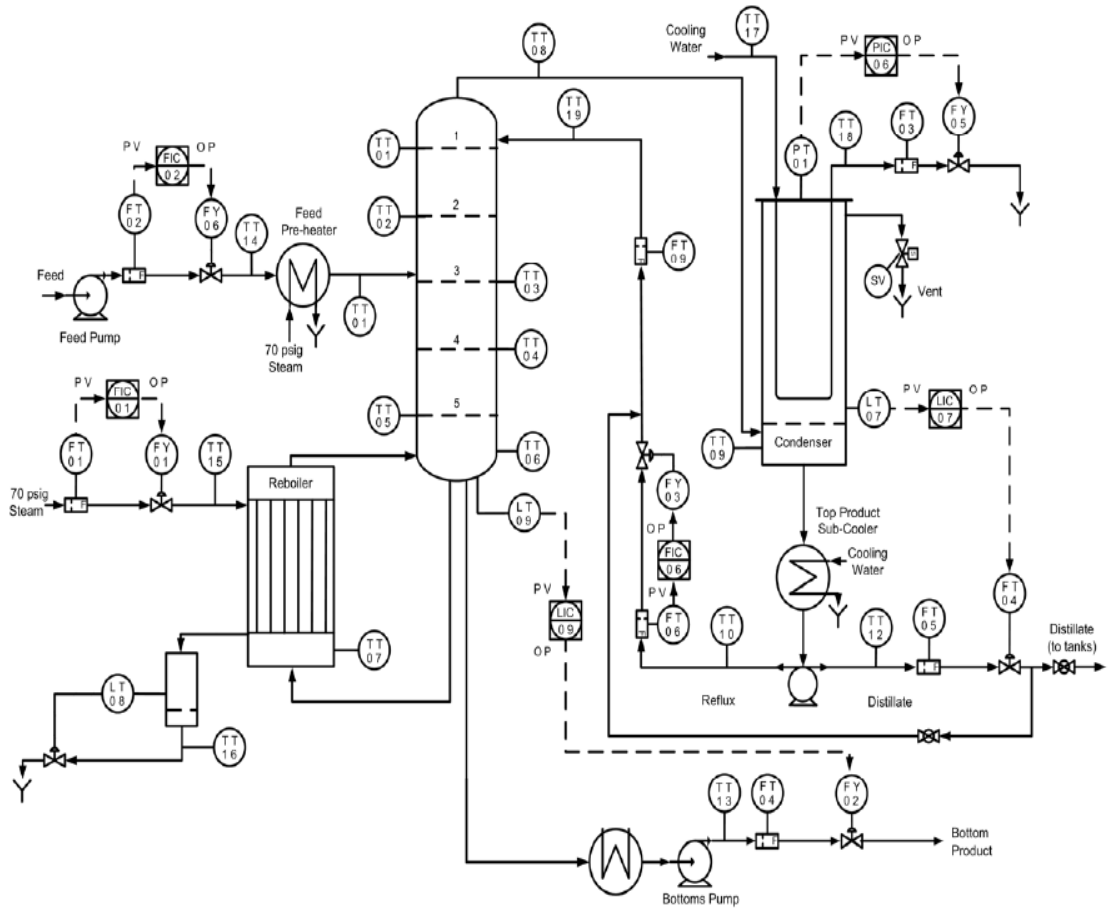

Figure 6.1: A continuous distillation column setup.

steady state operating modes. When the flow rate and temperature profiles shown by the software (LabView) remained constant for a period of 60 minutes, steady state condition was assumed for that particular mode. Triplicate liquid samples from each tray outlet and condenser bottom as well as one from the reboiler were taken and analyzed to minimize the measurement error. The liquid samples were also taken at 3 minutes time intervals only from the bottom of the condenser during the transition period between operating modes. For the steady state and transition period between two mode runs, the sampling time was set to 10 seconds, except the liquid samples that were .

6.3 Process Modeling and Validation

The development of a state estimation requires a process model. In Chapter 3, the nonlinear process model of the distillation process was developed from the first principle. Because we are considering a different distillation column, the process parameters, such as column and tray dimensions, tray efficiency, pressure drops,

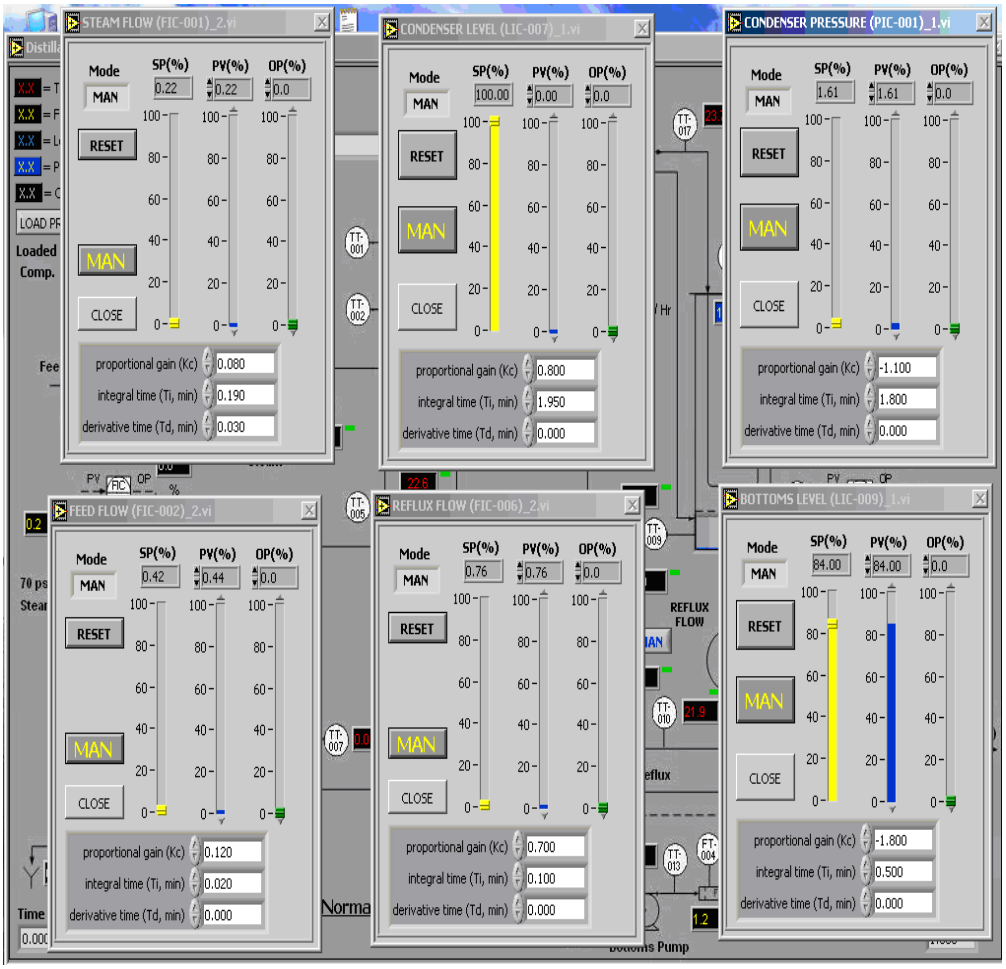

Figure 6.2: A distillation column multi-loop control system.

Table 6.1: Detailed dimensions of the column and trays.

Column diameter	$0.3m$
Tray active area	$0.0537m^2$
Hole diameter	$4.76 \times 10^{-3}m$
Open hole area	$0.00537m^2$
Tray thickness	$3.0 \times 10^{-3}m$
Outlet weir height	$0.063m$
Inlet weir height	$0.051m$
Weir length	$0.213m$
Liquid path length	$0.202m$
Tray spacing	$0.457m$

Table 6.2: Operating modes based on different vapor boilup rates.

Variables	Mode 1	Mode 2	Mode 3
Vapor boilup, V_m(kmol/h)	5.33	6.20	6.91
Reflux flow rate, R_m(kmol/h)	3.51	3.51	3.51
Distillate flow rate, D_m(kmol/h)	1.44	2.80	4.02
Feed flow rate, F_m(kmol/h)	5.89	5.89	5.89
Distillate composition of MeOH, x_D	0.8877	0.8577	0.8217
Feed composition of MeOH, z_m	0.6269	0.6269	0.6269

and production capacity will be different. However, the summarized hybrid process model of the distillation column under consideration will be of the following general form:

$$\begin{aligned} &\frac{dx_{i,j}}{dt} = f_m(x_{i,j}, y_{i,j}, V_m, R_m, F_m, z_m; \theta), \\ &T_i = g_m(x_{i,j}, \beta), \\ &m = \{1, 2, ..., l, ..., M\}, \quad i = \{1, ..., N_s\}, \quad j = \{1, ..., Nc - 1\}, \end{aligned} \tag{6.1}$$

where $x_{i,j}$ and T_i are the liquid composition of MeOH (mole fraction) and temperature on the stage i respectively. V_m (kmol/h) is the vapor boil up; R_m (kmol/h) is the reflux flow rate; F_m (kmol/h) is the feed flow rate; z_m is the feed composition while T_i is the temperature on stage i. By selecting a suitable sampling time, the hybrid dynamic model of a distillation process can be discretized and expressed in the form of Eq. (5.1).

The state estimation problem in this experimental work is to infer the composition of the methanol (i.e. the continuum state) in the distillate product using the available stage temperature measurements. In this study, a change in the system operating mode is caused by a change in the vapor boil up (V, kmol/h) with an unknown switching transition function. However, this transition function follows a hidden Markov model during the experiment. Figures 6.3 and 6.4 compare the steady state conditions of the three different operating modes as obtained from the experiment to those predicted by the process model. The results show that the predicted steady state profiles are able to capture the change in the system operating modes with a change in the column vapor boil up. The operating condition parameters for these three different modes are given in Table 6.2, while the hidden Markov model parameters are provided in Appendix D.

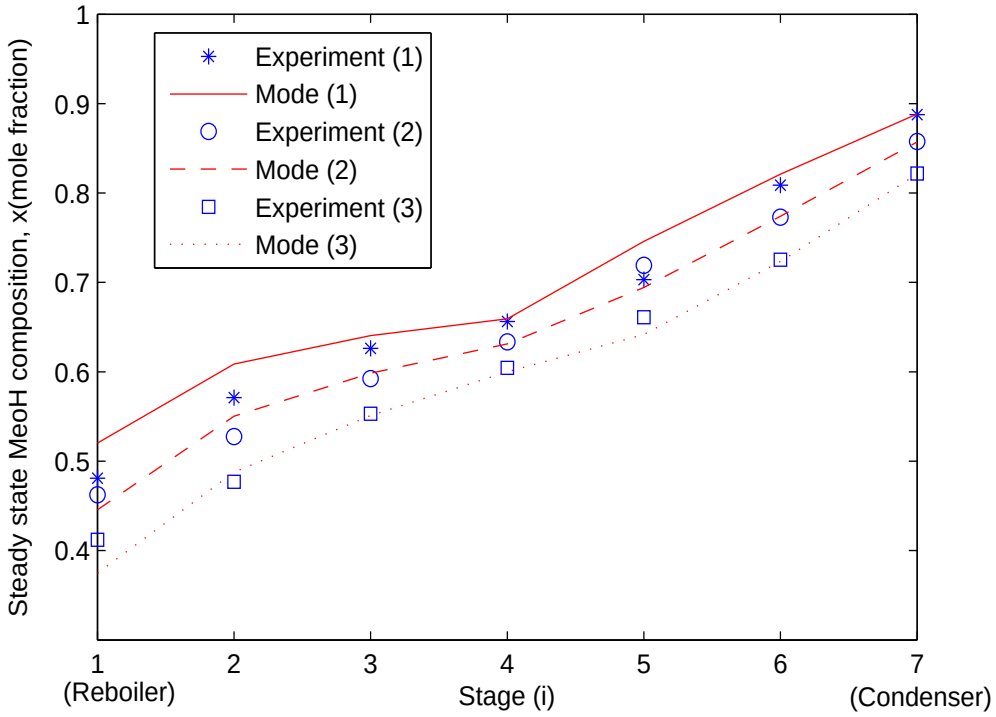

Figure 6.3: Steady state MeOH composition profiles for different operating modes.

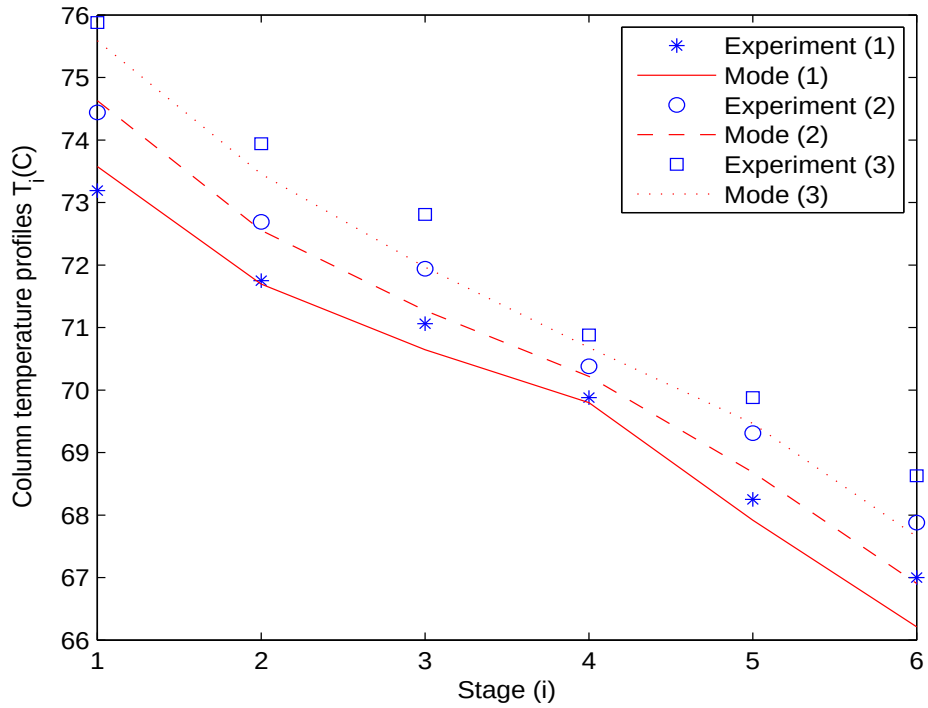

Figure 6.4: Steady state MeOH temperature profiles for different operating modes.

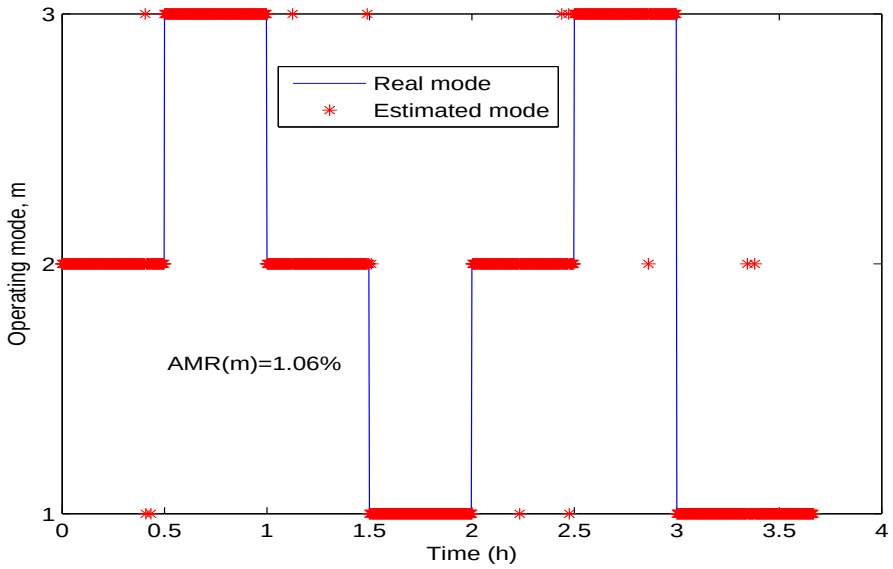

Figure 6.5: Noncontinuum state estimation: operating mode (m).

6.4 Results

6.4.1 HMHE performance

In order to test the performances of the proposed HMHE, measurements of temperatures from the thermocouple located on all of the column stages except the condenser are obtained at every 10 seconds and fed into the estimator online. Figures 6.5 to 6.8 show the performance of the HMHE in estimating the distillate product composition as well as the unknown switching operating modes. The continuum state dynamics shown in Figure 6.6 corresponds to the switch in operating modes shown in Figure 6.5, while the continuum state dynamics of Figure 6.8 follows a different switching modes shown in Figure 6.7. If we compare the two switching patterns, one can see that the HMHE performance is better (i.e., lower AMR(m)) in the results shown in Figures 6.5 and 6.6 than those shown in Figures 6.7 and 6.8. This is because the switching time is fairly constant and much longer in Figure 6.5 than that in Figure 6.7.

The HMHE performance is also tested using a different HMM parameters (see Appendix E), in which the switching pattern is much irregular with a faster switching time. The results are shown in Figures 6.9 and6.10. Even though the HMHE is able to capture the general trend of MeOH composition dynamics as well as the switching operating mode, the MHE performance in this case, is poorer than the previous results. The reason for this is because the rate of switching between one operating mode and another, in some instances, becomes faster than the natural system dynamics, i.e. switching occurs before the process settles to a steady state.

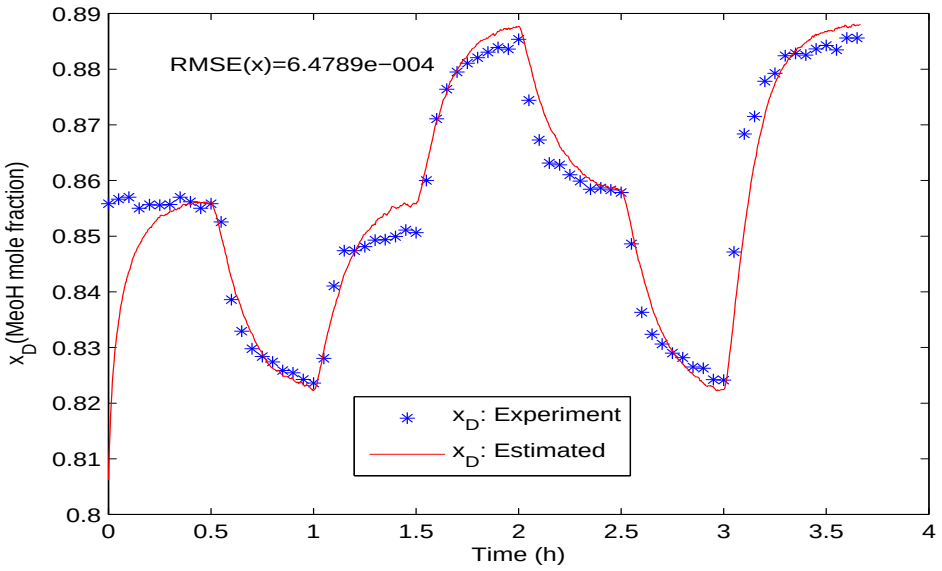

Figure 6.6: Continuum state estimation: Composition of MeOH in the distillate product.

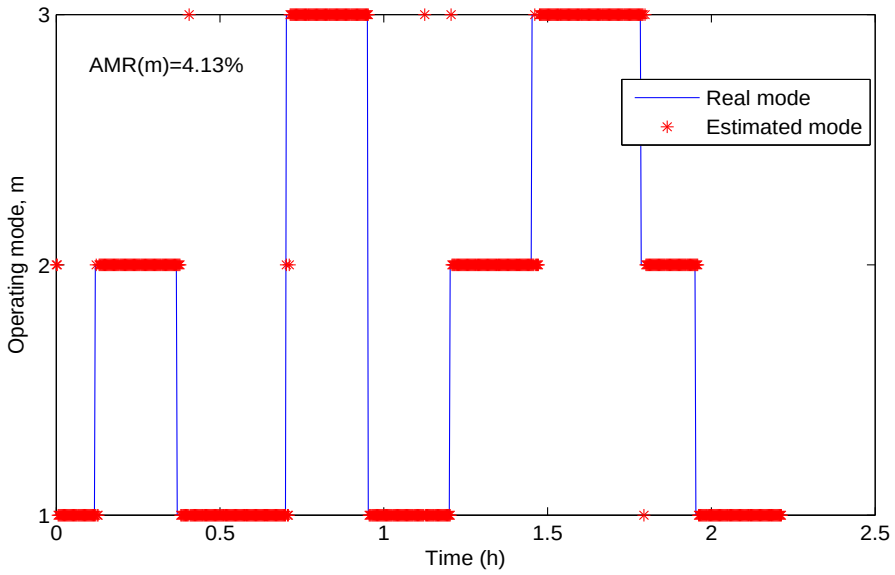

Figure 6.7: Noncontinuum state estimation: operating mode (m).

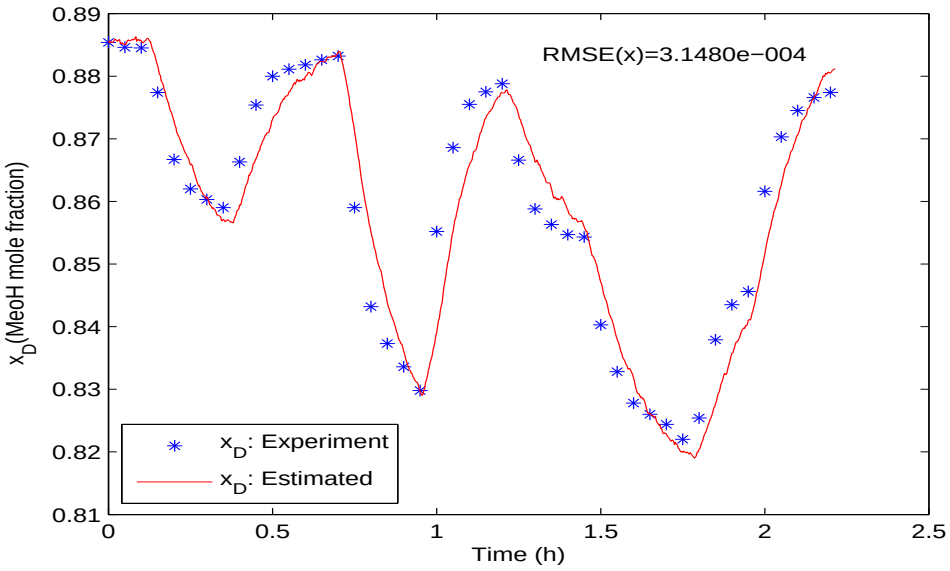

Figure 6.8: Continuum state estimation: Composition of MeOH in the distillate product.

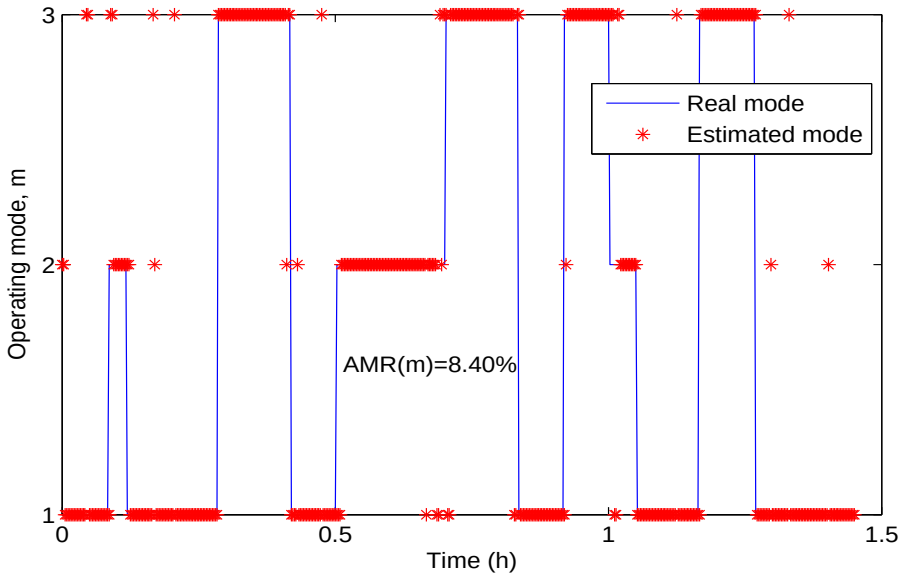

Figure 6.9: Noncontinuum state estimation: operating mode (m).

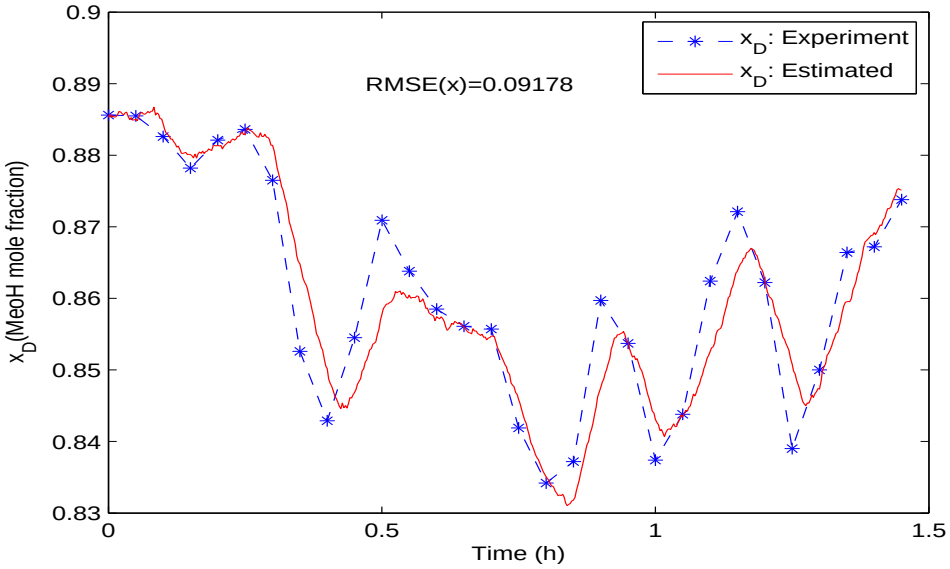

Figure 6.10: Continuum state estimation: Composition of MeOH in the distillate product.

Under this condition, the assumption of treating a change vapor boil up as a discrete-event state (i.e., sudden jump with no transition between operating modes) will no longer be valid. From practical point of view, HMHE will perform well as long as the rate of switching from one operating mode into another is slower than the system dynamics.

6.4.2 Effect of incorporating constraints

In order to assess the performance of the HMHE when using the available information about the controlled input variable (i.e., Reflux flow rate) and the process states (i.e., stage compositions) in constraining the continuum state as well as the noncontinuum state space, the following constraints are considered in HMHE implementation:

1. Continuum state constraint:

$$0 \leq x_{i,j} \leq 1, \tag{6.2}$$

2. Noncontinuum state space constraint:

$$R_m(k) < \bar{R}_m, \qquad m_k \in M_i : \quad M_i = 2, \tag{6.3}$$

$$R_m(k) \geq \bar{R}_m, \qquad m_k \in M_i : \quad M_i = 3. \tag{6.4}$$

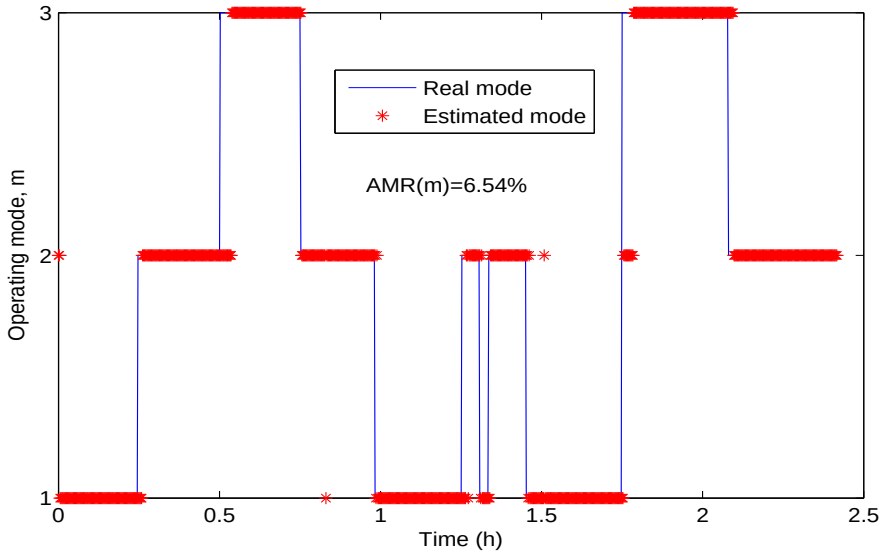

Figure 6.11: Noncontinuum state estimation: operating mode (m).

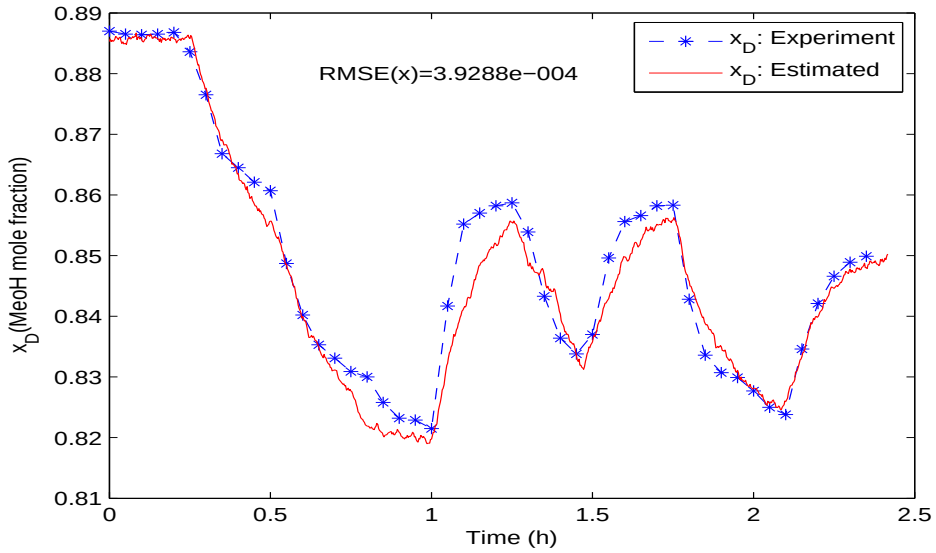

Figure 6.12: Continuum state estimation: Composition of MeOH in the distillate product.

Table 6.3: Effects of constraints on the HMHE performance.

	AMR(%)	RMSE(x)	CPU Time(min)
Constraints.	6.54	3.9281×10^{-4}	54
No constraints.	7.25	3.9692×10^{-4}	81

where $\bar{R}_m$ is the steady state reflux flow rate given in Table 6.2. Figures 6.11 and 6.12 show the performance of HMHE in estimating the operating mode (i.e., noncontinuum state) and the distillate composition (i.e., continuum state) when the constraints are included. The performance of HMHE when the constraints are incorporated are quantitatively compared with when there are no constraints and the results are summarized in Table 6.3. The Average Missing Rate (AMR), Root Mean Square Error (RMSE), as well as the computational time are much lower with better estimate of the states when the constraints are imposed.

6.5 Conclusion

In this chapter, extensive experimental investigation studies are carried out on a distillation process separating methanol-isopropanol mixture. This experimental work is aimed at examining the practical reliability of the developed hybrid moving horizon estimator that has the capability to estimate the composition of methanol in the distillate product as well as the operating modes using the available temperature measurements. The HMHE is shown to be effective not only in estimating a real-time liquid composition dynamics, but also in estimating a change in the operating mode as a function of time. The effect of constraints presence, process and measurement noise levels as well as horizon length variation on the estimation of the continuum and noncontinuum states are analyzed.

Chapter 7

Conclusion and Future Work Recommendations

7.1 Conclusion

In this work, the development and application of a noncontinuum state estimator, sequential hybrid estimator as well as simultaneous continuum and noncontinuum state estimator, which are based on a moving horizon estimation framework, are carried out for complex chemical processes. The success of this work shows that many process monitoring problems of a chemical process can be formulated as state estimation problems and be readily solved.

A sequential state estimation technique, which has the capability to monitor composition profiles of distillation processes under switching dynamics using the available temperature measurements, is investigated in Chapter 3. A distillation process is modeled as a hybrid nonlinear system with the column compositions considered as continuum states, while the operating modes are modeled as noncontinuum states. A moving horizon estimation algorithm is extended to incorporate a mode change detector and an operating mode estimator in order to estimate the column compositions as well as determine if and when there is a change (either desirably or undesirably) in the system operating modes. The proposed method is shown to be effective by testing it using both the simulation on a switching batch distillation process and the experiment on a lab-scale methanol-isopropanol continuous distillation system

An online noncontinuum state estimator, which is based on a moving horizon approach for switching systems that follow a HMM with either noncontinuum or continuum noisy measurements, is proposed in Chapter 4. The arrival cost, which summarizes the effect of past and *a prior* information on the current states, is developed. The effects of horizon length as well as constraints handling on MHENS performance are quantitatively analyzed. The simulation studies on a water tank system for a leakage detection problem as well as on a continuous stirred tank

reactor for an operating mode estimation problem have shown that the developed noncontinuum state estimator is effective.

A hybrid moving horizon estimator for simultaneous continuum and noncontinuum state estimation in a constrained switching dynamic system is developed in Chapter 5. We have shown that a hybrid state estimation, which is based on a moving horizon optimization technique, is a powerful tool in which further information about the system can be incorporated in estimation through constraints on both the continuum and noncontinuum states. A generalized arrival cost, which accounts for the cost due to mode transition states as well as due to the continuum state dynamics, is derived for hybrid moving horizon estimator. A series of simulation studies have shown that HMHE performs well in estimating both the continuum and noncontinuum states simultaneously.

In the last chapter, extensive experimental investigation studies are carried out on a distillation process separating methanol-isopropanol mixture. This experimental work is aimed at examining the practical reliability of the developed hybrid moving horizon estimator to infer a composition of the methanol in the distillate product as well as the operating modes using the available temperature measurements. The HMHE is shown to be effective not only in estimating a real-time liquid composition dynamics, but also in estimating a change in the operating mode as a function of time. The effects of constraints presence, process and measurement noise levels as well as horizon length variation on the estimation of the continuum and noncontinuum states are analyzed.

7.2 Future Work Recommendations

This work raises some challenging and unresolved problems that are potential candidate of further research interests. The future research directions that have been identified from this dissertation are as follows:

- **Computational issues:** The computational issues involved in implementing this technology have not been considered in this work. The main weakness of MHE and the associated algorithms that have been developed and discussed in this work such as MHENS, SHMHE, and HMHE lies on their online implementation issues when considering the enormous optimization steps involved. For nonlinear systems, computational difficulties often arise when one attempts to solve the optimization problems online. However, for most linear systems, the optimization problems can be reliably solved within a few seconds on a desktop computer using standard software.

- **Stability and convergence:** In this work, major efforts are directed into

the algorithm development with the stability and convergence examined only through simulation and experimental studies. The convergence of HMHE has not been theoretically proven and would need to be explored.

- **Industrial application:** Efficient implementation of MHENS as well as HMHE on large-scale industrial processes is of great practical importance. There is a need to further examine the practical reliability of a hybrid state estimator on actual industrial process data.

- **Hybrid state estimation in control system design and implementations:** One of the major needs of a state estimator is to be able to provide an immeasurable measurements to the controllers as in the case of a typical feedback control system. The practicality and implementation issues of combining a hybrid state estimator with a control system would have to be studied.

- **Estimator-based control of a hybrid system:** This thesis focuses mainly on the state estimation of a switching hybrid system given that both the output y and input u are known. We have not considered the control system design for a switching hybrid system. We have considered an open loop switching system in most of our simulation and experimental studies. However, in the last section of this work, we considered a situation where information were to be available from a change in the manipulated variable (i.e., input u) and showed how such information can be incorporated in the design of a hybrid moving horizon estimator in the form of a constraint. The Lyaounov-based model predictive controller (MPC) developed in the work of Mhaskar at. al (2005) [58] can be used in combination with a moving horizon based estimation technique proposed in this work, to develop a more effective nonlinear multivariable control system for a switched system.

Appendices

Appendix A

HMHE Objective Function Derivation

Given Eq. (5.8) as

$$\min_{\hat{m}_{T-N:T},\ \hat{x}_{T-N:T}} \{J_T\} : \quad J_T = \phi_{T-N} + J_{T-N+1:T}, \tag{1}$$

where

$$J_{T-N+1:T} = -\ln P(x_{T-N+1:T}, m_{T-N+1:T}, y_{T-N+1:T} | x_{T-N}, m_{T-N}), \tag{2}$$

the joint probability distribution of the noncontinuum state $m_{T-N+1:T}$ and the continuum state $x_{T-N+1:T}$ with the available measurement data $y_{T-N+1:T}$ can be expressed as

$$P(x_{T-N+1:T}, m_{T-N+1:T}, y_{T-N+1:T} | x_{T-N}, m_{T-N}) = \prod_{k=T-N+1}^{T} P(m_k|m_{k-1})$$
$$\prod_{k=T-N+1}^{T} P(x_k|x_{k-1}, m_k) \prod_{k=T-N+1}^{T} P(y_k|x_k, m_k). \tag{3}$$

If we take the logarithm of Eq. (3) and make use of $J_{T-N+1:T}$ as defined in Eq. (2), then, Eq. (1) we become

$$\min_{\hat{m}_{T-N:T},\ \hat{x}_{T-N:T}} \{J_T\} : \quad J_T = \phi_{T-N} - \sum_{k=T-N+1}^{T} \ln P(m_k|m_{k-1})$$
$$- \sum_{k=T-N+1}^{T} \ln P(x_k|x_{k-1}, m_k) - \sum_{k=T-N+1}^{T} \ln P(y_k|x_k, m_k). \tag{4}$$

If we assume that the continuum state x_k and the observation state y_k follow a Gaussian distribution, Eq. (4) can further be subdivided and defined as follows:

- Given the mode m_k and the state x_{k-1}, the conditional probability distribution of the state x_k with mean of $f_{m_k}(x_{k-1}, u_{k-1}; \theta)$ and covariance matrix of Q_k is:

$$P(x_k|x_{k-1}, m_k) = (2\pi)^{-n/2} {Q_k}^{-1/2} \exp\big[-\frac{1}{2}\{x_k - f_{m_k}(x_{k-1}, u_{k-1}; \theta)\}^T {Q_k}^{-1}\{x_k - f_{m_k}(x_{k-1}, u_{k-1}; \theta)\}\big], \tag{5}$$

- Conditioned on the mode m_k and x_k, the probability distribution of the observation y_k with the mean of $g_{m_k}(x_k; \beta)$ and covariance matrix of R_k is:

$$P(y_k|x_k, m_k) = (2\pi)^{-q/2} {R_k}^{-1/2} \exp\big[-\frac{1}{2}\{y_k - g_{m_k}(x_k; \beta)\}^T {R_k}^{-1}\{y_k - g_{m_k}(x_k; \beta)\}\big]. \tag{6}$$

If we define the following terms:

$$\begin{aligned} \hat{w}_{k-1} &= \hat{x}_k - f_{\hat{m}_k}(\hat{x}_{k-1}, u_{k-1}; \theta), \\ \hat{v}_k &= y_k - g_{\hat{m}_k}(\hat{x}_k; \beta), \end{aligned} \tag{7}$$

and by taking the negative logarithm of Eqs. (5) and (6), we have

$$-\ln P(x_k|m_k) = \mathcal{B}_k + \frac{1}{2}\hat{w}_{k-1}^T {Q_k}^{-1} \hat{w}_{k-1}, \tag{8}$$

$$-\ln P(y_k|x_k, m_k) = \mathcal{C}_k + \frac{1}{2} v_k^T {R_k}^{-1} v_k, \tag{9}$$

where $\mathcal{B}_k = -\ln(2\pi)^{-n/2} {Q_k}^{-1/2}$ and $\mathcal{C}_k = -\ln(2/\pi)^{-\frac{q}{2}} R_k^{-1/2}$. If we define $\gamma_{k-1}^{(i)}$, $\alpha_k^{(j)}$ and $\mathbb{P}_{k-1,k}^{(i,j)}$ as

$$\gamma_{k-1}^{(i)} = \begin{cases} 1 & if \quad i = \hat{m}_{k-1} \\ \\ 0 & if \quad i \neq \hat{m}_{k-1} \end{cases}, \tag{10}$$

$$\alpha_k^{(j)} = \begin{cases} 1 & if \quad j = \hat{m}_k \\ \\ 0 & if \quad j \neq \hat{m}_k \end{cases}, \tag{11}$$

and

$$\mathbb{P}_{k-1,k}^{(i,j)} := P(m_k = j | m_{k-1} = i), \quad \text{for} \quad i, j \in \mathbb{M}, \tag{12}$$

respectively, we can obtain Eq. (5.9) by substituting Eqs. (8)-(12) in Eq. (4) as

$$\begin{aligned} \min_{\{\hat{m}_{T-N:T}, \quad \hat{w}_{T-N:T}\}} J_T : \quad J_T &= \phi_{T-N} - \sum_{k=T-N+1}^{T} \sum_{i=1}^{M} \sum_{j=1}^{M} \gamma_{k-1}^{(i)} \alpha_k^{(j)} \ln \mathbb{P}_{k-1,k}^{(i,j)} \\ &+ \sum_{k=T-N}^{T-1} \sum_{j=1}^{M} \alpha_k^{(j)} \hat{w}_k^T {Q_k}^{-1} \hat{w}_k \quad + \quad \sum_{k=T-N+1}^{T} \sum_{j=1}^{M} \alpha^{(j)} \hat{v}_k^T {R_k}^{-1} \hat{v}_k + \mathcal{A}_k, \end{aligned} \tag{13}$$

where $\mathcal{A}_k = \mathcal{B}_k + \mathcal{C}_k$. Note that $\mathcal{A}_k$ is independent of the decision variables $\hat{m}_{T-N:T}$ and $\hat{w}_{T-N:T}$, and can be neglected in Eq. (13).

Appendix B

Arrival Cost Derivation

Given the following:

$$\phi_k^x = -\ln P(x_k|m_k, y_{0:k}). \tag{14}$$

Proof:

Using Bayesian rule, $P(x_k|m_k, y_{0:k})$ can be written as

$$P(x_k|y_{0:k}, m_k) = \frac{P(x_k|m_k) P(y_{0:k}|x_k, m_k)}{P(y_{0:k}|m_k)}, \tag{15}$$

which can also be written as

$$P(x_k|y_{0:k}, m_k) = \mathcal{D}_k P(x_k|m_k) P(y_{0:k}|x_k, m_k), \tag{16}$$

where $\mathcal{D}_k = P(y_{0:k}|m_k)^{-1}$. Using the conditional independency properties (see Figure 5.1):

$$P(x_k|y_{0:k}, m_k) = \mathcal{D}_k P(x_k|m_k) P(y_k|x_k, m_k). \tag{17}$$

Then, Eq. (14) becomes

$$\phi_k^x = -\ln \mathcal{D}_k - \ln P(x_k|m_k) - \ln P(y_k|x_k, m_k). \tag{18}$$

Following the same derivations and analysis in Appendix A, it is straight forward to see that both the second and the third term of Eq. (18) will become

$$-\ln P(x_k|m_k) = \mathcal{B}_k + \frac{1}{2}\hat{w}_{k-1}^T {P_k}^{-1} \hat{w}_{k-1}, \tag{19}$$

and

$$-\ln P(y_k|x_k, m_k) = \mathcal{C}_k + \frac{1}{2} v_k^T {R_k}^{-1} v_k, \tag{20}$$

Hence,

$$\phi_k^x = \frac{1}{2} w_{k-1}^T {P_k}^{-1} w_{k-1} + \frac{1}{2} v_k^T {R_k}^{-1} v_k + \mathcal{E}_k, \tag{21}$$

where $\mathcal{E}_k = \mathcal{B}_k + \mathcal{C}_k - \ln \mathcal{D}_k$.

Appendix C

Switching System Parameters

The parameters of the switching linear system of Section (5.4.1) are given as follows:

$$F^{(1)} = \begin{pmatrix} -0.211 & 0 \\ 0 & 0.521 \end{pmatrix}, F^{(2)} = \begin{pmatrix} 0.691 & 0 \\ 0 & -0.310 \end{pmatrix},$$

$$F^{(3)} = \begin{pmatrix} 0.153 & 0 \\ 0 & 0.410 \end{pmatrix}, \tag{22}$$

$$B^{(1)} = B^{(2)} = B^{(3)} = \begin{pmatrix} -2 \\ 1 \end{pmatrix}, \tag{23}$$

$$H^{(1)} = H^{(2)} = H^{(3)} = \begin{pmatrix} 1 & 0 \\ 0 & 1 \end{pmatrix}. \tag{24}$$

The transition probability matrix $\mathbb{P}$ is given as,

$$\mathbb{P} = \begin{pmatrix} 0.90 & 0.05 & 0.05 \\ 0.05 & 0.90 & 0.05 \\ 0.05 & 0.05 & 0.90 \end{pmatrix}. \tag{25}$$

when the constraint on the space span M_i as given in Eq. (5.35) is not active and

$$\mathbb{P} = \begin{pmatrix} 0.95 & 0.05 \\ 0.05 & 0.95 \end{pmatrix}. \tag{26}$$

when the constraint on the space span M_i as given in Eq. (5.35) is active.

Appendix D

Hidden Markov Model Parameters

$$\mathbb{P} = \begin{pmatrix} 0.9914 & 0.0058 & 0.0029 \\ 0.0083 & 0.9875 & 0.0042 \\ 0.0048 & 0.0048 & 0.9905 \end{pmatrix}. \tag{27}$$

Appendix E

Hidden Markov Model Parameters

$$\mathbb{P} = \begin{pmatrix} 0.9805 & 0.0078 & 0.0117 \\ 0.0196 & 0.9706 & 0.0098 \\ 0.0184 & 0.0061 & 0.9755 \end{pmatrix}. \tag{28}$$

Bibliography

[1] R. Aguilar-Lopez and R. Martinez-Guerra. Robust state estimation for repetitive operating mode process: Application to sequencing batch reactors. *Chem. Eng. Journal*, 126:155–161, 2007.

[2] A. Alessandri, M. Baglietto, and G. Battistelli. Minimum-distance receding-horizon state estimation for switching discrete-time linear system. In R. Findeisen, F. Allgwer, and L.T. Biegler, editors, *Assessment and Future Directions*. Springer-Verlag, 2007.

[3] A. Alessandri and P. Coletta. Switching observers for continuous-time and discrete-time linear systems. In *Proceedings of the American Control Conference*, pages 2516–2521, Arlington, VA, 2001. IEEE.

[4] A. Alessandri and P. Coletta. Design of observers for switched discrete-time linear systems. In *Proceedings of the American Control Conference*, pages 2785–2790, Denver, Colarado, 2003. IEEE.

[5] P.J. Antsaklis. A brief introduction to the theory and applications of hybrid systems. *Proceedings of the IEEE*, 88(7):879–887, 2000.

[6] M. Baglietto, G. Battistelli, and L. Scardovi. Active mode observation of switching linear systems. *Automatica*, 43:1442–1449, 2007.

[7] M. Baglietto, G. Battistelli, and L. Scardovi. Active mode observation of switching systems based on set-valued estimation of the continuous state. *Int. J. Robust Nonlinear Control*, 19:1521–1540, 2009.

[8] A. Balluchi, L. Benvenuti, M.D. Benedetto, and A.L. Sangiovanni-Vincentelli. Hybrid control of force transients for multi-point injection engines. *Int. J. Robust Nonlinear Control*, 11:515–539, 2001.

[9] R. Baratti, A. Bertucco, D. Alessandro, and M.A. Morbidelli. Development of a composition estimator for binary distillation columns. application to a pilot plant. *Chem. Eng. Sci.*, 50:541–550, 1995.

[10] R. Baratti, A. Bertucco, D. Alessandro, and M.A. Morbidelli. A composition estimator for multicomponent distillation columns development and experimental test on ternary mixtures. *Chem. Eng. Sci.*, 53:3601–3612, 1998.

[11] N. Bekiaris, G.A. Meskic, C.M. Radu, and M. Morari. Multiple steady states in homogeneous azeotropic distillation. *Ind. and Eng. Chem. Res.*, 32:2023–2038, 1993.

[12] A. Bemporad, D. Mignone, and M. Morari. Moving horizon estimation for hybrid systems and fault detection. In *Proceedings of the American Control Conference*, pages 2471–2475, San Diego, California, 1999. IEEE.

[13] B.W. Bequette. Nonlinear predictive control using multi-rate sampling. *The Can. J. Chem. Eng.*, 69(1):136–143, 1991.

[14] H. Bernhard, B.H. Korte, and J. Vygen. *Combinatorial optimization: Theory and algorithms*. Springer-Verlag, Heidelberg, 2008.

[15] L. Blackmore, S. Rajamanoharan, and B.C. Williams. Active estimation for switching linear dynamic systems. In *Conf. on Dec. and Cont.*, pages 137–144, San Diego, 2006. 45th, IEEE.

[16] Y. Boers and H. Driessen. Hybrid state estimation: a target tracking application. *Automatica*, 38:2153–2158, 2002.

[17] G. Böker and J. Lunze. Stability and performance of switching kalman filters. *Int. J. Control*, 75(16/17):1269–1281, 2002.

[18] W-S. Chen, B.R. Bakshi, P.K. Goel, and S. Ungarala. Bayesian estimation via sequential monte carlo sampling: unconstrained nonlinear dynamic systems. *Ind. and Eng. Chem. Res.*, 43:4012–4025, 2004.

[19] J. Ching, J.L. Beck, and K.A. Porter. Bayesian state and parameter estimation of uncertain dynamical systems. *Probabilistic Engineering Mechanics*, 21:81–96, 2006.

[20] E.A. Domlan, J. Ragot, and D. Maquin. Mode estimation for switching systems. *Proceedings of the American Control Conference*, New York, USA:11–13, 2007.

[21] A. Doucet and C. Andrieu. Iterative algorithms for state estimation of jump markov linear systems. *IEEE Transactions On Signal Processing*, 49(6):1215–1227, 2001.

[22] M.A. Duran and I.E. Grossmann. An outer approximation algorithm for a class of mixedinteger nonlinear programs. *Mathematical Programming*, 36:307–339, 1986.

[23] N.H. El-Farra, P. Mhaskar, and P.D. Christofides. Output feedback control of switched nonlinear systems using multiple lyapunov functions. *Systems and Control Letters*, 54:1163–1182, 2005.

[24] J. Evans and V. Krishnamurthy. Optimal sensor scheduling for hidden markov model state estimation. *Int. J. Control*, 74(18):1737–1742, 2001.

[25] G. Ferrari-Trecate, D. Mignone, and M. Morari. Moving horizon estimation for hybrid systems. In *Proceedings of American control conference*, pages 1684–1688, Chicago, Illinois, 2000.

[26] G. Ferrari-Trecate, D. Mignone, and M. Morari. Moving horizon estimation for hybrid systems. *IEEE Transactions on Automatic Control*, 47(10):1663–1676, 2002.

[27] P.K. Findeisen. *Moving horizon strategies for the constrained monitoring and control of nonlinear discrete-time systems*. PhD thesis, Chemical Engineering Department, University of Wisconsin-Madison, USA, 1997.

[28] C.A. Floudas and V. Visweswaran. A global optimization algorithm for certain classes of nonconvex nlps-i. *Computers and Chem. Engineering*, 14:1397–1417, 1990.

[29] D.G. Forney. The viterbi algorithm. *Proceedings of the IEEE*, 61(3), 1973.

[30] K.J Friston. Bayesian estimation of dynamical systems: An application to fmri. *NeuroImage*, 16:513–530, 2002.

[31] S. Ganguly and D.N. Saraf. Startup of a distillation column using nonlinear analytical model predictive control. *Ind. and Eng. Chem. Res.*, 32:1667–1675, 1993.

[32] B. Gendron and T.G. Cranic. Parallel branch-and-bound algorithms:survey and synthesis. *Operations Research*, 42(6):1042–1066, 1994.

[33] A.M. Geoffrion. A unifying review of linear gaussian models. *Journal Optimization and Theory Applications*, 10:237–260, 1972.

[34] S.Z. Ghahramani. A unifying review of linear gaussian models. *Neural Computation*, 11:305–345, 1999.

[35] G.C. Goodwin and D.E. Quevedo. Finite alphabet control and estimation. *International Journal of Control, Automation, and Systems*, 1(4):412–430, 2003.

[36] G.C. Goodwin and D.E. Quevedo. Moving horizon design of discrete coefficient fir filters. *IEEE Transactions On Signal Processing*, 53(6):412–430, 2005.

[37] E.L. Haseltine and J.B. Rawlings. Critical evaluation of extended kalman filtering and moving-horizon estimation. *Ind. and Eng. Chem. Res.*, 44:2451–2460, 2005.

[38] M.W. Hofbaur and B.C. Williams. Mode estimation of probalistic hybrid systems. In C.J. Tomlin and M.R. Greenstreet, editors, *HSCC*, volume LNCIS 2289, pages 253–266. Springer-Verlag, Berlin Heidelberg, 2002.

[39] M.W. Hofbaur and B.C. Williams. Hybrid estimation of complex systems. *Trans. on System, Man and Cybernetics Part-B, Cybernetics*, 34(5):2178–2191, 2004.

[40] Y. Hu and N.H. El-Farra. Robust fault detection and monitoring of hybrid process systems with uncertain mode transitions. *AIChE J.*, In press, 2010.

[41] B. Huang and S.L. Shah. *Performance assessement of control loops: Theory and applications*. Springer Verlag, Heidelberg, 1999.

[42] U. Onken J. Ghmeling and W. Arlt. Vapor-liquid equilibrium data collection. *Aqueous Organic Systems*, 1(1a):Chemistry Data Series, Dechema, Frankfurt, 1981.

[43] E.W. Jacobsen and S. Skogestad. Dynamics and control of unstable distillation columns. *Modeling, Identification and Control*, 14:59–72, 1990.

[44] E.W. Jacobsen and S. Skogestad. Multiple steady-states in ideal two-product distillation. *AIChE J.*, 37(4):499–511, 1991.

[45] E.W. Jacobsen and S. Skogestad. Instability of distillation columns. *AIChE J.*, 40(9):1466–1478, 1994.

[46] A.H. Jazwinski. Limited memory optimal filtering. *IEEE Transactions on Automatic Control*, 13(5):558–563, 1968.

[47] M. Jelali and B. Huang (Eds). *Detection and diagnosis of stiction in control loops: State of the art and advanced methods*. Springer, Verlag, 2010.

[48] B. Joseph and C.B. Brosilow. Inferential control of processes: Parts i, ii and iii. *AIChE J.*, 24:485–509, 1978.

[49] S.J. Julier and J.K. Uhlmann. Unscented filtering and nonlinear estimation. *Proceedings of the IEEE*, 92(2):401–421, 2004.

[50] R.E. Kalman. A new approach to linear filtering and prediction problems. *Transactions of the ASME, Journal of Basic Engineering*, 82:35–45, 1960.

[51] A. Kienle, M. Groebel, and E.D. Gilles. Multiple steady states in binary distillation columns-theoretical and experimental results. *Chemical Engineering Science*, 50(17):2691–2703, 1995.

[52] T. Kraus, P. Kuhl, L. Wirsching, H.G. Bock, and M. Diehl. A moving horizon state estimation algorithm applied to the tennessee eastman benchmark process. In *IEEE Inter. Conf. on Multisensor Fusion and Integration for Intelligent Systems*, Heidelberg, Germany, 2006.

[53] L. Lang and E.D. Gilles. Nonlinear observers for distillation columns. *Chem. Eng. Sci.*, 14:1297–1301, 1990.

[54] P. De Larminat, D. Sarlat, and Y. Thomas. Invariant imbedding and filtering: a moving horizon criterion. *JACC*, Austin, 1974.

[55] U.N. Lerner. *Hybrid Bayesian networks for reasons about complex systems*. PhD thesis, Computer Science Department, Stanford University, USA, 2003.

[56] J.B. Mare and J.A. De Dona. Moving horizon estimation of constrained nonlinear systems by carleman approximations. In *Proceedings of the IEEE*, pages 2147–2152, San Diego, USA, 2006.

[57] T. Mejdell and S. Skogestad. Composition estimator in a pilot-plant distillation column using multiple temperature. *Ind. and Eng. Chem. Res.*, 30(12):2555–2564, 1991.

[58] P. Mhaskar, N.H. El-Farra, and P.D. Christofides. Predictive control of switched nonlinear systems with scheduled mode transitions. *IEEE Transactions on Automatic Control*, 50:1670–1680, 2005.

[59] R. Monroy-Loperena and J. Alvarez-Ramirez. Output-feedback of reactive batch distillation columns. *Ind. and Eng. Chem. Res.*, 39:378–386, 2000.

[60] K.R. Muske. *Linear model predictive control of chemical processes*. PhD thesis, The University of Texas, USA, PhD thesis 1996.

[61] K.R. Muske and J.B. Rawlings. Model predictive control with linear models. *AIChE J.*, 39(2):262–287, 1993.

[62] R.M. Oisiovici and S.L. Cruz. State estimation of batch distillation columns using an extended kalman filter. *Chem. Eng. Sci.*, 55:4667–4680, 2000.

[63] M.J. Olanrewaju and M.A. Al-Arfaj. Estimator-based control of reactive distillation: Application of an extended kalman filtering. *Chem. Eng. Sci.*, 61(10):3386–3399, 2006.

[64] M.J. Olanrewaju and M.A. Al-Arfaj. Impact of disturbance magnitudes and directions on the dynamic behavior of a generic reactive distillation. *Chemical Engineering and Processing*, 45:140–149, 2006.

[65] M.J. Olanrewaju, B. Huang, and A. Afacan. Online composition estimation and experiment validation of distillation processes with switching dynamics. *Chem. Eng. Sci.*, 65:1597–1608, 2010.

[66] M. Park and D. Miller. Low-delay optimal map state estimation in hmm's with application to symbol decoding. *IEEE Sig. Pro. Let.*, 4(10):289–292, 1997.

[67] L. Pina and M.A. Botto. Simultaneous state and input estimation of hybrid systems with unknown inputs. *Automatica*, 42:755–762, 2006.

[68] C.C. Qu and J. Hahn. Computation of arrival cost for moving horizon estimation via unscented kalman filtering. *Journal of process control*, 19(2):358–363, 2009.

[69] E. Quintero-Marmol, L.W. Luyben, and C. Georgakis. Application of an extended luenberger observer to the control of multicomponent batch distillation. *Ind. and Eng. Chem. Res.*, 30:1870–1879, 1991.

[70] L.R. Rabiner. Tutorial on hidden markov models and selected applications in speech recognition. *Proceedings of the IEEE*, 77(2):257–286, 1989.

[71] C.V. Rao. *Moving horizon strategies for the constrained monitoring and control of nonlinear discrete-time systems*. PhD thesis, Chemical Engineering Department, University of Wisconsin-Madison, USA, 2000.

[72] C.V. Rao and J.B. Rawlings. Constrained process monitoring: Moving horizon approach. *AIChE J.*, 48(1):97–109, 2002.

[73] C.V. Rao, J.B. Rawlings, and D.Q. Mayne. Constrained state estimation for nonlinear discrete-timesystems: Stability and moving horizon approximations. *IEEE Transactions On Automatic Control*, 48(2):243–258, 2003.

[74] J.B. Rawlings and B.R. Bakshi. Particle filtering and moving horizon estimation. *Computers and Chemical Engineering*, 30:1529–1541, 2006.

[75] A. Rios-Bolivar and F. Szigeti. Binary distillation column control based on state and input observability. In *ro. of the 10th Mediterranean Conference on Control and Auto.*, Lisbon, Portugal, 2002.

[76] D. Robertson. *Moving horizon strategies for the constrained monitoring and control of nonlinear discrete-time systems*. PhD thesis, Auburn University, USA, PhD thesis 1996.

[77] D.G. Robertson, J.H. Lee, and J.B. Rawlings. A moving horizon-based approach for least squares state estimation. *AIChE J.*, 42:2209–2224, 1996.

[78] C. Rowe and J. Maciejowski. Min-max moving horizon estimation for a class of hybrid systems. In *Conference on Decision and Control*, Maui, Hawaii, 2003.

[79] R.Y Rubinstein and D.P. Kroese. *Simulation and the Monte Carlo method*. John Wiley, Hoboken, 2008.

[80] L. Ruokang and H.O. Jon. Fault detection and diagnosis in a closed-loop nonlinear distillation process: application of extended kalman filters. *Ind. and Eng. Chem. Res.*, 30:898–908, 1991.

[81] L.P. Russo and R.E. Young. Moving-horizon state estimation applied to an industrial polymerization process. In *Proceedings of American Control Conference*, pages 1129–1133, San Diego, USA, 1999.

[82] T. Schon, F. Gustufsson, and A. Hunsson. A note on state estimation as a convex optimization problem. *IEEE*, VI:61–64, 2003.

[83] R. Senthil, K. Janarthanan, and J. Prakash. Nonlinear state estimation using fuzzy kalman filter. *Ind. and Eng. Chem. Res.*, 45(25):8678–8688, 2006.

[84] D. Simon. h_∞ filtering with inequality constraints for aircraft turbofan engine health estimation. *Proceedings of the IEEE Conference on Decision & Control*, 45th:3291–3296, 2006.

[85] H.W. Sorenson. *Kalman filtering: Theory and application*. IEEE Press, New York, 1985.

[86] B.J. Spivey, J.D. Hedengren, and T.F. Edgar. Constrained nonlinear estimation for industrial process fouling. *Ind. and Eng. Chem. Res.*, 49:7824–7831, 2010.

[87] K. Sundmacher and A. Kienle. *Reactive distillation: status and future directions*. Willey-VCH, Weinheim, 2003.

[88] Y.A. Thomas. Linear quadratic optimal estimation and control with receding horizon. *JACC*, 11:19–21, 1975.

[89] M.L. Tyler, K. Asano, and M. Morari. Application of moving horizon estimation based fault detection to cold tandem steel mill. *Int. J. Control.*, 73(5):427–438, 2000.

[90] B.D. Tyreus and W.L. Luyben. Tuning pi controllers for integrator/dead time processes. *Ind. and Eng. Chem. Res.*, 31:2625–2628, 1992.

[91] S. Ungarala. Computing arrival cost parameters in moving horizon estimation using sampling based filters. *Journal of process control*, 19(9):1576–1588, 2009.

[92] S. Ungarala, Z. Chen, and K. Li. Bayesian state estimation of nonlinear systems using approximate aggregate markov chains. *Ind. and Eng. Chem. Res.*, 45:4208–4221, 2006.

[93] R. Vidal and A. Chiuso S. Soatto. Observability and identifiability of jump linear systems. pages 3614–3619, Las Vegas, NE, 2002.

[94] J. Viswanathan and I.E. Grossamann. A combined penalty function and outer-approximation method for minlp optimization. *Computers & Chem. Eng*, 14(7):769–782, 1990.

[95] V.N.Kiva and B.M. Alukhanova. Multiple steady states of distillation and its realisation. *Computers & Chemical Engineering*, 21:S541–S546, 1997.

[96] J. Wang. Complex dynamics in a nonlinear chemical system switching between two stable stationary states. *Journal of Chemical Physics*, 17(9):3626–3630, 2003.

[97] R. Xiong and M.A. Gallivan. Moving horizon estimation for in situ monitoring of chemical vapor deposition process. In *Proceedings of American Control Conference*, New York,USA, 2007.

[98] V.M. Zavala and L.T. Biegler. Optimization-based strategies for the operation of low-density polyethylene tubular reactors: Moving horizon estimation. *Computers and Chemical Engineering*, 33:379–390, 2009.

[99] V.M. Zavala, C.D. Laird, and L.T. Biegler. A fast computational framework for large scale moving horizon estimation. Cancun, Mexico, 2007.

[100] V.M. Zavala, C.D. Laird, and L.T. Biegler. A fast moving horizon estimation algorithm based on nonlinear programming sensitivity. *Journal of Process Control*, 18:876–884, 2008.

[101] M. Zeitz. The extended luenberger observer for nonlinear systems. *Systems and Control Letters*, 9(2):149–156, 1987.